ARL-TR-9411 ● FEB 2022

DEVCOM ARMY RESEARCH LABORATORY

# In-situ Atmospheric Intelligence for Hybrid Power Grids: Volume 4 (Climate Impacts on Tactical Power Generation – Part I), Sensor Comparison and Site Characterization

by Gail Vaucher and Sophia Bergen

## NOTICES

### Disclaimers

The findings in this report are not to be construed as an official Department of the Army position unless so designated by other authorized documents.

Citation of manufacturer's or trade names does not constitute an official endorsement or approval of the use thereof.

Destroy this report when it is no longer needed. Do not return it to the originator.

ARL-TR-9411 ● FEB 2022


# In-situ Atmospheric Intelligence for Hybrid Power Grids: Volume 4 (Climate Impacts on Tactical Power Generation – Part I), Sensor Comparison and Site Characterization

**Gail Vaucher**
*DEVCOM Army Research Laboratory*

**Sophia Bergen**
*Reserve Officers' Training Corps Internship, Cornell University*

# REPORT DOCUMENTATION PAGE

*Form Approved*
*OMB No. 0704–0188*



| 1. REPORT DATE *(DD-MM-YYYY)* | 2. REPORT TYPE | 3. DATES COVERED (From - To) |
|---|---|---|
| February 2022 | Technical Report | 1 October 2020–31 December 2021 |

**4. TITLE AND SUBTITLE**
In-situ Atmospheric Intelligence for Hybrid Power Grids: Volume 4 (Climate Impacts on Tactical Power Generation – Part I), Sensor Comparison and Site Characterization

**5a. CONTRACT NUMBER**

**5b. GRANT NUMBER**

**5c. PROGRAM ELEMENT NUMBER**

**6. AUTHOR(S)**
Gail Vaucher and Sophia Bergen

**5d. PROJECT NUMBER**

**5e. TASK NUMBER**

**5f. WORK UNIT NUMBER**

**7. PERFORMING ORGANIZATION NAME(S) AND ADDRESS(ES)**
DEVCOM Army Research Laboratory
ATTN: FCDD-RLC-ED
White Sands Missile Range, NM 88002

**8. PERFORMING ORGANIZATION REPORT NUMBER**
ARL-TR-9411

**9. SPONSORING/MONITORING AGENCY NAME(S) AND ADDRESS(ES)**

**10. SPONSOR/MONITOR'S ACRONYM(S)**

**11. SPONSOR/MONITOR'S REPORT NUMBER(S)**

**12. DISTRIBUTION/AVAILABILITY STATEMENT**
Approved for public release: distribution unlimited.

**13. SUPPLEMENTARY NOTES**

**14. ABSTERACT**
Expanding power diversity has the potential to reduce electrical grid vulnerability and inconsistencies. The integration of renewables, such as combining photovoltaic with traditional power resources, is just one example. Foreknowledge of meteorological conditions can significantly advance hybridized power integration and optimization. This report documents the foundational "Climate Impacts on Tactical Power Generation (Part I)" project, which investigated the meteorological data required to build prognostic atmospheric models needed to optimize power resource hybridization. Six key meteorological variables from the co-located Meteorological Measurement Tripod #2 and A-1830 sensor suites were reviewed. These independently calibrated suites were approximately 30 m apart on a flat, single-story roof in a southwestern US desert. Twenty-one days of collocated data (2021 June) were prepared for comparison. Local effects and cloud shadowing were evident in the very few comparison-plot outlier points. The slightly skewed wind speed comparison plot was a function of local building airflow. The statistical results showed most variables were within the sensor accuracy. Overall, the comparison showed strong agreement between resources, and systematic differences were linked to the atmospheric character of the sampling site. Future work includes climate impacts on tactical power-grid applications.

**15. SUBJECT TERMS**
Climate Impacts on Tactical Power Generation, atmospheric sensor comparison, MMT2, cloud shadow effects, building airflow, atmospheric intelligence, tactical hybrid power, PV

| 16. SECURITY CLASSIFICATION OF: | | | 17. LIMITATION OF ABSTRACT | 18. NUMBER OF PAGES | 19a. NAME OF RESPONSIBLE PERSON |
|---|---|---|---|---|---|
| a. REPORT | b. ABSTRACT | c. THIS PAGE | | | Gail Vaucher |
| Unclassified | Unclassified | Unclassified | UU | 86 | 19b. TELEPHONE NUMBER (Include area code) (575) 678-2334 |

## Contents


**List of Figures** v

**List of Tables** vii

**Acknowledgments** viii

**Executive Summary** ix

**1. Introduction** 1

1.1 Tactical Power Applications 1

1.2 Disaster Relief Applications 2

1.3 Climate Impacts on Tactical Power Generation 2

1.4 Meteorological Variables Used in This Study 3

1.4.1 Pressure 3

1.4.2 Temperature 3

1.4.3 Relative Humidity 4

1.4.4 Solar Radiation 4

1.4.5 Wind Speed and Wind Direction 4

1.5 Data Applications: Relevance to Larger Projects 5

**2. Methods** 6

2.1 Data Resources 6

2.2 Data Preparation 8

2.2.1 Data Quality Control Assessment 8

2.2.2 Timestamp Check 11

2.2.3 Variable Unit Check 11

2.3 Pre-Analysis Data Preparations 12

2.3.1 Nighttime Solar Radiation 12

2.3.2 Light and Variable Wind Conditions 12

2.4 Data Comparison Program 13

2.5 Analysis: Sensor Comparison Techniques 13

2.5.1 Qualitative Data Comparison 13

2.5.2 Quantitative Data Comparison 13

**3. Results and Discussion 14**

3.1 Qualitative Analyses/Results 16

3.2 Quantitative Analyses/Results 17

3.2.1 SR Outliers, a Function of Cloud Shadow Timing 17

3.2.2 Skewed WS Comparison Reveals Site Character 19

3.2.3 WD Comparison Implies Site Airflow Character 20

3.2.4 Error Analysis in Context 20

3.2.5 Sensor Accuracy Reviewed 21

3.3 Climatological Patterns from the Statistical Analyses 21

**4. Summary and Conclusions 22**

**5. Future Climate Impacts on Tactical Power Generation, Part II 23**

**6. References 24**

**Appendix A. MMT2 and A-1830 Raw Data Plots 26**

**Appendix B. Daily MMT2 vs. A-1830 Comparison Plots 38**

**Appendix C. Daily Comparison-Error Analysis Tables 61**

**Appendix D. Verification of Error Calculations 70**

**List of Symbols, Abbreviations, and Acronyms 73**

**Distribution List 74**

## List of Figures


Fig. 1 Top-down roof view of MMT2 (M) and A-1830 (A) locations on the nearly flat roof ..... 7

Fig. 2 SR scatter plots with (left) and without (right) the daily local shadowing event. Points removed are circled in red ..... 9

Fig. 3 2021 Jun 15, MMT2/A-1830 SR data. Pink boxes show the nighttime and routine sensor shadowing data ..... 10

Fig. 4 Light and variable winds at the A-1830 site, on 2021 Jun 05. Threshold value is 3.09 m/s ..... 12

Fig. 5 2021 June 05 WSs sampled by the MMT2 and A-1830 anemometers. The pink line is the light and variable threshold ..... 13

Fig. 6 Total data set scatter plots comparing MMT2 and A-1830 thermodynamic data ..... 15

Fig. 7 Total data set scatter plots comparing MMT2 and A-1830 dynamic data ..... 15

Fig 8 MMT2 and A-1830 data for 2021 Jun 20. Red circle notes the (A-1830, MMT2) contrasting SR values cause by local cloud cover ..... 18

Fig. 10 Cumulative WS comparison trend reinforces 1994 NOAA wind tunnel, building airflow pattern findings ..... 20

Fig. A-1 2021 Jun 05, MMT2 vs. A-1830 raw data plots ..... 27

Fig. A-2 2021 Jun 06, MMT2 vs. A-1830 raw data plots ..... 27

Fig. A-3 2021 Jun 07, MMT2 vs. A-1830 raw data plots ..... 28

Fig. A-4 2021 Jun 08, MMT2 vs. A-1830 raw data plots ..... 28

Fig. A-5 2021 Jun 09, MMT2 vs. A-1830 raw data plots ..... 29

Fig. A-6 2021 Jun 10, MMT2 vs. A-1830 raw data plots ..... 29

Fig. A-7 2021 Jun 11, MMT2 vs. A-1830 raw data plots ..... 30

Fig. A-8 2021 Jun 12, MMT2 vs. A-1830 raw data plots ..... 30

Fig. A-9 2021 Jun 13, MMT2 vs. A-1830 raw data plots ..... 31

Fig. A-10 2021 Jun 14, MMT2 vs. A-1830 raw data plots ..... 31

Fig. A-11 2021 Jun 15, MMT2 vs. A-1830 raw data plots ..... 32

Fig. A-12 2021 Jun 17, MMT2 vs. A-1830 raw data plots ..... 32

Fig. A-13 2021 Jun 18, MMT2 vs. A-1830 raw data plots ..... 33

Fig. A-14 2021 Jun 19, MMT2 vs. A-1830 raw data plots ..... 33

Fig. A-15 2021 Jun 20, MMT2 vs. A-1830 raw data plots ..... 34

Fig. A-16 2021 Jun 21, MMT2 vs. A-1830 raw data plots ..... 34

Fig. A-17 2021 Jun 22, MMT2 vs. A-1830 raw data plots ..... 35
Fig. A-18 2021 Jun 25, MMT2 vs. A-1830 raw data plots ..... 35
Fig. A-19 2021 Jun 26, MMT2 vs. A-1830 raw data plots ..... 36
Fig. A-20 2021 Jun 27, MMT2 vs. A-1830 raw data plots ..... 36
Fig. A-21 2021 Jun 28, MMT2 vs. A-1830 raw data plots ..... 37
Fig. B-1 2021 Jun 05, MMT2 vs. A-1830 data comparison ..... 40
Fig. B-2 2021 Jun 06, MMT2 vs. A-1830 data comparison ..... 41
Fig. B-3 2021 Jun 07, MMT2 vs. A-1830 data comparison ..... 42
Fig. B-4 2021 Jun 08, MMT2 vs. A-1830 data comparison ..... 43
Fig. B-5 2021 Jun 09, MMT2 vs. A-1830 data comparison ..... 44
Fig. B-6 2021 Jun 10, MMT2 vs. A-1830 data comparison ..... 45
Fig. B-7 2021 Jun 11, MMT2 vs. A-1830 data comparison ..... 46
Fig. B-8 2021 Jun 12, MMT2 vs. A-1830 data comparison ..... 47
Fig. B-9 2021 Jun 13, MMT2 vs. A-1830 data comparison ..... 48
Fig. B-10 2021 Jun 14, MMT2 vs. A-1830 data comparison ..... 49
Fig. B-11 2021 Jun 15, MMT2 vs. A-1830 data comparison ..... 50
Fig. B-12 2021 Jun 17, MMT2 vs. A-1830 data comparison ..... 51
Fig. B-13 2021 Jun 18, MMT2 vs. A-1830 data comparison ..... 52
Fig. B-14 2021 Jun 19, MMT2 vs. A-1830 data comparison ..... 53
Fig. B-15 2021 Jun 20, MMT2 vs. A-1830 data comparison ..... 54
Fig. B-16 2021 Jun 21, MMT2 vs. A-1830 data comparison ..... 55
Fig. B-17 2021 Jun 22, MMT2 vs. A-1830 data comparison ..... 56
Fig. B-18 2021 Jun 25, MMT2 vs. A-1830 data comparison ..... 57
Fig. B-19 2021 Jun 26, MMT2 vs. A-1830 data comparison ..... 58
Fig. B-20 2021 Jun 27, MMT2 vs. A-1830 data comparison ..... 59
Fig. B-21 2021 Jun 28, MMT2 vs. A-1830 data comparison ..... 60
Fig. D-1 MATLAB validation of error equations ..... 72

## List of Tables


Table 1 MMT2 and A-1830 sensor suite descriptions and specifications ..... 8

Table 2 Statistical analysis of MMT2 vs. A-1830 for the total June 2021 data set (21 days) ..... 15

Table 3 2021 Jun 06, MMT2 data sampled while cloud traversed site ..... 17

Table 4 Concurrent MMT2 and A-1830 data showing two 2021 Jun 20 cases of extreme SR contrasts caused by cloud shadowing ..... 19

Table 5 Sensor accuracy and cumulative MAE comparison ..... 21

Table C-1 2021 Jun 05, MMT2 vs. A-1830 statistical comparison ..... 62

Table C-2 2021 Jun 06, MMT2 vs. A-1830 statistical comparison ..... 62

Table C-3 2021 Jun 07, MMT2 vs. A-1830 statistical comparison ..... 63

Table C-4 2021 Jun 08, MMT2 vs. A-1830 statistical comparison ..... 63

Table C-5 2021 Jun 09, MMT2 vs. A-1830 statistical comparison ..... 63

Table C-6 2021 Jun 10, MMT2 vs. A-1830 statistical comparison ..... 64

Table C-7 2021 Jun 11, MMT2 vs. A-1830 statistical comparison ..... 64

Table C-8 2021 Jun 12, MMT2 vs. A-1830 statistical comparison ..... 64

Table C-9 2021 Jun 13, MMT2 vs. A-1830 statistical comparison ..... 65

Table C-10 2021 Jun 14, MMT2 vs. A-1830 statistical comparison ..... 65

Table C-11 2021 Jun 15, MMT2 vs. A-1830 statistical comparison ..... 65

Table C-12 2021 Jun 17, MMT2 vs. A-1830 statistical comparison ..... 66

Table C-13 2021 Jun 18, MMT2 vs. A-1830 statistical comparison ..... 66

Table C-14 2021 Jun 19, MMT2 vs. A-1830 statistical comparison ..... 66

Table C-15 2021 Jun 20, MMT2 vs. A-1830 statistical comparison ..... 67

Table C-16 2021 Jun 21, MMT2 vs. A-1830 statistical comparison ..... 67

Table C-17 2021 Jun 22, MMT2 vs. A-1830 statistical comparison ..... 67

Table C-18 2021 Jun 25, MMT2 vs. A-1830 statistical comparison ..... 68

Table C-19 2021 Jun 26, MMT2 vs. A-1830 statistical comparison ..... 68

Table C-20 2021 Jun 27, MMT2 vs. A-1830 statistical comparison ..... 68

Table C-21 2021 Jun 28, MMT2 vs. A-1830 statistical comparison ..... 69

## Acknowledgments

The authors wish to thank Mr Robert Brice for his work with the Meteorological Measurement Tripod instrumentation; the Army Test and Evaluation Command – Meteorology Department (Mr Blaine Thomas and Mr Scott Startz) for their provision of meteorological comparison data; and Mr John Raby for his consistently excellent technical reviews and meteorological insights. Finally, a special thanks goes to the DEVCOM ARL Technical Publishing Branch for its technical editing excellence, specifically to Ms Carol Johnson and Ms Jessica Schultheis.

## Executive Summary

Power diversity, as a strategy, has significant potential for reducing the vulnerability of remote-site electrical resource continuity. The integration of renewable energy, such as combining photovoltaic power with traditional generator and battery power resources, is just one application of this concept. Exploiting foreknowledge of meteorological conditions while employing atmospheric-dependent power resources can significantly advance hybridized power optimization. Applications of this work include both the tactical and disaster relief environments.

This report documents the findings of a two-part "Climate Impacts on Tactical Power Generation" project. In Part I (documented here), the foundational atmospheric data resource for a US Army Combat Capabilities Development Command Army Research Laboratory tactical hybrid-power research investigation was evaluated. This task also served to document foundational meteorological concepts needed for Part II (tactical climate applications).

The evaluated data included six key meteorological variables: pressure, temperature, relative humidity, solar radiation, wind speed, and wind direction. A description of what each variable represents, how they are sampled, their units, and a general description of their applications are provided, and set the study's foundation.

The two data sets being compared include these six atmospheric variables sampled from the Meteorological Measurement Tripod #2 (MMT2) and the A-1830. Both sensor suites were located in the desert southwest United States, and mounted on the same single-story, flat building roof (MMT2 on the north, center of the roof, and the A-1830 on the west side of the same roof). The suite sensors were calibrated within a similar time period, which prompted the following thesis: *A data comparison between the independently calibrated MMT2 and A-1830 sensor suites should yield extremely similar, if not overlapping, patterns. Any systematic differences between these calibrated sensors could be a function of the sampling site's atmospheric character.*

The study used 21 days of 2021 June data. The data preparation included a quality control assessment, timestamp check, and variable unit check. Before the comparison was initiated, the known systematic trends were addressed, such as all nighttime solar radiation (SR = 0 $W/m^2$), and "light and variable" wind data were removed.

Qualitative and quantitative analyses stemmed from daily and cumulative comparison scatter plots and statistical evaluations. By definition, A-1830 data

were labeled as “truth” in this comparison. The statistics calculated included the standard deviation, mean absolute error (MAE), mean bias error, and root mean square error. The percent of variable data used in the cumulative comparison review was also tallied.

The qualitative results showed the two sensor suites have strong agreement. Quantitative results confirmed the favorable findings and demonstrated significant impacts from local effects. For example, from the very few comparison-plot outlier points, one could see the effects of cloud shadowing over the individual data resources, even when only 30 m separated their locations.

The error analysis showed solar radiation to have the largest standard deviation and MAE; however, in the context of the variable’s maximum magnitude sampled, the spread was 4% of that max solar radiation value. In contrast, the wind speed showed a small standard deviation that was 38% of the maximum wind speed reported during the 21-day study.

Reviewing the sensor accuracy in the context of the MAE, most thermodynamic variables show an MAE less than the sensor accuracy. The two exceptions (relative humidity and wind speed) were explained. Relative humidity accuracy was defined for an environment at a single temperature. The relative humidity data represented samples taken from temperatures spanning a range of over 25 °C.

The wind speed exception was vindicated when a known building airflow pattern explained the systematic differences between sensors as a function of their specific locations. That is, sensors mounted above a flat roof center experience accelerated flow, and windward-mounted sensors respond to the flow rising up the windward wall and encountering a convergence with the horizontal flow across the roof.

In summary, the MMT2 and A-1830 sensor suite data comparison showed good agreement between resources, and systematic differences were indeed linked to the sampling site’s atmospheric character.

# 1. Introduction

Reducing the vulnerability of remote-site electrical resources can be accomplished through the advancement of power diversity. One method for reducing this susceptibility is by integrating renewable energy, such as photovoltaic (PV) power generation, with traditional generator and battery power resources. Optimizing the hybridized power requires current and future knowledge of atmospheric conditions, which is the focus of this research. Applications of this work include both the tactical and disaster relief environments.

## 1.1 Tactical Power Applications

Military operations require consistent and reliable power sources to maintain command and control centers, medical support, communication, weapons systems, and equipment. Offensive, defensive, and stability missions are reliant on access to electricity.

According to ATP 3-34.45 (HQDA 2018), a tactical power source refers to a source output of less than 200 V that is maintained by either a single unit or individual Soldiers. These electric power sources include generators, fuel cells, and hybrid power. Power storage is installed, operated, and maintained by individual units. Individual power sources, which are worn or carried, include batteries, fuel cells, small PV panels, and lightweight generators. Since they are for individual units, tactical power systems have limited capacity and distribution (HQDA 2018).

Given the independent and unpredictable nature of unit missions, mobility and detection are important factors when considering tactical electric power. DOD standard low-voltage mobile generators burn kerosene-based fuels. They can deliver power to single or multiple loads through spot generation, or to multiple loads when several power sources are connected through a distribution network. Despite the efficiency advantages, closely placed generators in distribution networks can emit electromagnetic, visual, auditory, and infrared signals. This detection vulnerability strengthens the argument for considering alternate power resources, or as a minimum, cover and concealment when planning tactical power distribution systems.

In addition to low-voltage generators, tactical environments can employ the use of fuel, fuel cells, and renewables. Fuel cells, like batteries, produce electricity through a chemical reaction. They are energy-dense, quiet, and release no harmful emissions. However, they must constantly be supplied with one-time-use materials. Examples of alternative renewable energy systems include solar, wind, and thermal energy. Hybridizing power into multiple, coherent integrated energy sources

reduces the reliance on batteries, and minimizes the dependence on one-time-use fossil fuels.

## 1.2 Disaster Relief Applications

Public Law 109-58 and the *Energy Policy Act of 2005* prompted a significant advancement in renewable energy research and technology (ACORE 2021). Since that time, there has been an active integration of the quickly improved and commercialized renewable energy technologies. For example, critical traffic controls, emergency message boards, and radio repeaters along evacuation routes are often seen powered by isolated PV panels. In Bayonne, New York, a commercial-scale hybrid (solar/diesel) backup system (installed in 2004) acted as a power source when Hurricane Sandy (an October 2012 event) caused the provision of local electricity to fail for an extended time. This same hurricane prompted New York City industry partners to collaborate on how to integrate the over 600 solar arrays functioning on city rooftops for any subsequent natural disaster.

By the mid-2010s, there were over 20 solar-powered community sirens (tornado warnings) and PV-powered meters monitoring river water levels for flooding in Florida. Working with the National Renewable Energy Laboratory, the Florida Solar Energy Center designed/built PV disaster trailers that provided electricity for disaster medical teams and so on. As the renewable energy technology advances, the need to optimize the integration in a way that the benefits outweigh the investment is the next phase (Vaucher 2016).

## 1.3 Climate Impacts on Tactical Power Generation

The title project, “Climate Impacts on Tactical Power Generation”, was designed as a two-part investigation. The long-term goal is to investigate how climate elements affect tactical power generation and operations. The Earth’s climate is always dynamic. This perpetually changing nature creates an ongoing challenge to electrical power generation planners, as well as managers of global operations. Consequently, there is a need to investigate environmental trends and patterns that can potentially become strengths and opportunities for various mission applications, such as tactical power generation.

With a focus on isolated, mobile, power production, Part I of this study concentrated on assessing and characterizing the primary meteorological variables used by climatologists. Phase II will focus on more specific climatological patterns and their potential tactical applications.

This report documents the initial phase. Six key meteorological variables and their character were examined in the context of an atmospheric data quality assessment. Understanding that each sampling location is unique, the general location chosen for this baseline study was southern New Mexico during the traditionally dry portion of the late spring/early summer time. In the next section, each of the variables investigated is described.

## 1.4 Meteorological Variables Used in This Study

Six meteorological variables were defined as relevant to the tactical environment. These parameters included four thermodynamic parameters—pressure (P), temperature (T), relative humidity (RH), solar radiation (SR)—and two dynamic terms—wind speed (WS) and wind direction (WD). Each variable is explained in the following sections.

### 1.4.1 Pressure

Pressure (P) is the defined as the force applied per unit area ("Pressure" n.d.). It is measured in pascals, bars, millibars, atmospheres, and newtons per meters squared ($N/m^2$). On a molecular level, this parameter can be visualized as the momentum transferred to a surface as molecules collide against it. The commonly used sensor is a barometer. Conventional barometers use the displacement of mercury against a marked tube to quantify P magnitudes. Current digital sensors convert output voltages to a P reading. In the atmosphere, sharp swings in P over a 24-h period are not typical—except when a cold/warm front passes over a sensor.

### 1.4.2 Temperature

Temperature (T) is defined as the average translational kinetic energy of the molecules in a body, and is used as a metric for hotness and coldness (Lower 2021). It is also used to indicate the direction in which heat energy will spontaneously flow. Colder temperatures are attributed to slower-moving molecules, whereas hotter temperatures are attributed to faster collisions. When molecules are moving with greater speeds, higher temperatures values are reported, along with more space between molecules. Conventional liquid thermometers exploit this characteristic. At high temperatures, the increased space between molecules results in material expansion. Conversely, materials reduce in size at colder temperatures. Mercury or alcohol enclosed within a marked glass tube expertly demonstrates these properties in a "thermometer" sensor. An alternative method for measuring T uses a digital temperature sensor, called a thermistor. Here, the resistance across a voltage drop is used to measure T. T is measured in units of Fahrenheit, Celsius, or Kelvin ("Temperature" n.d.).

### 1.4.3 Relative Humidity

RH is the "moisture content (i.e., water vapor and so on) of the atmosphere, expressed as the amount of moisture that can be retained by the atmosphere at a given temperature and pressure without condensation" (NWS 2009c). To quantify this value, RH is defined as the ratio between the water vapor present in the atmosphere and the amount of water vapor the atmosphere can retain (NWS 2009c), and is reported in units of percent:

$$\frac{Moisture\ Present}{Maxiumum\ Moisture\ Capacity} \times 100. \quad (1)$$

RH and T are inseparably linked. As previously mentioned, molecules at higher temperatures are moving with greater speeds, generating physical space between the molecules. The existence of more volume between molecules effectively increases the denominator of Eq. 1, resulting in a lower RH. At lower temperatures, where there is less space between molecules, a higher RH occurs. RH is measured using a hygrometer. Contemporary digital hygrometers, like the digital barometer, measure voltage change, which is then converted into a percentage measurement (NWS 2009c).

### 1.4.4 Solar Radiation

SR is the electromagnetic radiation emitted from the sun transmitted through the atmosphere to the surface. SR is sampled by a pyranometer and measure in watts per meters squared ($W/m^2$). The pyranometer uses a thermopile sensor that produces a response proportional to the sunlight it receives. The more sunlight, the hotter the sensor gets and the greater the current. The diurnal SR cycle is fairly consist in that when the sun is near the horizons (sunrise/sunset), SR values are near zero, and when the sun reaches its highest point (zenith), the sensor yields its maximum output. Electronically, the pyranometer produces a "cosine response", in that it varies with the cosine of the angle between the sun and zenith (Campbell Scientific, Inc. 2009).

### 1.4.5 Wind Speed and Wind Direction

WS describes the rate at which air is flows over a surface (NWS 2009e). WS is measured using an anemometer. A common sensor used is a cup anemometer. This instrument consists of cups attached to horizontal bars, which are connected to one vertical rod. As the wind blows, the cups respond by rotating around the rod. The number of rotations per unit time is correlated to the WS. Units of measure include knots, meter per second (m/s), and miles per hour.

WD is expressed as the direction from which air is flowing and is measured using cardinal degrees (NWS 2009d). WD units are based on a 360° compass, with north defined as 0° or 360°. Note: In meteorology, north is considered 0° or 360°, east is 90°, south is 180°, and west is 270°.

A common analog WD sensor is a weathervane, and often accompanies a cup anemometer. Weathervanes have an arrow that rotates over a vertical rod with four fixed cardinal directions representing north, south, east, and west positions on a center rod. With ambient air movement, the vane automatically points in the direction from which the wind is moving.

Examples of research-grade anemometers are wind monitors and sonic anemometers. The wind monitors appear as wingless aircraft with a propeller. The spinning propeller produces an AC sine wave signal, whose frequency is proportional to the WS.[*] The WD is determined by a 10K-ohm precision conductive plastic potentiometer. With a constant voltage applied to this potentiometer, the analog voltage output is directly proportional to azimuth angle. Visually, the miniaturized, wingless aircraft device responds to the flow of air by bringing the propeller into the wind and the tail downwind in the airflow. Thus, enabling the observer to validate the airflow orientation. The wind monitors used for this project are listed in Table 1 in Section 2.

The sonic anemometer (not part of this study) uses disturbances in sound waves to calculate the velocity of the wind. They require no moving parts and little physical maintenance (NWS 2009d; RM Young 2004; "Wind direction" n.d.).

## 1.5 Data Applications: Relevance to Larger Projects

The data used for this project were sampled by the Meteorological Measurement Tripod #2 (MMT2) sensor suite. The MMT2 resource services multiple applications from hazmat decision aids, to model development and "real time" operations. Multiple diagnostic and prognostic model development projects depend on these data as representative atmospheric descriptors and for building correlation relationships. Thus, its adherence to "truth" is critical. A model is only as good as the data used to develop it. (For more information on the MMT2, see Section 2.)

Tactical power optimization is another application, which leans heavily on the six atmospheric parameters selected for this study. Power optimization research relies on real-world atmospheric data to construct, improve, and test simulations against real-world conditions. Knowledge of current and future atmospheric conditions are

[*] Three sine wave signals are produced for each rotation.

key elements in the power optimization routines. (For more information on power optimization, see ARL-TR-9060 [Vaucher et al. 2020].)

Finally, the exercise of comparing sensors provides a foundational understanding for Part II of this project. By understanding the meteorological parameters and recognizing the regional atmospheric character, this knowledge will enable a richer understanding of longer-term climatic patterns for the studied environment. Extracting normal and unusual atmospheric behaviors relies on an informed perspective. This study provides an initial assessment reference.

# 2. Methods

This study was subdivided into three steps. First, meteorological data representing the six primary atmospheric variables were extracted from recently calibrated sensor time series. These data were used to characterize each parameter. Next, data from a second independently calibrated sensor suite located about 30 m from the first tripod were extracted and concurrent time series were compared. Finally, patterns and trends were noted in the context of the larger applications, such as those anticipated for Part II of the "Climate Impacts on Tactical Power Generation" project.

In this section, the atmospheric data sets and their preparations are described, followed by a summary of the sensor comparison techniques.

## 2.1 Data Resources

The primary data source was sampled by the Meteorological Measurement Tripod (MMT) sensor suite located in a southwestern New Mexico desert location. The MMT is also known as the "Local-Rapid Evaluation of Atmospheric Conditions (L-REAC®) Sensor Suite Module". The original purpose of this data resource was to serve as real-time atmospheric measurement input to an airborne hazard decision aid, designed and built by the US Army Combat Capabilities Development Command Army Research Laboratory (Vaucher 2011). The L-REAC® Sensor Suite Module system was temporarily relocated to "Site B", and the sensor suite name was changed to MMT. With the relocation, a dual-purpose was initiated. The "newly named" system output 1) continued as the real-time atmospheric data resource for L-REAC applications, and 2) provided 24/7 data for characterizing the ambient meteorological conditions for multiple projects, such as a tactical hybridized power optimization testbed.

A complete update to all the MMT sensors occurred in March 2021. Subsequent data files were labeled, "MMT2", to flag the new sensor hardware. A nearby Army

Test and Evaluation Command (ATEC) meteorological sensor suite, called the "A-1830", completed its periodic recalibration, prompting a DEVCOM Army Research Laboratory–ATEC collaboration based on the following thesis: S*ince both meteorological sensor suites underwent nearly coincident calibrations, a data comparison between the independently calibrated MMT2 and A-1830 should yield extremely similar, if not overlapping, patterns. This comparison could also reveal local forcing effects generated by the subtle sensor placement differences on the same rooftop.* To prove or disprove these concepts became one of the underlying goals of this study.

Both physical locations of the MMT2 and ATEC sensor suites were on top of the same one story building, situated in Tularosa Basin, New Mexico. Thirty meters separated the sensor stands (Fig. 1). The MMT2 was located at the north and center position of a nearly flat, rectangular roof. The ATEC sensors were located on the west side of this same roof, midway between the north-south edges. Aside: Prevailing winds for this site were primarily from the west and southwest quadrants. The roof's level positioned the sensors on the top side of the atmosphere's local canopy layer. No significant obstacles (trees, taller buildings, etc.) were nearby, only buildings of similar heights. To the west of this site (~16 km away) were the approximately 8000 ft tall, zagged Organ Mountains (Desert Peaks National Monument), which routinely cast shadows over the site near sunset. About 65 km (~40 miles) to the east, the Sacramento Mountains provided a near-horizontal silhouette during the pre-dawn hour.

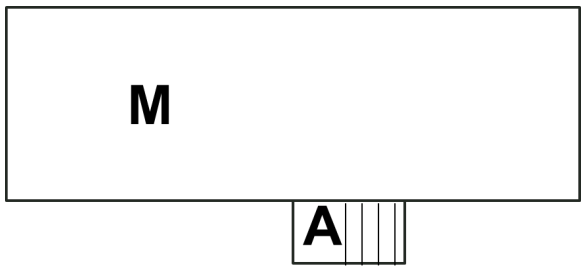


**Fig. 1 Top-down roof view of MMT2 (M) and A-1830 (A) locations on the nearly flat roof**

The specific height above the roof for each MMT2 and A-1830 sensor are shown in Table 1, along with the variable/sensor types, models, and units used. Comparing the two sensor suites, all sensors had closely aligned processes for acquiring the data, as well as equivalent potential capabilities.

**Table 1 MMT2 and A-1830 sensor suite descriptions and specifications**

| Variable | Sensor | Description | Units | MMT2 Sensor (Height above Roof) | A-1830 Sensor (Height above Roof) |
|---|---|---|---|---|---|
| **Pressure** | Barometer | Capacitive sensor measures amount of voltage to change current. Pressure measured using output voltage. | mb | Vaisala PTB110 (1 m) | Vaisala PTB110 (1 m) |
| **Temperature** | Thermometer | 2000mV excitation, measured voltage drop across resistor. Resistance used in Steinhart-hart equation to solve for temperature. | °C | Campbell Scientific T107 (0.7 m and 5.7 m) | Rotronics HC2-S3 (2 m) |
| **Temperature/ Relative Humidity** | Thermometer/ Hygrometer | Temperature measured with capacitive sensor. Relative humidity with resistive sensor. | °C and % | E+E Elektronik EE181 (2 m) | Rotronics HC2-S3 (2 m) |
| **Solar Radiation** | Pyranometer | For MMT2, PV sensor converts current to a voltage, and for A-1830, Thermopile heats up and temperature different is converted to voltage. | W/m$^2$ | Kipp/Zonen CMP3 (2 m) | Li-COR LI-200X (2 m) |
| **Anemometer** | Wind Speed/ Wind Direction | Propeller rotation produces AC sine wave with frequency proportional to wind speed. Output signal is an analog voltage proportional to wind direction. | m/s & degrees | RM Young 05305 (6 m) | RM Young 05305 (2 m) |

## 2.2 Data Preparation

Preparing the data for comparison consisted of extracting and analyzing two concurrent data sets. A total of 21 days of data, representing 2021 June 5–28, were evaluated. These 21 June days were chosen since they included a full or nearly complete 24 h of data.* The MMT2 sensor suite was defined as the "variable" in this comparison study, and the A-1830 data were labeled the "standard" or "truth".

All data were reported in 1-min intervals. Most MMT2 sensors collected data every 10 s, which were then averaged into one data output per minute. Other sensors simply sampled once per minute. The net result was that each data file consisted of a full day's worth of 1-min samples, or 1440 lines of data, as validated by Eq. 2:

$$\frac{1\ data\ point}{1\ minute} \times \frac{60\ minutes}{1\ hour} \times \frac{24\ hours}{1\ day} = \frac{1{,}440\ data\ points}{1\ day}. \quad (2)$$

### 2.2.1 Data Quality Control Assessment

Examining 1-day periods, each time series was checked for data anomalies. The few found were evaluated on a case-by-case basis. Where the irregularity was extensive and its cause explainable, the anomaly period was extracted from both data resources to preserve the 1-to-1 comparison, for example, the following:

* As part of the data preparation, the rare missing data were identified, investigated, and a cause determined. The handling of the three missing data points is discussed in Section 2.2.1.

1) **Daily Shadow Effects**: For all 21 days of this study, the A-1830 measurement for SR abruptly decreased at about 0830 Mountain Standard Time (MST) and returned to "normal" values around 0900 MST. Based on correspondence with the A-1830 data managers, it was determined that this daily SR drop and recovery was the result of a local shadow passing over the A-1830 pyranometer during the month of June. Given the consistent nature of this event, the 31-min time interval was defined as an explainable systematic occurrence that did not represent the local climate. Therefore, these 31 data points were removed from both the A-1830 and MMT2 data time series and were not included in the statistical analysis.

   The impact of removing these values is seen in a scatter plot of concurrent MMT2 versus A-1830 pyranometer values (Fig. 2). On the left graph, the 2021 Jun 05 scatter plot includes the 31 data points between 0830–0930 MST. On the right side, the 31 points are removed. The artificial concentration of points around 700–800 W/m$^2$ on the MMT2 axis (shown in the left plot with a red circle) is removed. The error calculations produced by the absence of these points, became more consistent with historical local climate expectations. Aside: The shadow effect appears as a square wave in the daily time series (Fig. 3).

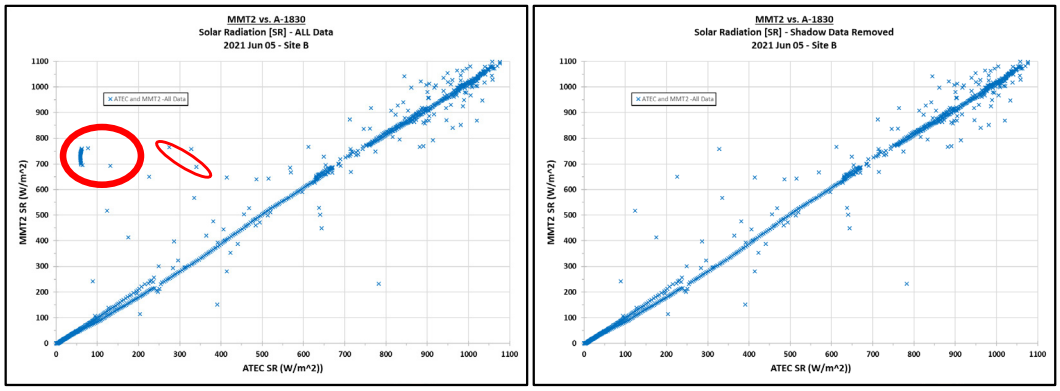


**Fig. 2 SR scatter plots with (left) and without (right) the daily local shadowing event. Points removed are circled in red.**

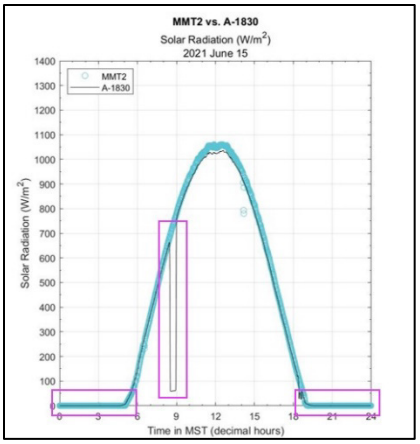


**Fig. 3 2021 Jun 15, MMT2/A-1830 SR data. Pink boxes show the nighttime and routine sensor shadowing data**

2) **Missing Data**: As part of the data preparation, each file was checked for containing exactly 1440 data lines (see Section 2.2). If the number of lines was fewer, the missing data were noted and examined for its impact.

   To enable the two-data-set comparison, the MMT2 and A-1830 sensor suites must have a measured value for each variable at every minute. There were three instances where one of the comparison files was incomplete; one variable entry was missing. To maximize the statistical analysis, a linear average was employed to create the missing single point, without significantly biasing the statistical results. The three missing points included the following:

   a. A-1830 SR: 2021 Jun 12 (Julian Day 163), 1402 MST.

      The A-1830 SR value for 2021 Jun 12, 1402 MST, was missing. Consequently, the A-1830 SR values at 1401 MST (954 $\frac{W}{m^2}$ ) and 1403 MST (951.2 $\frac{W}{m^2}$ ) were averaged. The result (952.6 $\frac{W}{m^2}$) was assigned to the A-1830, 2021 Jun 12, 1402 MST data point.

   b. MMT2 Temperature: 2021 Jun 22 (Julian Day 173), 1433 MST.

      The MMT2 temperature sample for 2021 Jun 22, 1433 MST, was missing. MMT 1432 MST (34.68 °C) and 1434 MST (34.62 °C) were averaged; and the result (34.65 °C) was set as the missing temperature for 1433 MST.

   c. MMT2 Temperature: 2021 Jun 27 (Julian Day 178), 1157 MST.

      One MMT2 temperature sample was missing. MMT2 1156 MST (23.87 °C) and 1158 MST (23.35 °C) were averaged, with the result

(23.61 °C) being assigned to the missing MMT2 temperature for 2021 Jun 27, 1157 MST.

### 2.2.2 Timestamp Check

With the data anomalies identified and resolved, the comparison method sought to confirm that each data resource represented the same 1-min moment in time. MST (a.k.a. "sun time") was selected for the common time zone unit. Using sun time generally allows the zenith (highest) sun position for the day to occur at or near midday.

A calibrated, common time resource between the two sensor suites was investigated. The sensors suites' automated timestamps were taken from their supporting computer clocks. These computer clocks were routinely updated through internet resources. The findings implied that the timestamp source for both data sets were calibrated from this same precise atomic clock, namely, the US Naval Observatory Atomic Clock.

All time data were converted into decimal hours. These units were chosen to enable a clear demonstration of the time series over a full 24-h cycle. The conversion program began with the original 2-digit time entry (hhmm), split the variable into hour (hh) and minutes (mm), and then calculated a decimal hour using the following equation:

$$Decimal\ Hours = hh + \left(\frac{mm}{60\ minutes/1\ hr}\right), \tag{3}$$

where hh is the number of hours on a 24-h clock, and mm is the number of minutes in a 60-min hour. As an example, hhmm = 0145, would be interpreted as 1 h and 45 min or,

$$1\ hour + \left(\frac{45\ minutes}{\frac{60\ minutes}{1\ hour}}\right) = 1.75\ decimal\ hours$$

The use of decimal hours enabled an easier visualization of the 24-h pattern displayed from both weather stations.

### 2.2.3 Variable Unit Check

The meteorological variable units were examined for consistency. As explained earlier, each parameter had a variety of possible units. For example, T could be reported in degrees Celsius (°C), degrees Fahrenheit (°F), and Kelvin (K). For this study, all T quantities were stored as °C. For the other variable units, see Table 1.

## 2.3 Pre-Analysis Data Preparations

Once the data quality was addressed, the preparation phase pursued the removal of all known systematic patterns that might distract or inhibit a fruitful analysis. Two of these patterns included nighttime SR values (0 W/m$^2$) and "light and variable" wind conditions. Both are described in next sections.

### 2.3.1 Nighttime Solar Radiation

SR measurements were sampled 24/7. Before sunrise and after sunset, all SR values were 0 W/m$^2$. Nighttime sensor results reporting SR less than 0 were understood as normal sensor noise and reset to 0 W/m$^2$. To simplify the numeric analysis, only daylight (nonzero) data were considered. There were no cases where both SR sensors reported zero values during daylight hours (i.e., solar eclipse). Figure 3 demonstrates the pre-sunrise and post-sunset portions of the SR time series. The routine A-1830 sensor shadowing data (black line, square wave shape) are also notated on this graphic.

### 2.3.2 Light and Variable Wind Conditions

WS and WD presented a unique challenge for the statistical analysis. When WSs are less than 6 kt, or 3.09 m/s (NWS 2021e), they are considered "light (WS) and variable (WD)". This natural random variability in the WD justified the exclusion of any wind data when the WS value was below the 3.09-m/s threshold. Figure 4 demonstrates the light and variable character of WS and WD above and below the threshold over the A-1830 site on 2021 Jun 05. The red line signifies the threshold WS value. Figure 5 shows a WS comparison of the two sensor suites for this same day.

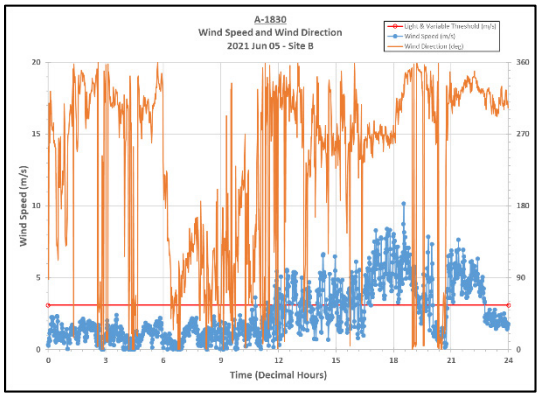


**Fig. 4 Light and variable winds at the A-1830 site, on 2021 Jun 05. Threshold value is 3.09 m/s.**

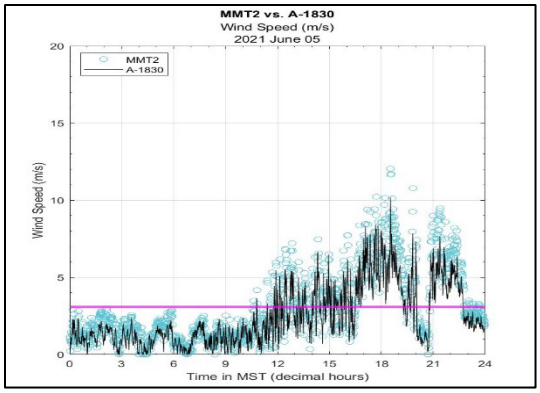


**Fig. 5 2021 June 05 WSs sampled by the MMT2 and A-1830 anemometers. The pink line is the light and variable threshold.**

## 2.4 Data Comparison Program

A MATLAB program was developed to facilitate the MMT2 versus A-1830 data comparison. This program included elements of both the data preparation and pre-analysis techniques. This program read the data files, verified time step alignment, identified missing data locations, performed applicable data quality control, and generated plots for each of the meteorological variables. The code also presumed that the nighttime SR values (0 $W/m^2$) were removed, as were the "light and variable" wind conditions. The results of this program were used as informational resources for both a qualitative and quantitative data comparison, which is described in the next section.

## 2.5 Analysis: Sensor Comparison Techniques

The analysis tools used to capture the similarities and contrasts between the two independent meteorological data resources were divided into two techniques: a qualitative data comparison and a quantitative data comparison.

### 2.5.1 Qualitative Data Comparison

The qualitative data comparison focused on whether one sensor's time series tended to report higher or lower values than the other. It looked at the trends found under clear and cloudy skies, as well as the nighttime versus daytime conditions. These observations were confirmed after the differences between concurrent sampling were also evaluated.

### 2.5.2 Quantitative Data Comparison

The quantitative data comparison focused on statistically describing the difference between concurrent sampling. The statistical parameters reported included standard

deviation, mean bias error (MBE), mean absolute error (MAE), and root mean squared error (RMSE).

The standard deviation captured the variation about the mean differences. Whereas the MBE showed the overall over- or underestimation of differences from the "truth" system. The MAE provided a measure of how close the variable sensor was to the "truth" sensor, irrespective of an over/underestimation. The RMSE reported absolute difference between the measured value and the "true" value.

## 3. Results and Discussion

The original thesis was that a data comparison between the independently calibrated MMT2 and A-1830 sensor suites should yield extremely similar, if not overlapping, patterns. Also, any systematic differences between these calibrated sensors could help to define the atmospheric character of the sampling site.

As described earlier, this study generated individual plots for 21 days of 2021 June data. The raw data figures are included in Appendix A. Their corresponding two-site comparison scatter plots and error analyses are included in Appendixes B and C, respectively. In addition to the daily figures, all the data files were compiled into a single, cumulative resource from which statistics representing the entire 21 days were calculated. Figures 6 and 7 show the amalgamated scatter plots of the thermodynamic and dynamic variables, respectively. A statistical description of this cumulative data resource is tabulated in Table 2. A hand-calculation, verifying the selected statistical functions used in the numerical analyses, is found in Appendix D.

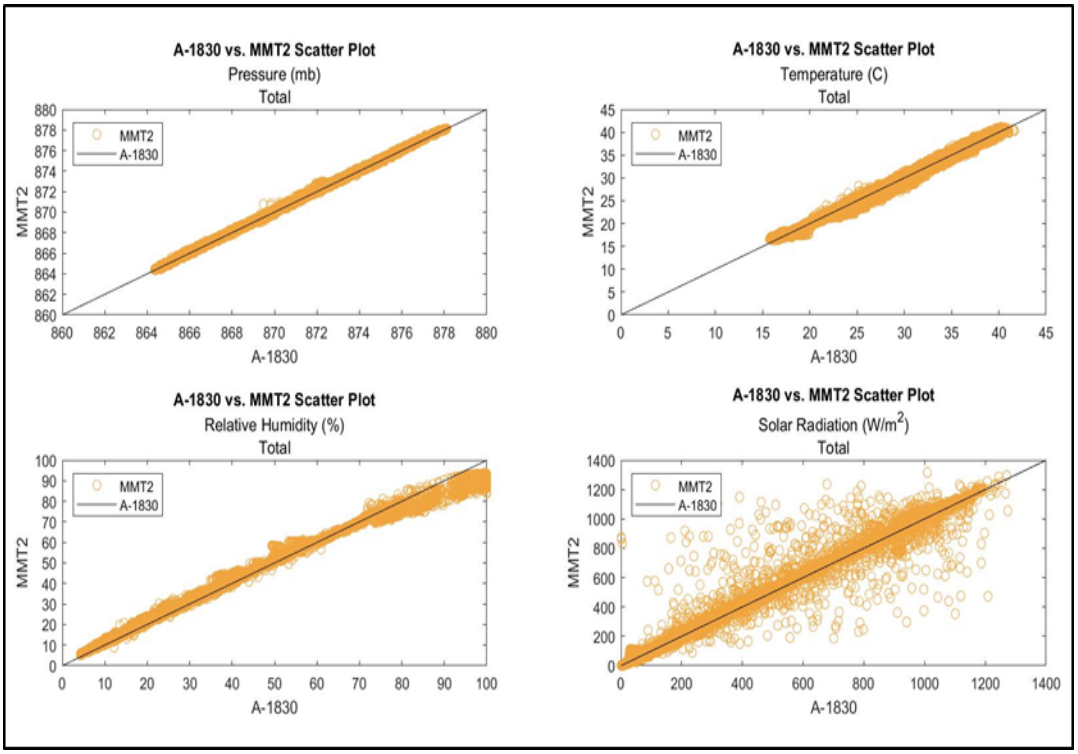


**Fig. 6 Total data set scatter plots comparing MMT2 and A-1830 thermodynamic data**

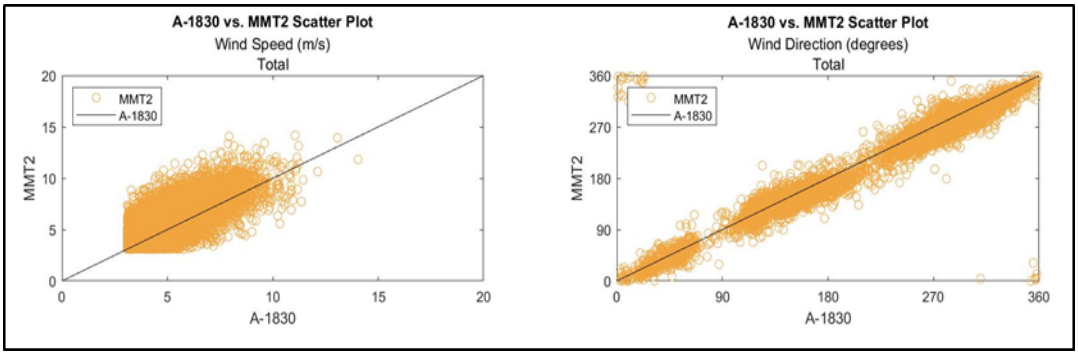


**Fig. 7 Total data set scatter plots comparing MMT2 and A-1830 dynamic data**

**Table 2 Statistical analysis of MMT2 vs. A-1830 for the total June 2021 data set (21 days)**

| 2021 Jun 05–28 (21 days of data) | STD | MAE | MBE | RMSE | Percent of data included |
|---|---|---|---|---|---|
| **P (mb)** | 0.52 | 0.13 | 0.51 | 0.12 | 100 |
| **T (°C)** | 0.42 | 0.31 | 0.42 | 0.07 | 100 |
| **RH (%)** | 2.29 | 1.71 | 2.05 | 1.02 | 100 |
| **SR ($\frac{W}{m^2}$)** | 52.95 | 22.27 | 52.04 | 9.77 | 57 |
| **WS - u (m/s)** | 5.74 | 4.57 | –0.012 | 5.74 | 40 |
| **WS – v (m/s)** | 5.70 | 4.54 | 0.07 | 5.70 | 40 |

## 3.1 Qualitative Analyses/Results

Reviewing the cumulative scatter plots qualitatively, all variables show the bulk of the coincident MMT2 and A-1830 data fell around the perfect agreement, the diagonal line. This observation favorably re-enforces the main concept of the thesis. Examining the data more closely, the following observations were gleaned:

- *P and T*: MMT2 versus A-1830 P and T plots show good agreement, staying within their respective ranges.
- *RH*: For the 0% to 70% RH range, MMT2 reports higher RH than A-1830. The 60%–75% RH range has a tight RH match. In the 70%–100% range, MMT2 underestimates RH with respect to the A-1830 sensor (i.e., A-1830 is higher than MMT2).
- *SR*: The SR plot has strong agreement between pyranometer sensors and a wider overall spread than the other thermodynamic variables. The daily max/min values appear to be consistent between both systems. Several extreme-contrast cases were observed from the cumulative comparison plots. These are elaborated on in Section 3.2.
- *WS*: The truncated appearance of WS values is a result of the exclusion of "light and variable" winds. Both systems reported maximum WS around 15 m/s, with the bulk of the high WS magnitude around 10 m/s. The MMT2 WS showed a tendency toward higher magnitudes than the A-1830 values. A reason for this characteristic is likely a function of the natural local wind flow patterns, which is explained in Section 3.2.
- *WD*: Both MMT2 and A-1830 showed the 0° and 360° north references linked. A tri-modal grouping of WD was apparent in the 21-day accumulation of values:
    - Group 1 ranged from 0° to 90°, with a waning of data count around 90º.
    - Group 2 spanned 91°–220°, as the data population thinned at 220°.
    - Group 3 covered the 221°–360° interval, with the 360°/0° direction showing a smaller number of data points.

  The question still to be resolved is whether this three-group pattern in June is "real" for all the surrounding Tularosa Valley or if it is a local effect. Another observation is the tendency for the MMT2 WD magnitudes to be less than the A-1830 WD values. This curious pattern is explored in a later section.

## 3.2 Quantitative Analyses/Results

Reviewing the results quantitatively exposed both site-specific characteristics and atmospheric event correlations. The examples that follow start with investigating variable outliers and conclude with a closer look at the tabulated statistical results.

### 3.2.1 SR Outliers, a Function of Cloud Shadow Timing

The atypical SR data in the cumulative comparison plots reveals the significant impact of local cloud shadowing. For example, the SR cumulative comparison showed an MMT2 point in the 300 W/m$^2$ range, while the A-1830 value was in the 1100 W/m$^2$ range. Another contrasting point placed the MMT2 at approximately 900 W/m$^2$, while A-1830 reported a value of approximately 200 W/m$^2$. To explain these patterns, the SR response to cloud cover needs to be examined. Consider the 2021 Jun 06, 1437–1446 MST case.

Table 3 shows the 10-min extraction of MMT2 data for 2021 Jun 06, 1437–1446 MST. The MMT2 data start and end with SR in the 815-860 W/m$^2$ range (a reasonable clear sky value for that time of day. When the cloud overshadows the sensor, the change in SR (Delta SR) plummets quite quickly. Between sample 1438 MST and 1439 MST, the SR value drops 60%, or 446 W/m$^2$, in just 1 min! This means that if one sensor was in the sun and the other was not, the SR values could report significantly different magnitudes yet both be documenting "truth" for their location. Based on the 21 days of data reviewed, a 30-m separation is far enough to capture some of these contrasting occurrences.

**Table 3 2021 Jun 06, MMT2 data sampled while cloud traversed site**

| Line (#) | Julian Day (2021 Jun 6) | Time (hhmm) | SR (W/m2) | Delta SR (W/m2) | Pressure (mb) | WS (m/s) | WD (degrees) |
|---|---|---|---|---|---|---|---|
| 1 | 157 | 1437 | 856 | N/A | 865.49 | 5.1 | 280 |
| 2 | 157 | 1438 | 747 | -109 | 865.49 | 5.8 | 263 |
| 3 | 157 | 1439 | 301 | -446 | 865.46 | 5.4 | 264 |
| 4 | 157 | 1440 | 201 | -100 | 865.36 | 6.6 | 251 |
| 5 | 157 | 1441 | 204 | 3 | 865.43 | 4.7 | 258 |
| 6 | 157 | 1442 | 227 | 23 | 865.46 | 9.0 | 263 |
| 7 | 157 | 1443 | 250 | 23 | 865.54 | 7.4 | 276 |
| 8 | 157 | 1444 | 374 | 124 | 865.49 | 5.5 | 270 |
| 9 | 157 | 1445 | 446 | 72 | 865.50 | 5.3 | 275 |
| 10 | 157 | 1446 | 817 | 371 | 865.43 | 4.5 | 249 |

In the cumulative SR scatter plot (Fig. 6), the graph starts with two outliner cases where the A1830 and MMT2 sensors show extreme contrasts in magnitudes. In both cases, the A-1830 sensor reported near 0 W/m$^2$ and the MMT2 sample was in the 800-W/m$^2$ range. After investigating these cases, both cases were found to occur on 2021 Jun 20 (Fig. 8*). Observing the SR time series at 1424 MST, the A-1830 and MMT2 values were 0 and 887 W/m$^2$, respectively. The other event occurred at 1500 MST, where the A-1830 and MMT2 values were 0.7 and 873 W/m$^2$ (Fig. 8). The consistent saw-tooth time series surrounding these events and reported by both SR sensors (Table 4) is a clear indication that clouds were occulting the sun, as they passed over the site. The occasional reduced SR magnitude discrepancies between the two sensors indicate a spatial dependency in the cloud shadow effect. That is, one sensor was reporting from a darker region than the other sensor. As to the cause for the extreme SR data point outliers (dropping to 0 W/m$^2$), based on the A-1830 sensors' height above the roof, this reported sample was likely caused by a bird resting on the shaded sensor for the 1-min sampling time period. While a 1-min period may seem like a long time for resting wildlife, in the June desert heat, an unchallenged shaded area is valued by most living creatures. Thus, the interpretation is reasonable.

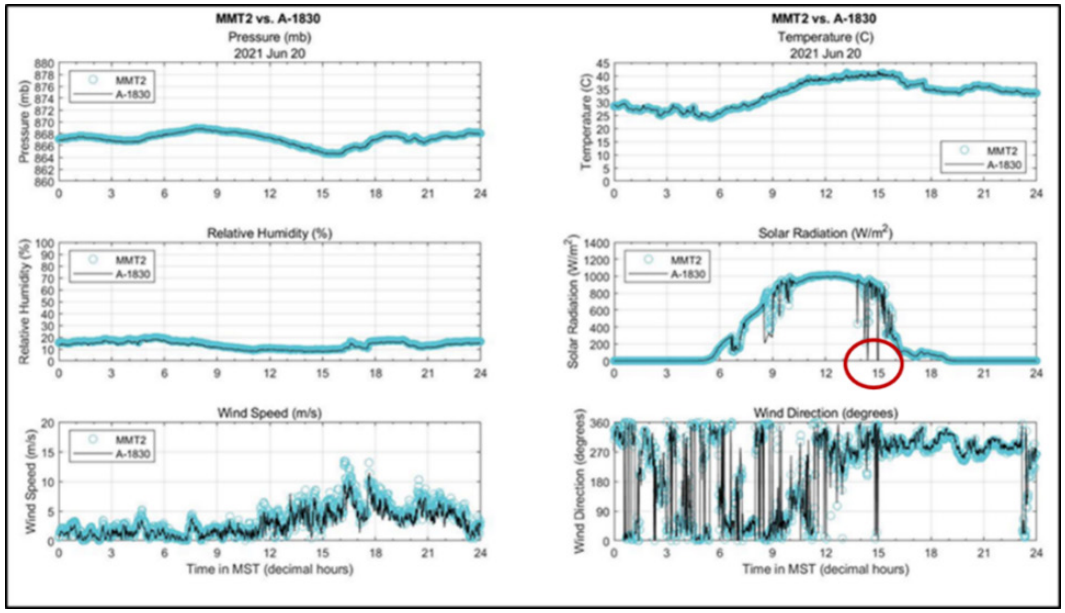


**Fig 8 MMT2 and A-1830 data for 2021 Jun 20. Red circle notes the (A-1830, MMT2) contrasting SR values cause by local cloud cover.**

* Figure 8 is Fig. A-5 with the area of interest highlighted in a red circle.

**Table 4 Concurrent MMT2 and A-1830 data showing two 2021 Jun 20 cases of extreme SR contrasts caused by cloud shadowing**

**A-1830 was in shadow; MMT2 in sunlight**

**(A-1830, MMT2) = (0 W/m², 887 W/m²)**

| A-1830, Date/Time | P (mb) | T(C) | RH(%) | WS(m/s) | WD(deg) | SR(W/m^2) |
|---|---|---|---|---|---|---|
| 6/20/2021 14:22 | 865.32 | 39.65 | 8.11 | 0.37 | 344 | 930.2 |
| 6/20/2021 14:23 | 865.34 | 40.24 | 7.95 | 0.55 | 278 | 360.5 |
| 6/20/2021 14:24 | 865.35 | 40.99 | 7.66 | 1 | 333 | 0 |
| 6/20/2021 14:25 | 865.27 | 41.13 | 7.62 | 1.23 | 316 | 86.5 |
| 6/20/2021 14:26 | 865.11 | 40.79 | 7.74 | 4.93 | 329 | 362.6 |
| 6/20/2021 14:27 | 865.27 | 40.01 | 8.01 | 4.68 | 272 | 391.2 |
| 6/20/2021 14:28 | 865.25 | 39.88 | 8.07 | 2.41 | 287 | 887.7 |
| 6/20/2021 14:29 | 865.2 | 39.97 | 8.06 | 4.97 | 323 | 954 |

| MMT2-JD 171, Time (hhmm) | P (mb) | T(C) | RH(%) | WS(m/s) | WD(deg) | SR(W/m^2) |
|---|---|---|---|---|---|---|
| 1422 | 865.38 | 39.15 | 9.16 | 1.994 | 202.3 | 934 |
| 1423 | 865.31 | 39.39 | 9.16 | 0.363 | 197.5 | 928 |
| 1424 | 865.36 | 39.78 | 9.16 | 1.945 | 336.2 | 887 |
| 1425 | 865.37 | 39.97 | 9.17 | 1.949 | 334.6 | 573.3 |
| 1426 | 865.31 | 40.02 | 9.16 | 3.087 | 326.8 | 457.4 |
| 1427 | 865.27 | 39.91 | 9.23 | 5.467 | 316.6 | 555 |
| 1428 | 865.28 | 39.74 | 9.16 | 4.149 | 266.6 | 461.3 |
| 1429 | 865.28 | 39.5 | 9.23 | 3.523 | 290.1 | 932 |

**(A-1830, MMT2) = (0.7 W/m², 873 W/m²)**

| A-1830, Date/Time | P (mb) | T(C) | RH(%) | WS(m/s) | WD(deg) | SR(W/m^2) |
|---|---|---|---|---|---|---|
| 6/20/2021 14:55 | 864.89 | 39.88 | 8.25 | 1.25 | 19 | 868.2 |
| 6/20/2021 14:56 | 864.88 | 40.3 | 8.09 | 1.21 | 278 | 863.3 |
| 6/20/2021 14:57 | 864.88 | 40.97 | 7.85 | 1.07 | 337 | 164.6 |
| 6/20/2021 14:58 | 864.87 | 41.68 | 7.56 | 2.33 | 322 | 1.4 |
| 6/20/2021 14:59 | 864.9 | 41.58 | 7.55 | 1.92 | 3 | 4.9 |
| 6/20/2021 15:00 | 864.89 | 41.45 | 7.66 | 2.76 | 328 | 0.7 |
| 6/20/2021 15:01 | 864.76 | 41.45 | 7.58 | 4.03 | 346 | 442.8 |
| 6/20/2021 15:02 | 864.75 | 40.33 | 8.04 | 3.71 | 342 | 800.5 |
| 6/20/2021 15:03 | 864.75 | 40.14 | 8.17 | 2.56 | 315 | 868.2 |

| MMT2-JD 171, Time (hhmm) | P (mb) | T(C) | RH(%) | WS(m/s) | WD(deg) | SR(W/m^2) |
|---|---|---|---|---|---|---|
| 1455 | 864.94 | 39.53 | 9.62 | 1.725 | 24.86 | 881 |
| 1456 | 864.91 | 39.7 | 9.49 | 0.779 | 346.9 | 873 |
| 1457 | 864.9 | 40.01 | 9.36 | 2.164 | 322.5 | 871 |
| 1458 | 864.89 | 40.16 | 9.23 | 2.919 | 349.3 | 865 |
| 1459 | 864.91 | 40.03 | 9.36 | 4.168 | 346.1 | 834 |
| 1500 | 864.9 | 40.16 | 9.23 | 2.605 | 351 | 873 |
| 1501 | 864.88 | 40.12 | 9.23 | 5.674 | 322.5 | 890 |
| 1502 | 864.88 | 39.47 | 9.42 | 4.843 | 328.8 | 892 |
| 1503 | 864.87 | 39.38 | 9.58 | 4.671 | 323.7 | 893 |

### 3.2.2 Skewed WS Comparison Reveals Site Character

The MMT2 wind speeds showed a tendency toward higher magnitudes than the A-1830 values (Fig. 7). This slightly skewed nature may be a function of the roof sensor placement. The MMT2 instrument was centered on the roof, and the A-1830 was mounted on the windward building edge. Based on published NOAA wind tunnel building flow studies, a sensor mounted above the roof center (MMT2) will encounter accelerated velocities. A sensor on the roof's upwind building side (A-1830) will experience the vertical winds scaling the side of the building and a confluence flow at the edge of the building side and rooftop, as shown in Fig. 10 (Vaucher 2011). Both anemometers acquired 2-D WS samples. Resolving the systematically slower velocities of the A-1830 sensor might be done better, if 3-D wind sensors were employed in both locations. Another approach for the future is to reanalyze the WS data, as a function of wind direction.

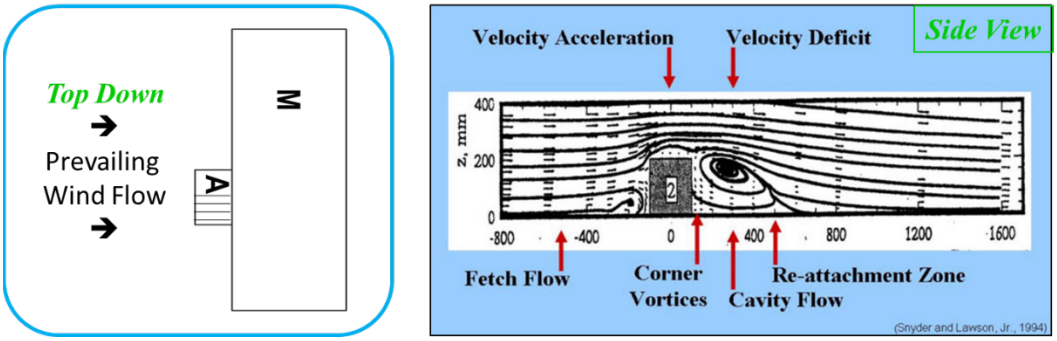


**Fig. 10 Cumulative WS comparison trend reinforces 1994 NOAA wind tunnel, building airflow pattern findings. From Snyder and Lawson (1994) and/or Vaucher (2011, Fig. 1).**

### 3.2.3 WD Comparison Implies Site Airflow Character

In Fig. 7, the WD scatterplot shows a pattern of MMT2 magnitudes being slightly "less than" the A-1830 magnitudes. Because the magnitudes represent a directional orientation, this pattern needs to be examined in the context of a compass. In other words, the MMT2 directions are frequently skewed counterclockwise relative to the A-1830 directions. In meteorological terms, this shift in direction is called a "backing" and a clockwise directional shift would be "veering".

Since the two sensors are technically at different heights with the MMT2 above the A-1830 sensor, the observation is reworded in the context a vertical profile, starting with the lower sensor: Airflow over the common building shows a "backing" difference between the A-1830 and MMT2 sensor heights and locations. The mounted sensor height difference is relatively small, so the normal directional shear at low levels that is associated with tornadic development is not appropriate. However, the pattern is noteworthy in the context of the local building effect (NWS 2009a, 2009b).

### 3.2.4 Error Analysis in Context

The scatter plots coupled with the corresponding statistical analyses characterize the MMT2 sensors with respect to the A-1830 sensor suite. However, it is important to put the error magnitudes in perspective with their respective populations and their sampled magnitudes.

The greatest standard deviation and MBE was from the SR sensor. This attribute is confirmed with the SR scatter plot that shows a visually wider spread of cumulative, coincident SR values (Fig. 6). Specifically, the standard deviation and MBE was about 52 W/m$^2$. In the context of SR magnitude range expected for the given data set, the (A-1830) SR maximum value was about 1350 W/m$^2$. This means that the

SR "spread" represents slightly less than 4% of the maximum potential radiation range sampled and is not necessarily a significant concern.

In contrast, the WS components have an average standard deviation of 5.7 m/s. The maximum WS measurement was about 15 m/s; thus, this standard deviation represents 38% of the data range. This error is technically large, yet is also consistent with the local forcing effect impacts, as described earlier.

### 3.2.5 Sensor Accuracy Reviewed

The MAE for each variable was compared to the sensor accuracy, as defined in their respective sensor manuals. Table 5 shows the results.

**Table 5 Sensor accuracy and cumulative MAE comparison**

| Variable | Sensor accuracy | MAE |
|---|---|---|
| **P** | ±0.6 mb between 0 and 40 °C | 0.13 mb |
| **T** | ±0.4 °C between –24 to 48 °C | 0.31 °C |
| **RH** | ±0.8% RH at 23 °C | 1.71% |
| **SR** | ±0.5% max | 22.27 $\frac{W}{m^2}$ (1.6%) |
| **WS** | ±0.3 m/s | 4.57 m/s |
| **WD** | N/A | N/A |

MAEs fall within the instrument's accuracy range for P, T, and SR. However, the errors were larger than the sensor accuracy for RH and WS. Note: The RH accuracy was determined for an environment whose temperature was 23 °C. The MAE for these 21 days represents RH for environments having temperatures between 15 and 43 °C. This context could explain the larger MAE. The much larger WS MAE value is likely a function of the systematic influence of local building airflow, as explained earlier.

## 3.3 Climatological Patterns from the Statistical Analyses

The percent of data used for the error analyses was included in Table 2. This tally provided subtle comments on the climatological character of the site.

For example, at this location, during the month of June, about 60% of WSs fell below the threshold for "light and variable" winds. This implies a predominance of calm conditions during the June month. Examining the daily results shows that June's tendency for calm conditions also includes contrasting extremes: On June 6, 90% of the WSs were above the threshold (a windy day), and on June 28, 1% was above the threshold (extended calm).

Regarding the reduced number of SR data points, this result is easily explained by recalling that all nighttime data were removed. The summer solstice (one of the longest sunlight days) occurs in June. Based on the SR percent data used, one might say that about 57% of the total June hours experienced sunlight at the sampling site. It would be interesting to conduct another study with December data (winter solstice/shortest day) to complete the climatological outline of daylight hours reported over this site for a single year.

## 4. Summary and Conclusions

Advancing power diversity has the capacity for reducing the vulnerability and interruptions of isolated electrical grids. The value-added by integrating renewables, such as combining PV, and traditional power resources, is strengthened with the foreknowledge of meteorological conditions. This report documents the first of a two-part "Climate Impacts on Tactical Power Generation" project. The results establish a foundational atmospheric data resource for a DEVCOM ARL tactical hybrid-power research investigation, along with the follow on, "Climate Impacts on Tactical Power Generation", Part II (tactical climate applications).

Six key meteorological variables (P, T, RH, WS, WD, and SR) were reviewed regarding what the variables represent, how they are sampled, their units, and general descriptions of their applications. Two co-located data resources (MMT2 and A-1830) containing these six variables were compared based on the thesis: *A data comparison between the independently calibrated MMT2 and A-1830 sensor suites should yield extremely similar, if not overlapping, patterns. Any systematic differences between these calibrated sensors could be a function of the sampling site's atmospheric character.* The study used 21 days of 2021 June data. Data preparation was discussed in Section 2, along with the extraction of known systematic trends, such as nighttime SR and "light and variable" wind.

Qualitative and quantitative data analyses stemmed from daily and cumulative comparison scatter plots and statistical evaluations. With A-1830 data labeled as "truth" for this comparison, "error" statistics were calculated. Percent of variable data used was also included in the tabulated daily and cumulative results.

Strong agreement was concluded from the qualitative assessment. Quantitative analyses confirmed the favorable findings. Local effects were evident in the very few comparison-plot outlier points. Cloud shadowing over the individual data resources, even when separated by only 30 m, explained the rare SR data variations. The slightly skewed nature of the WS comparison was understood to be a function of the normal local building flow patterns. The statistical results showed most variables to be within the sensor accuracy. RH fell outside the threshold, but, in the

context of its single T environment, versus the 21 days of multiple T environments, the results were accepted. The WS results exceeding the sensor accuracy were linked to the local building flow patterns—and accepted as explainable.

In summary, the MMT2 and A-1830 sensor suite data comparison showed good agreement between resources, and systematic differences were linked to the atmospheric character of the sampling site.

## 5. Future Climate Impacts on Tactical Power Generation, Part II

"Climate Impacts on Tactical Power Generation" Part II will focus on the tactical climate applications. In preparation for that investigation, four "lessons learned" are highlighted:

- *P and T*: P and T aligned well in the comparison; instilling confidence in the measurements. RH difference were explainable; however, for extra confidence, extracting RH while the environment was at 23 °C (the temperature used for calibrating the RH sensor) might be informative.
- *SR*:
    - SR was extremely sensitive to cloud cover; future comparisons might focus only on clear sky or fully overcast conditions.
    - As a climate exercise, examining SR as a function of WS and WD would also be educational.
- *WS comparison*:
    - WS comparison showed a clear skewed nature. This curious feature might be explored by employing 3-D wind sensors.
    - June reported a significantly large amount of "light and variable" periods. Repeating the comparison during a high-wind month might strengthen the comparison.
- *Climatology*: Finally, the study examined 21 days of June. The question remains, were the observed trends consistent with those of the larger climatological regional area (the Tularosa Valley, New Mexico)?

## 6. References


[ACORE] Selected US Department of Defense goals, priorities and requirements for renewable energy. American Council on Renewable Energy; c2021 [accessed 2015 May 14]. http://www.acore.org/dod-energy-goals.

Campbell Scientific, Inc. CMP3-L pyranometer instruction manual (rev 2/09). Campbell Scientific, Inc; c2009.

[HQDA]. ATP 3-34.45. Electric power generation and distribution. Headquarters, Department of the Army (US); 2018.

Lower S. 2.2: Energy, heat, and temperature. Chemistry LibreTexts; n.d. [last updated 2021 Mar 3; accessed 2021 Aug 13]. https://chem.libretexts.org/Bookshelves/General_Chemistry/Book%3A_Chem1_(Lower)/02%3A_Essential_Background/2.02%3A_Energy_Heat_and_Temperature.

[NWS] Backing [glossary entry]. National Weather Service; 2009a [updated 2009 June 25; accessed 2022 Feb 14]. https://forecast.weather.gov/glossary.php?letter=b.

[NWS] Relative humidity [glossary entry]. National Weather Service; 2009c [updated 2009 June 25; accessed 2021 Aug 13]. https://forecast.weather.gov/glossary.php?word=RH#:~:text=Relative%20Humidity%20%2D%20a%20dimensionless%20ratio,both%20moisture%20content%20and%20temperature.

[NWS] Veering [glossary entry]. National Weather Service; 2009b [updated 2009 June 25; accessed 2022 Feb 14]. https://forecast.weather.gov/glossary.php?letter=v.

[NWS] Wind direction [glossary entry]. National Weather Service; 2009d [updated 2009 June 25; accessed 2021 Aug 13]. https://forecast.weather.gov/glossary.php?word=wind%2Bdirection.

[NWS] Wind speed [glossary entry]. National Weather Service; 2009e [updated 2009 June 25; accessed 2021 Aug 13]. https://forecast.weather.gov/glossary.php?word=Wind%2BSpeed.

RM Young. Meteorological instruments, instructions, wind monitor, model 05103L (Rev H102811). RM Young Company; 2004.

Pressure. Encyclopedia Britannica, Inc.; n.d. [accessed 2021 Aug 13]. https://www.britannica.com/science/pressure.

Snyder W, Lawson R Jr. Wind-tunnel measurements of flow fields in the vicinity of buildings. 8th Conference on Applied Air Pollution Meteorology with A&WMA; 1994 Jan; Nashville, TN. AMS; Boston. p 244–250.

Temperature. Encyclopedia Britannica, Inc.; n.d. [accessed 2021 Aug 13]. https://www.britannica.com/science/temperature.

Vaucher G, Berman M, Parker G, Lee M, D'Arcy S, Jane R, Price T. In-situ atmospheric intelligence for hybrid power grids: volume 2 (automated data flow tests). CCDC Army Research Laboratory (US); 2020 Sep. Report No.: ARL-TR-9060.

Vaucher G. Atmospheric input for renewable energy microgrids (educating 'smart grids'). 7th Conference on Weather, Climate, Water and the New Energy Economy and 2nd Conference on Applied Climatology; Session: Adapting to Climate Variability and its Impacts on Energy Sector Resilience, Part 1; American Meteorological Society Annual Meeting, 2016 Jan 13.

Vaucher, G. Local-Rapid Evaluation of Atmospheric Conditions (L-REAC) system, volume 4 (system evaluation). Army Research Laboratory (US); 2011 Dec. Report No.: ARL-TR-5848.

Wind direction. Encyclopedia Britannica, Inc.; n.d. [accessed 2021 Aug 13]. https://www.britannica.com/science/winddirection.

# Appendix A. MMT2 and A-1830 Raw Data Plots

Appendix A displays the 21 days of 2021 June raw meteorological data plots used in this study. The US Army Combat Capabilities Development Command Army Research Laboratory Meteorological Measurement Tripod #2 (MMT2) data are shown as blue circles; the Army Test and Evaluation Command A-1830 data are displayed as an unmarked black line. Samples were logged every 1 min, totaling 1440 samples/day. The 24-h plots include all six meteorological variables: pressure (in mb), temperature (in °C), relative humidity (in %), solar radiation (in W/m$^2$), wind speed (in m/s), and wind direction (in °).

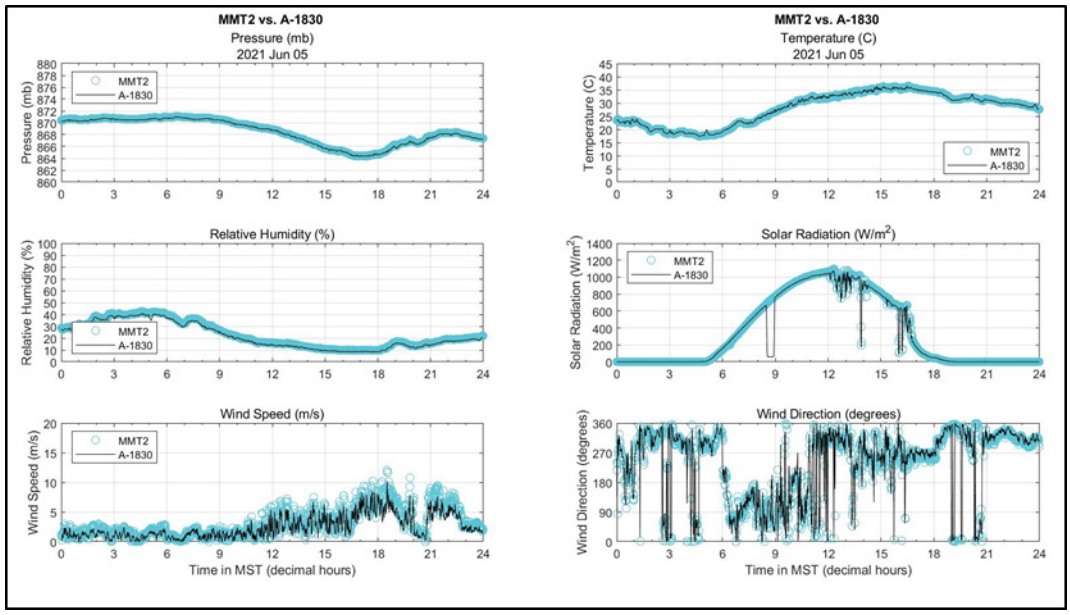


**Fig. A-1 2021 Jun 05, MMT2 vs. A-1830 raw data plots**

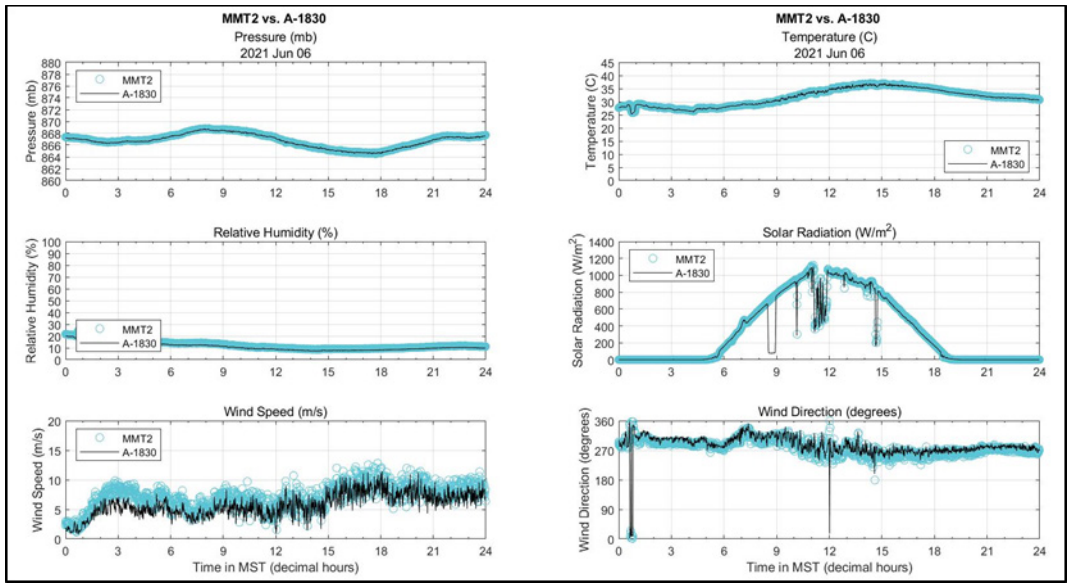


**Fig. A-2 2021 Jun 06, MMT2 vs. A-1830 raw data plots**

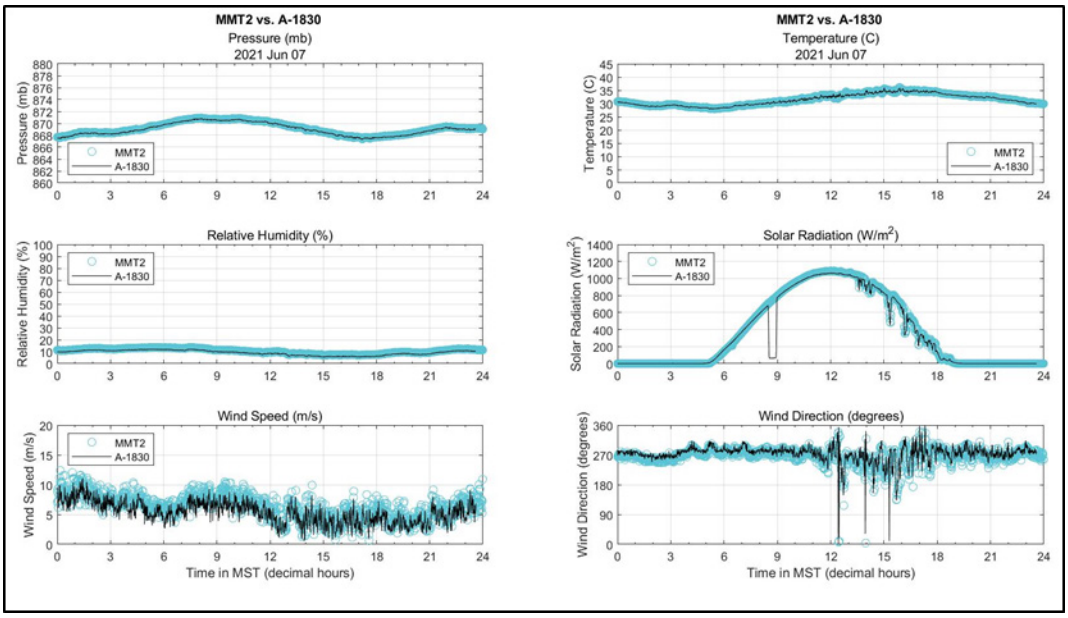


**Fig. A-3 2021 Jun 07, MMT2 vs. A-1830 raw data plots**

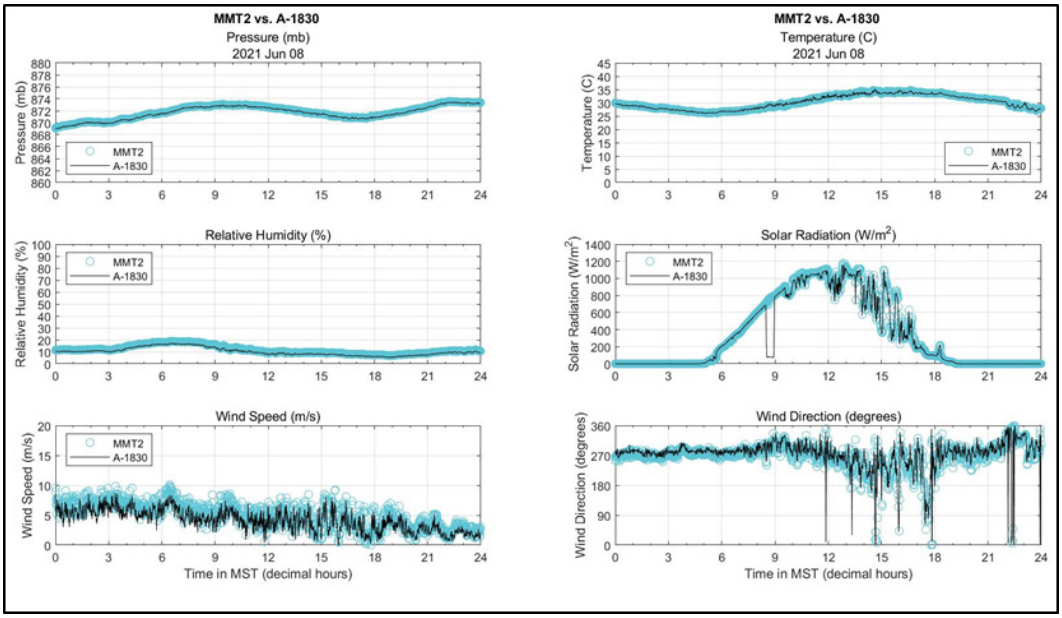


**Fig. A-4 2021 Jun 08, MMT2 vs. A-1830 raw data plots**

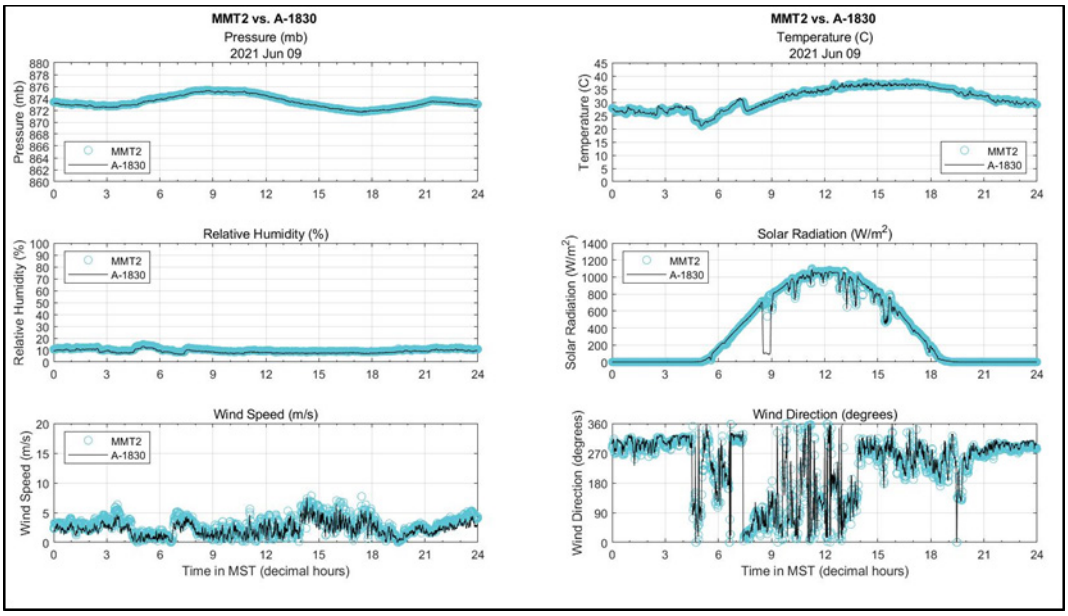


**Fig. A-5  2021 Jun 09, MMT2 vs. A-1830 raw data plots**

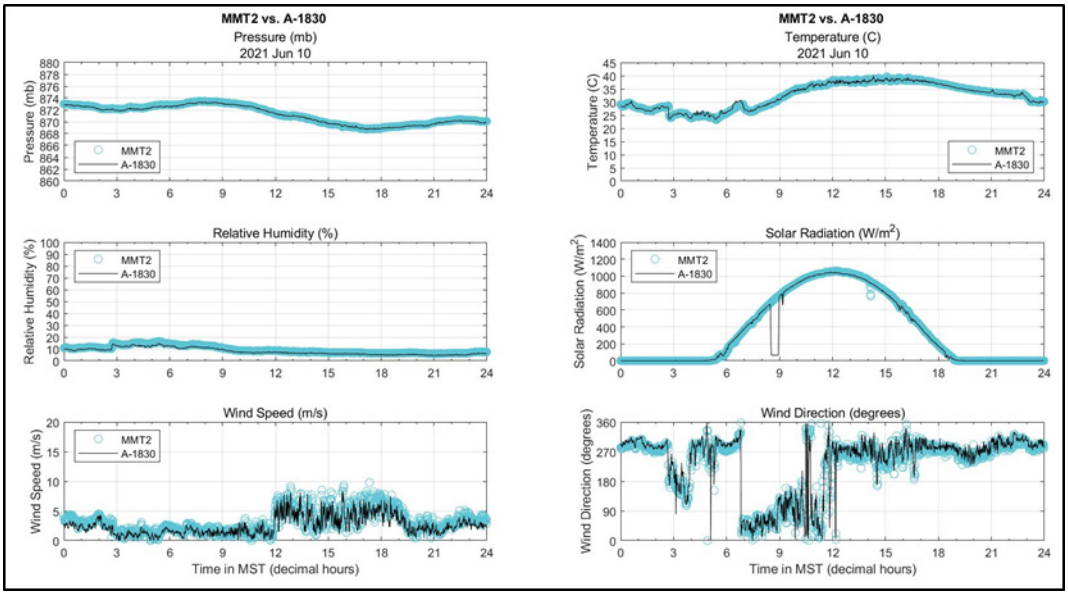


**Fig. A-6  2021 Jun 10, MMT2 vs. A-1830 raw data plots**

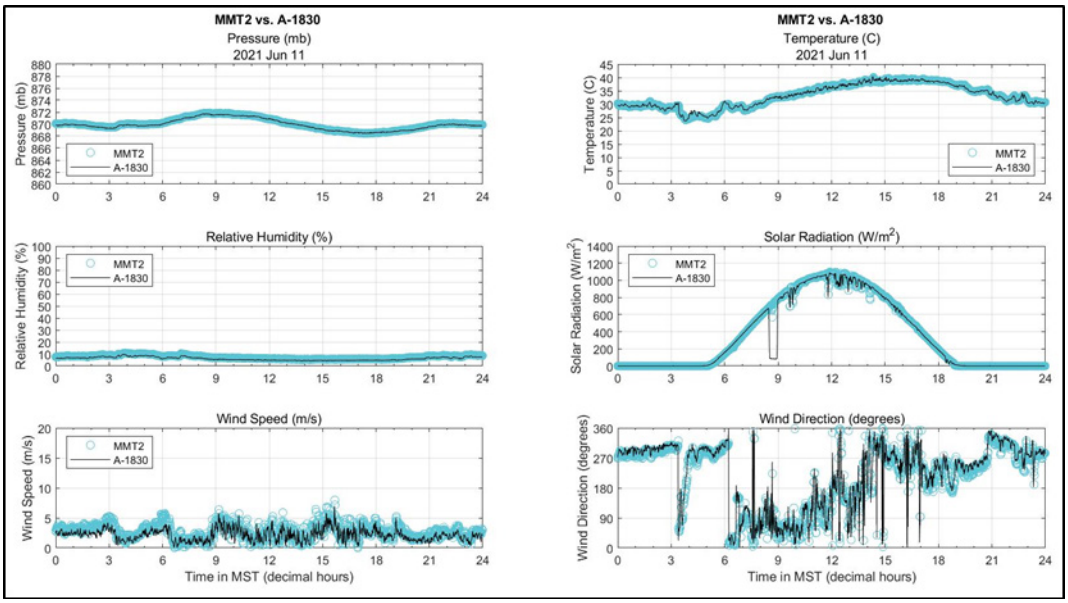


**Fig. A-7 2021 Jun 11, MMT2 vs. A-1830 raw data plots**

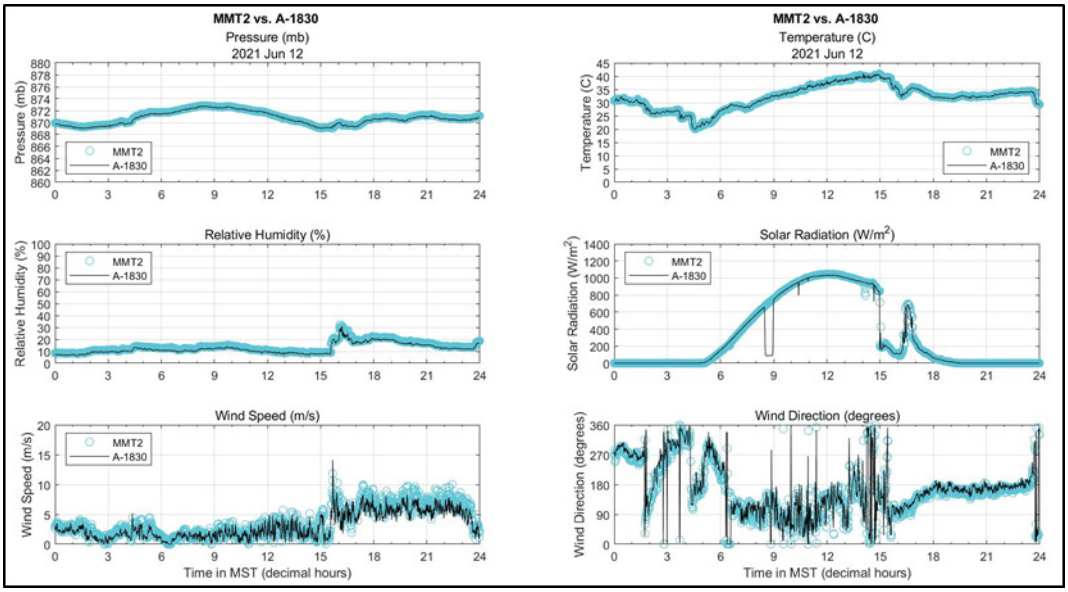


**Fig. A-8 2021 Jun 12, MMT2 vs. A-1830 raw data plots**

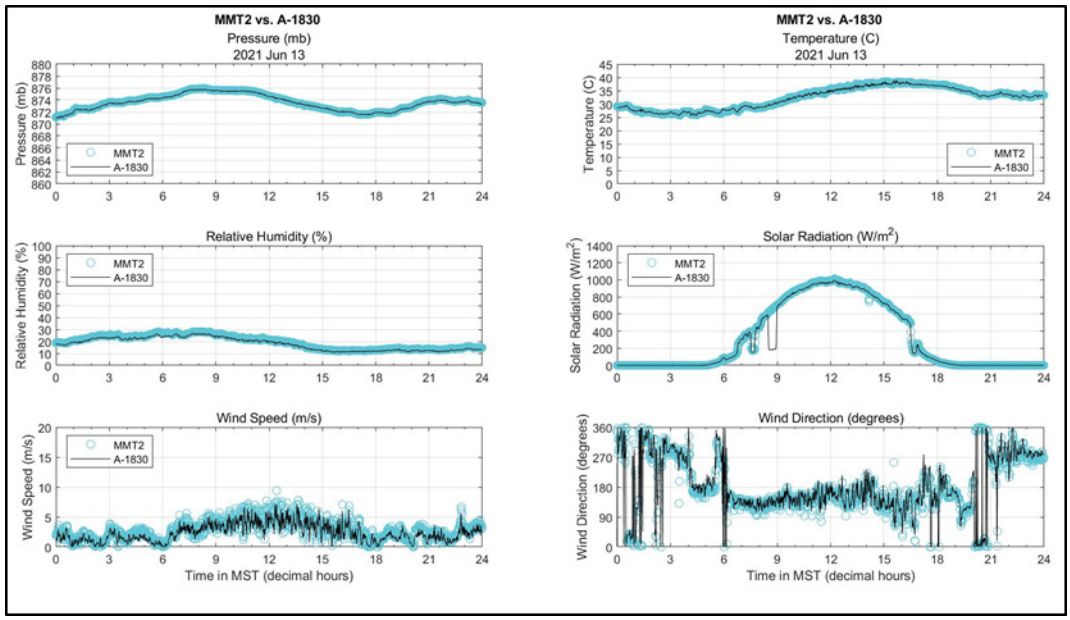


**Fig. A-9 2021 Jun 13, MMT2 vs. A-1830 raw data plots**

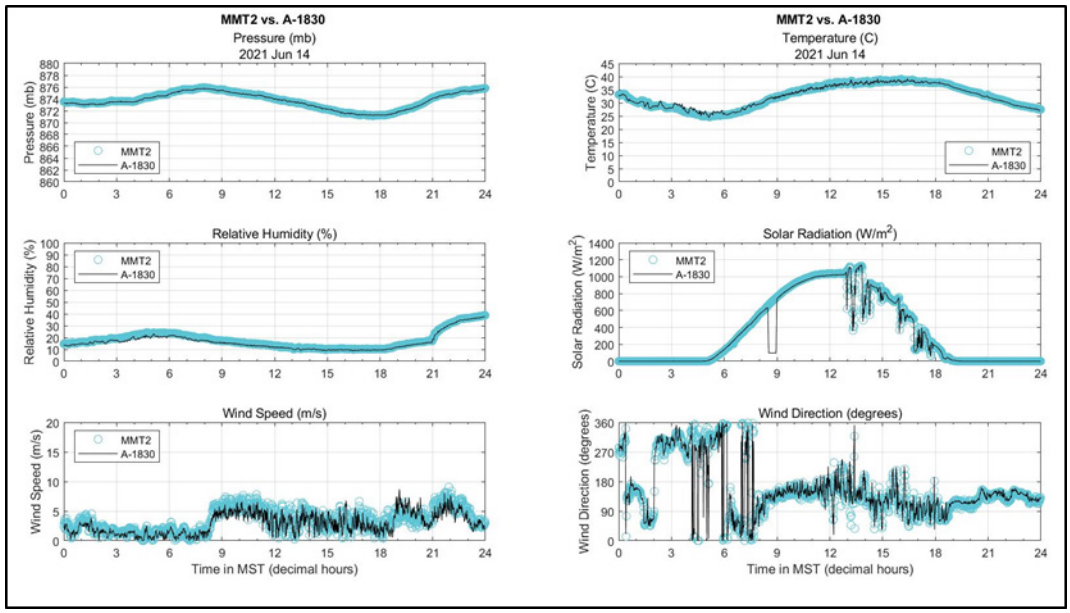


**Fig. A-10 2021 Jun 14, MMT2 vs. A-1830 raw data plots**

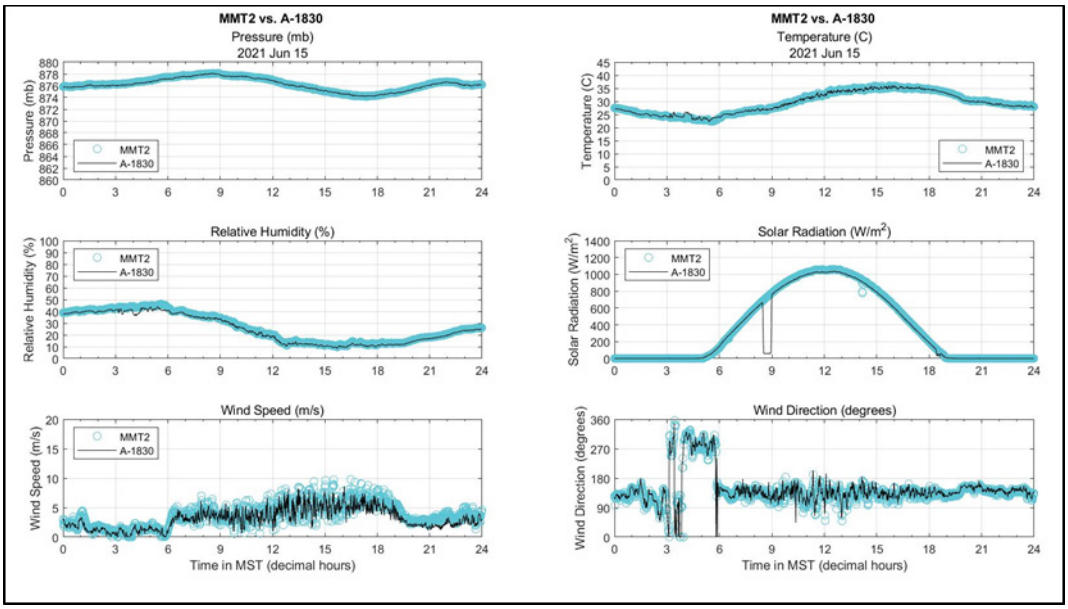


**Fig. A-11 2021 Jun 15, MMT2 vs. A-1830 raw data plots**

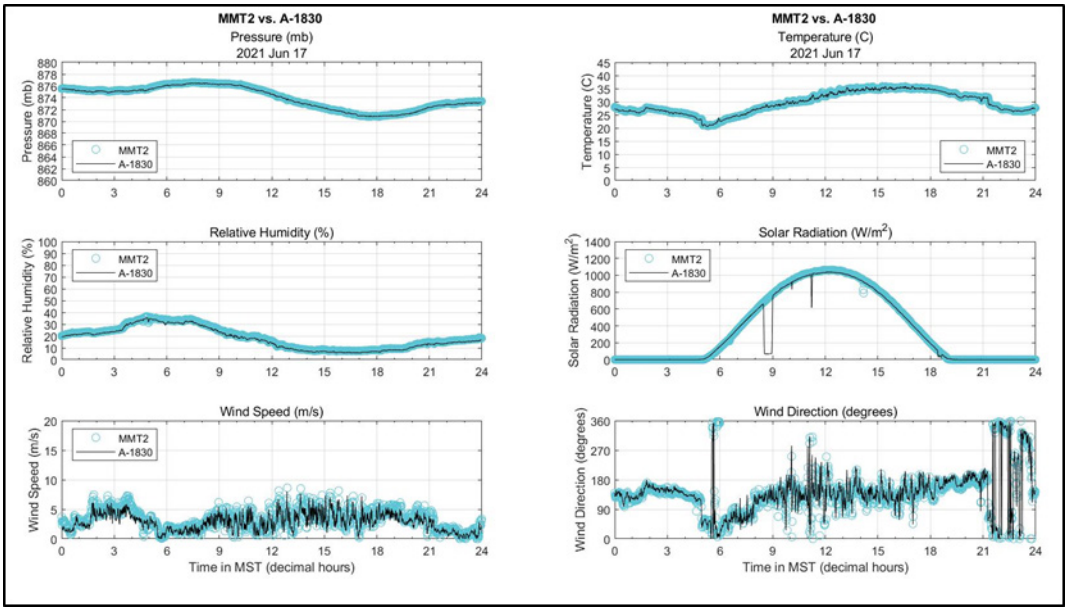


**Fig. A-12 2021 Jun 17, MMT2 vs. A-1830 raw data plots**

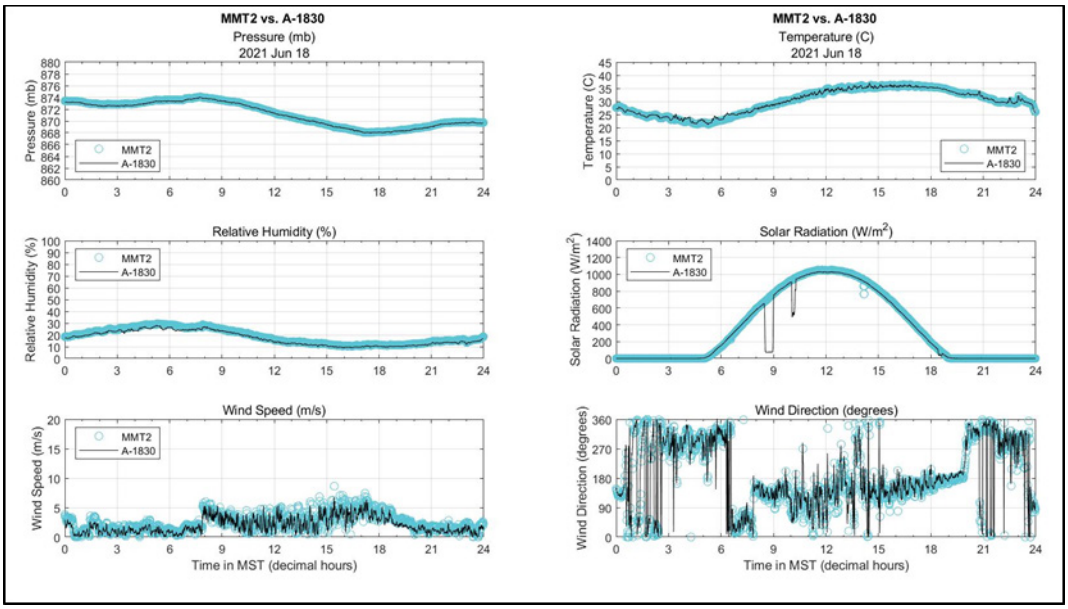


**Fig. A-13 2021 Jun 18, MMT2 vs. A-1830 raw data plots**

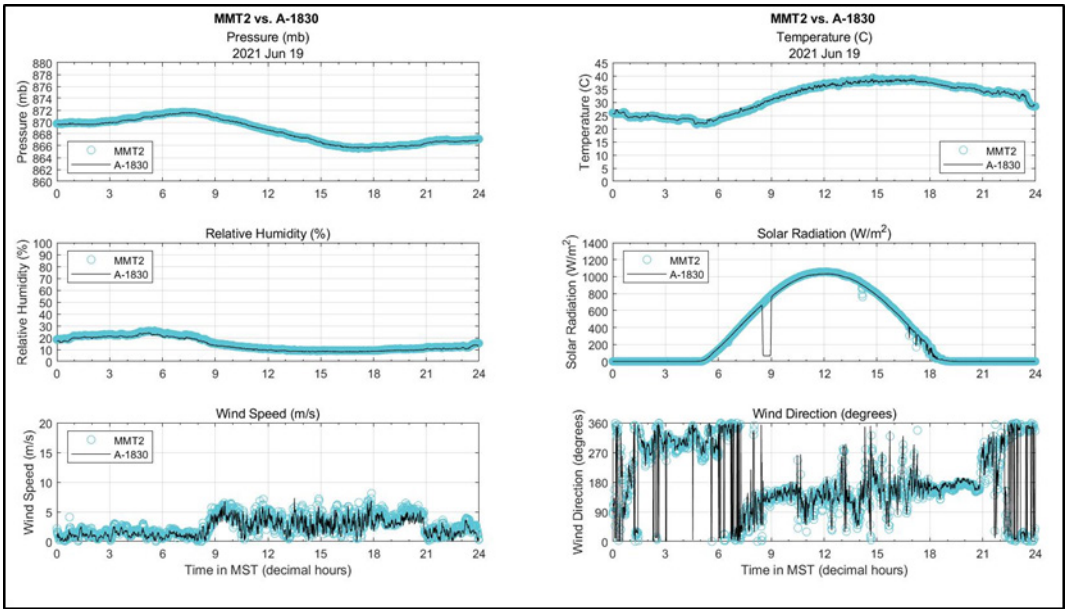


**Fig. A-14 2021 Jun 19, MMT2 vs. A-1830 raw data plots**

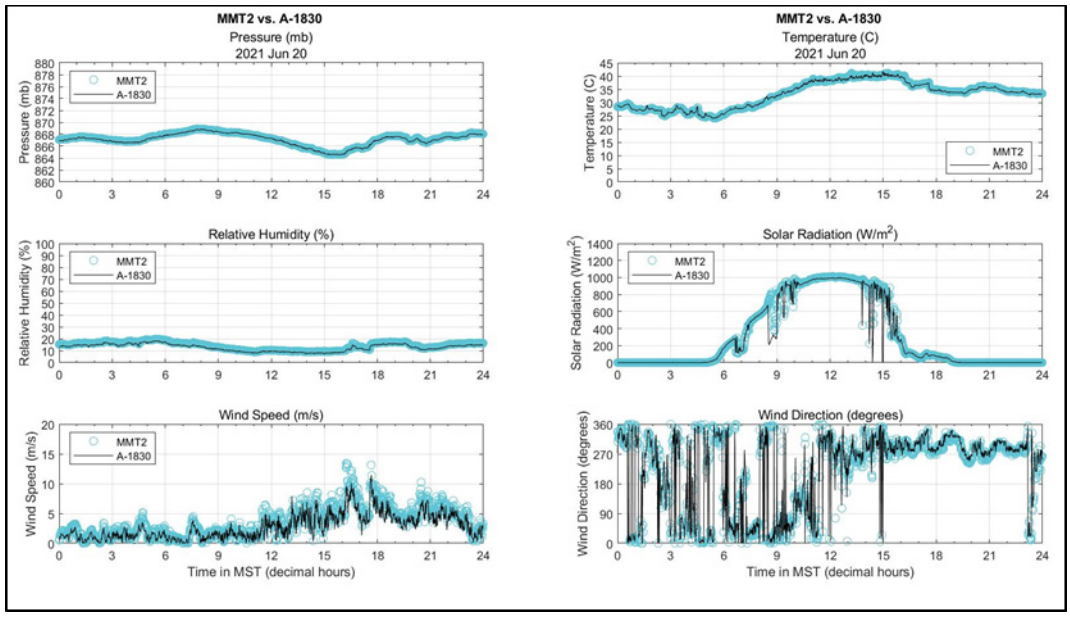


**Fig. A-15 2021 Jun 20, MMT2 vs. A-1830 raw data plots**

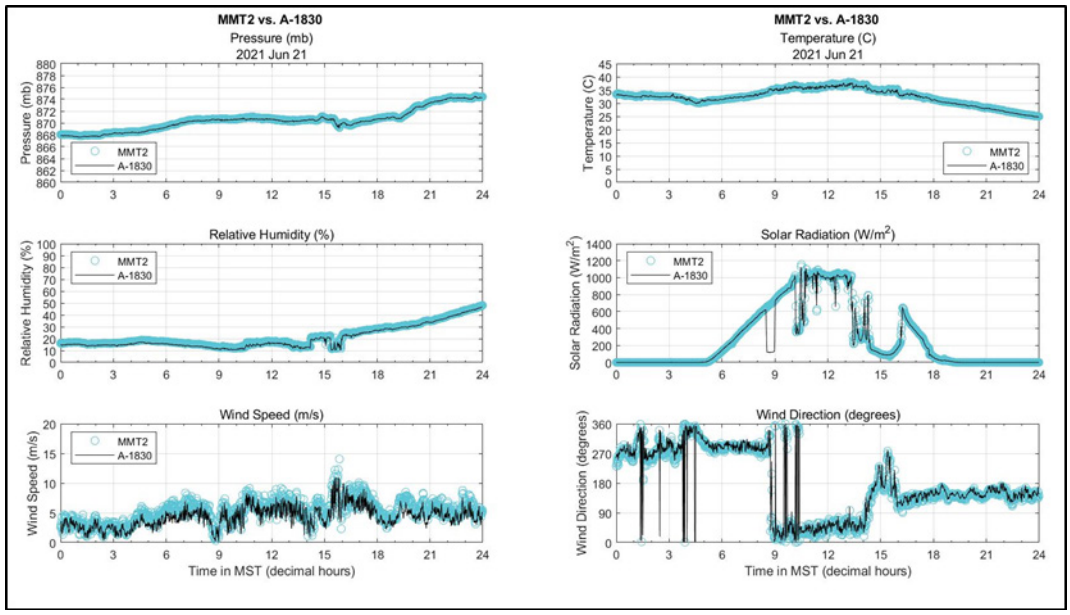


**Fig. A-16 2021 Jun 21, MMT2 vs. A-1830 raw data plots**

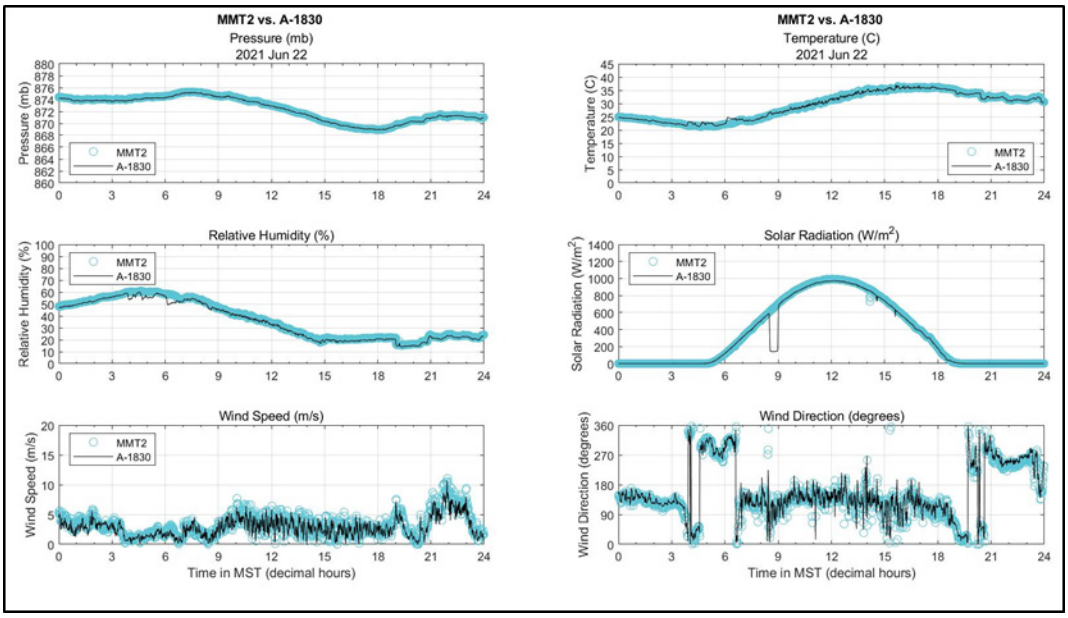


**Fig. A-17 2021 Jun 22, MMT2 vs. A-1830 raw data plots**

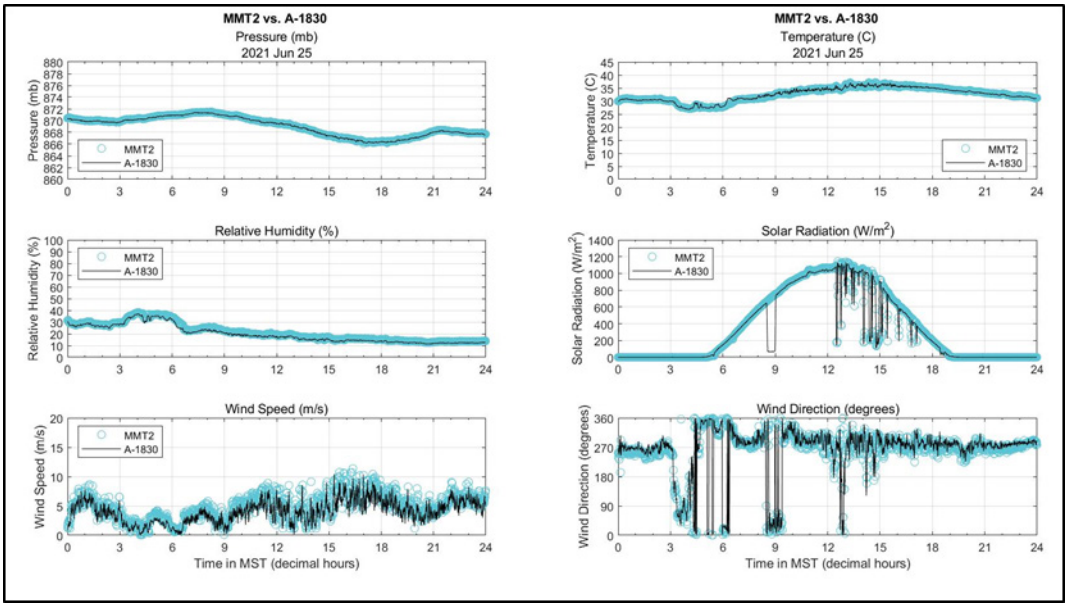


**Fig. A-18 2021 Jun 25, MMT2 vs. A-1830 raw data plots**

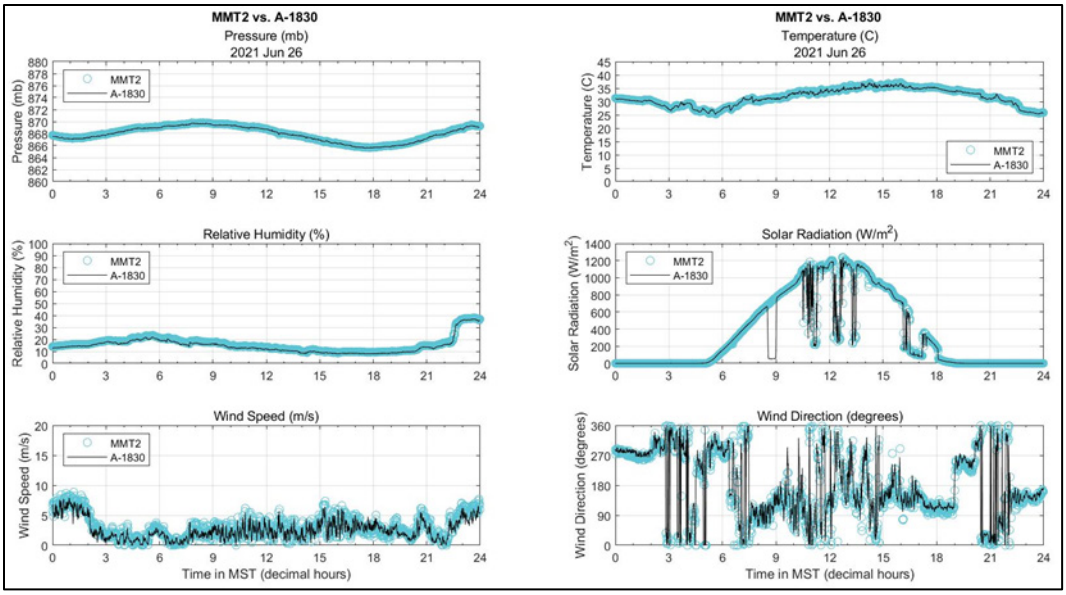


**Fig. A-19 2021 Jun 26, MMT2 vs. A-1830 raw data plots**

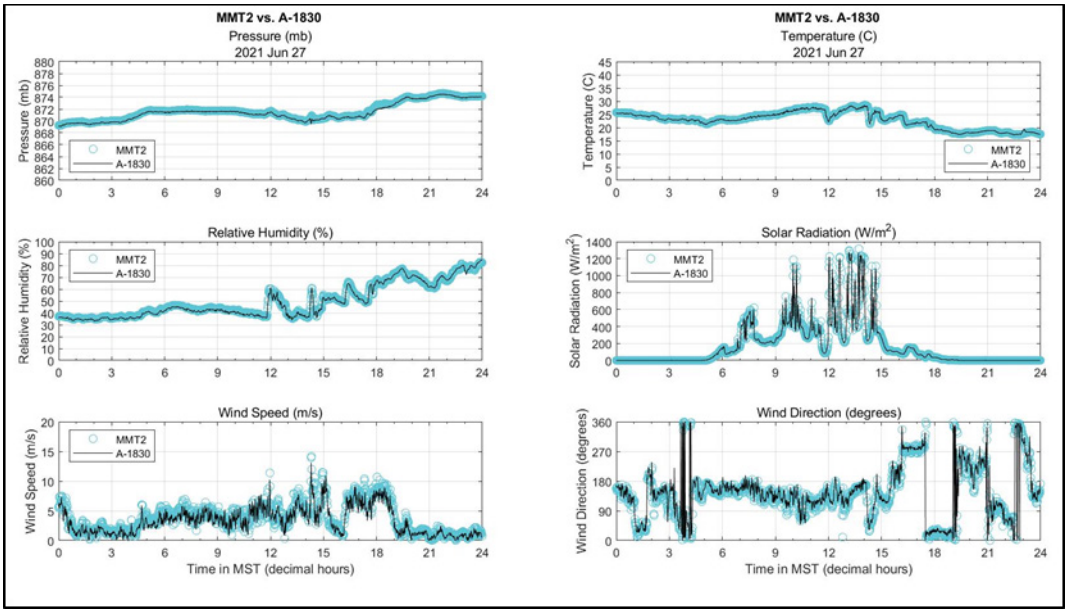


**Fig. A-20 2021 Jun 27, MMT2 vs. A-1830 raw data plots**

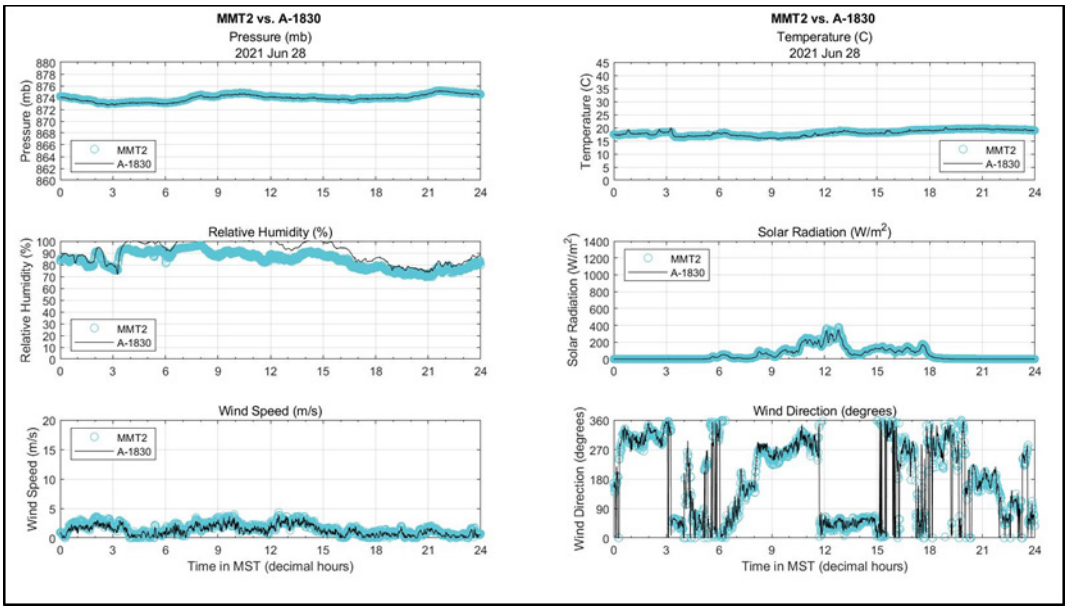


**Fig. A-21 2021 Jun 28, MMT2 vs. A-1830 raw data plots**

## Appendix B. Daily MMT2 vs. A-1830 Comparison Plots

Appendix B displays the 21 days of 2021 June, processed, Meteorological Measurement Tripod #2 (MMT2) versus A-1830 meteorological data compared in this study. For the comparison, the A-1830 data were defined as the "standard". A "perfect" fit line is showed as a diagonal line from lower left to upper right. Each plot represents meteorological variables sampled over a single day; local midnight to local midnight, 24-h period. Time is documented in Mountain Standard Time. The thermodynamic data—pressure (in mb), temperature (in °C), relative humidity (in %), solar radiation (in $W/m^2$)—are grouped together, and followed by the dynamic variables of wind speed (in m/s) and wind direction (in °).

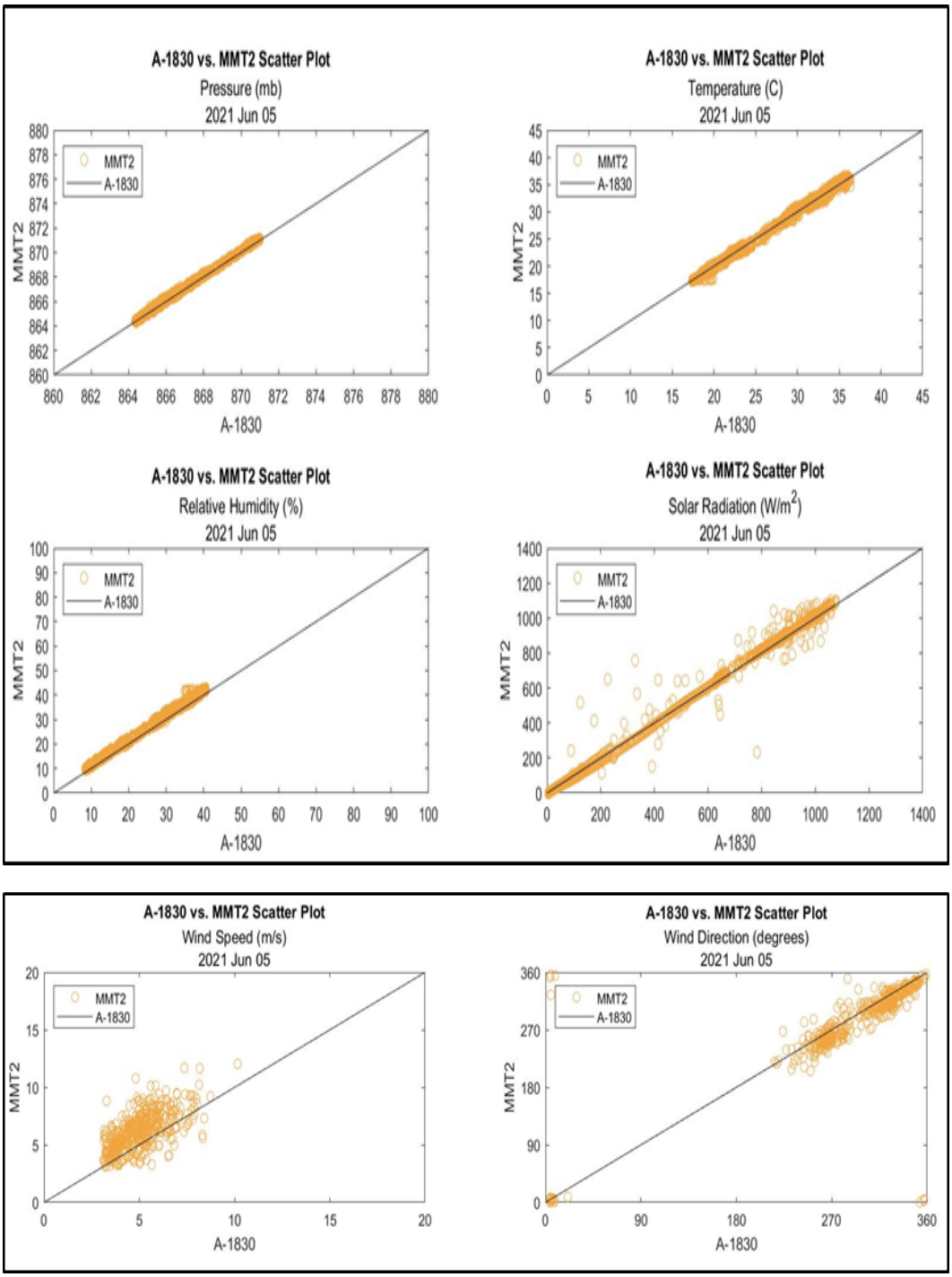


**Fig. B-1 2021 Jun 05, MMT2 vs. A-1830 data comparison**

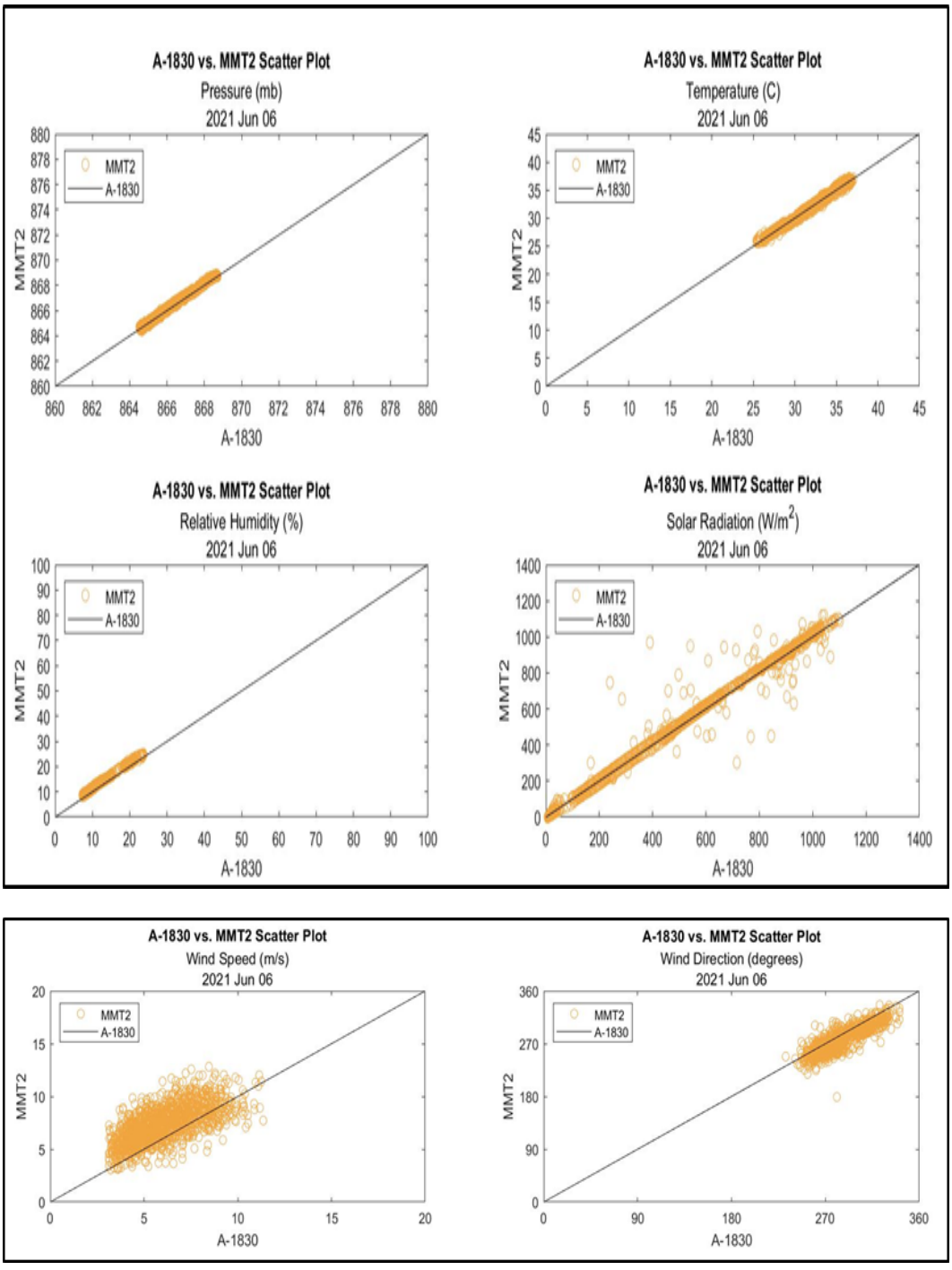


**Fig. B-2 2021 Jun 06, MMT2 vs. A-1830 data comparison**

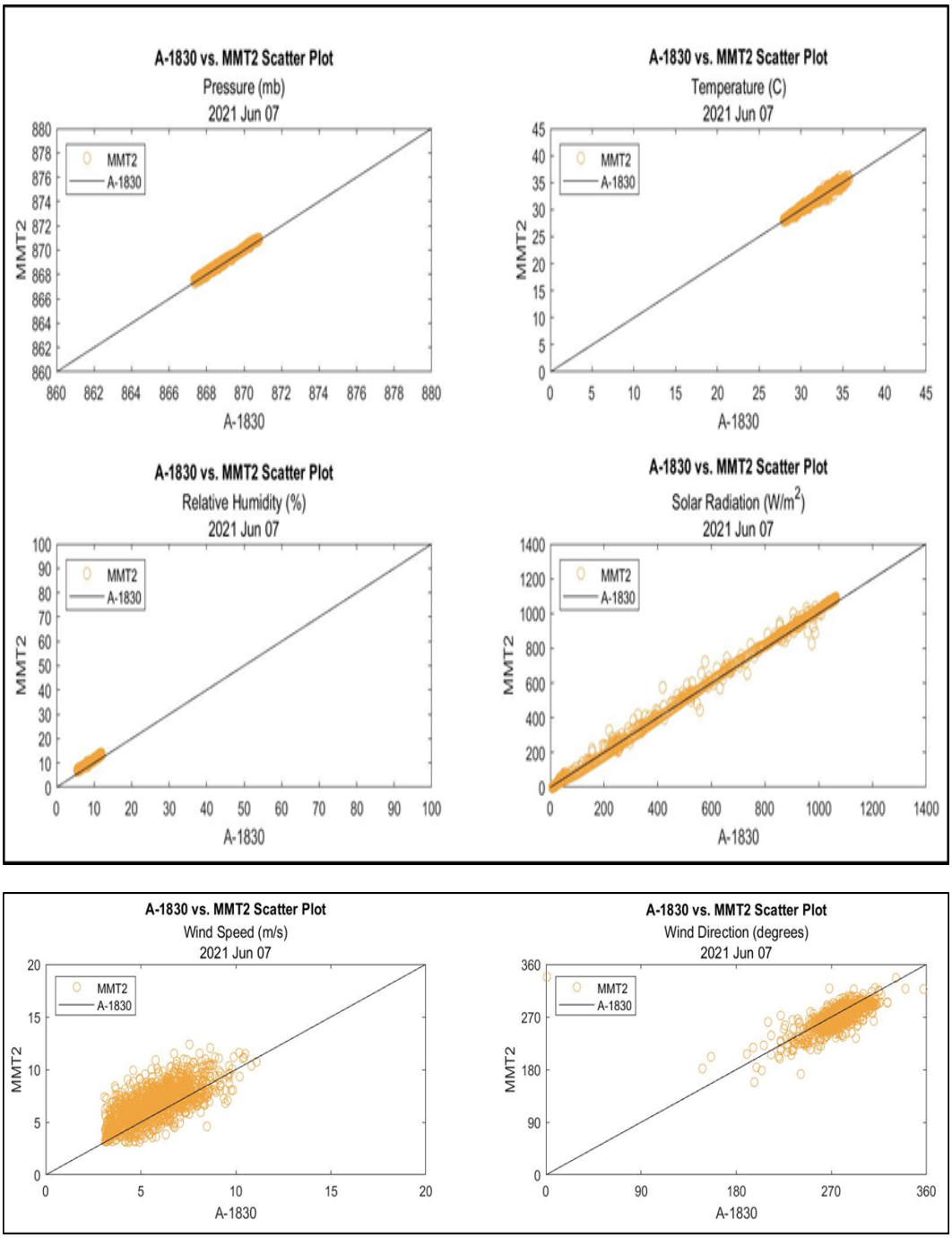


**Fig. B-3 2021 Jun 07, MMT2 vs. A-1830 data comparison**

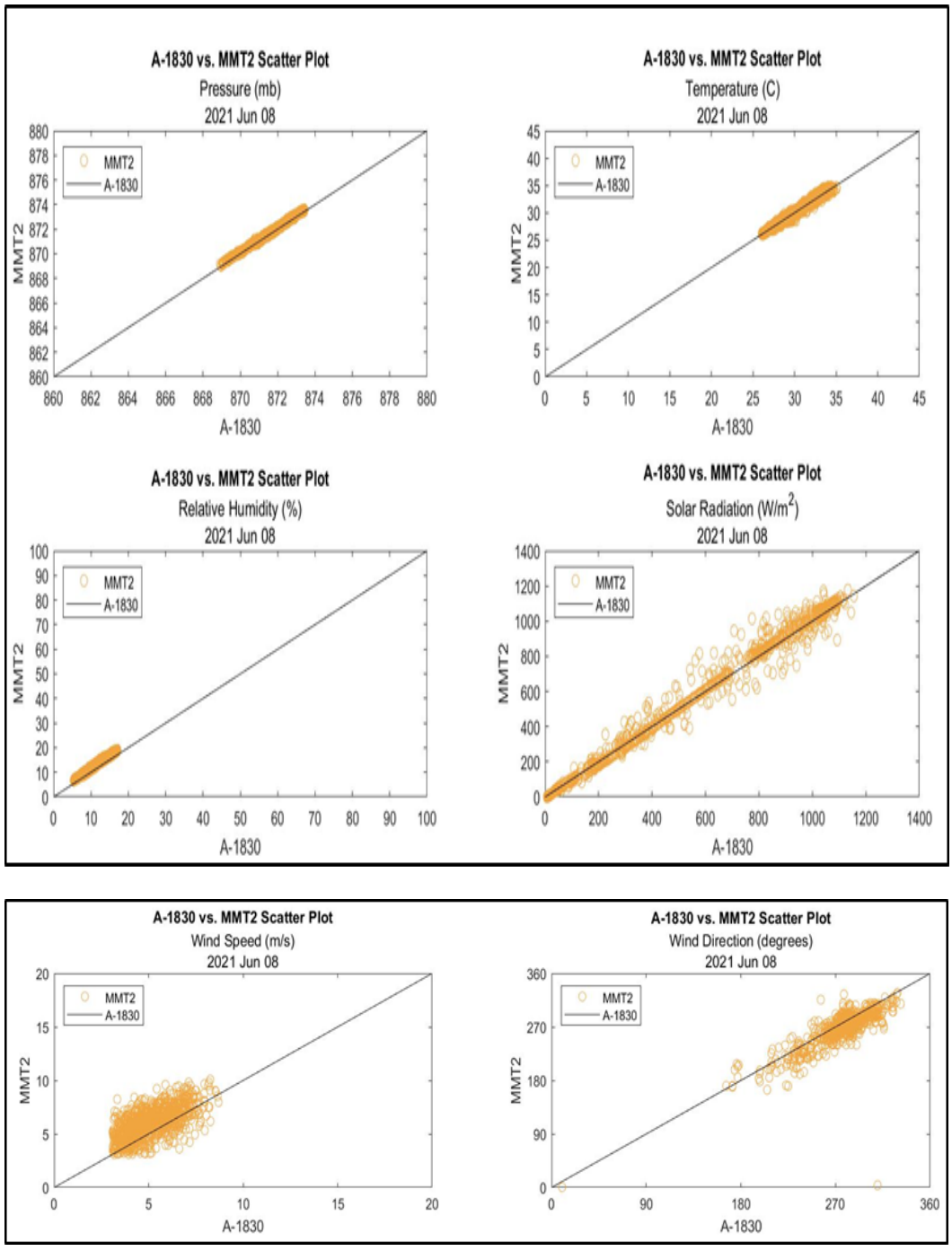


**Fig. B-4 2021 Jun 08, MMT2 vs. A-1830 data comparison**

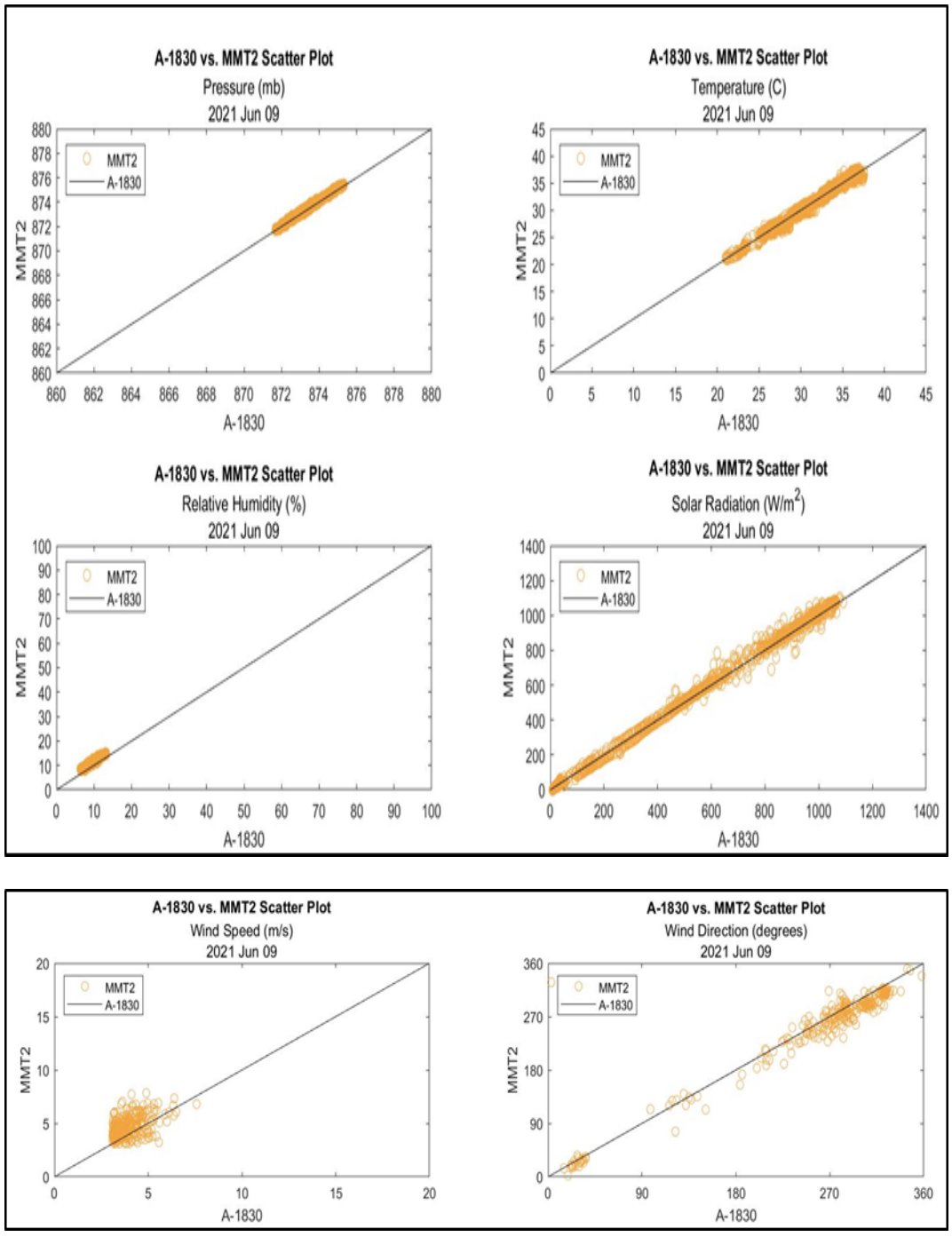


**Fig. B-5 2021 Jun 09, MMT2 vs. A-1830 data comparison**

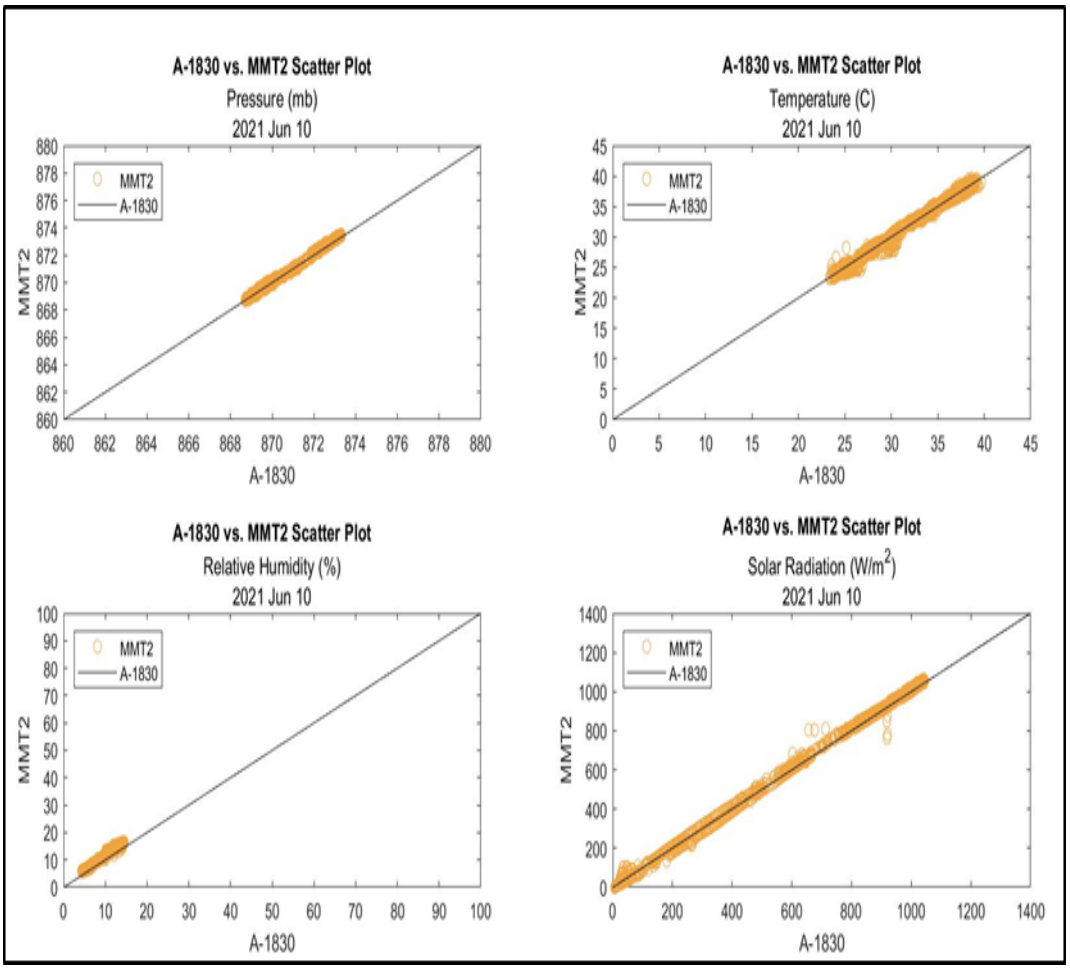


**Fig. B-6 2021 Jun 10, MMT2 vs. A-1830 data comparison**

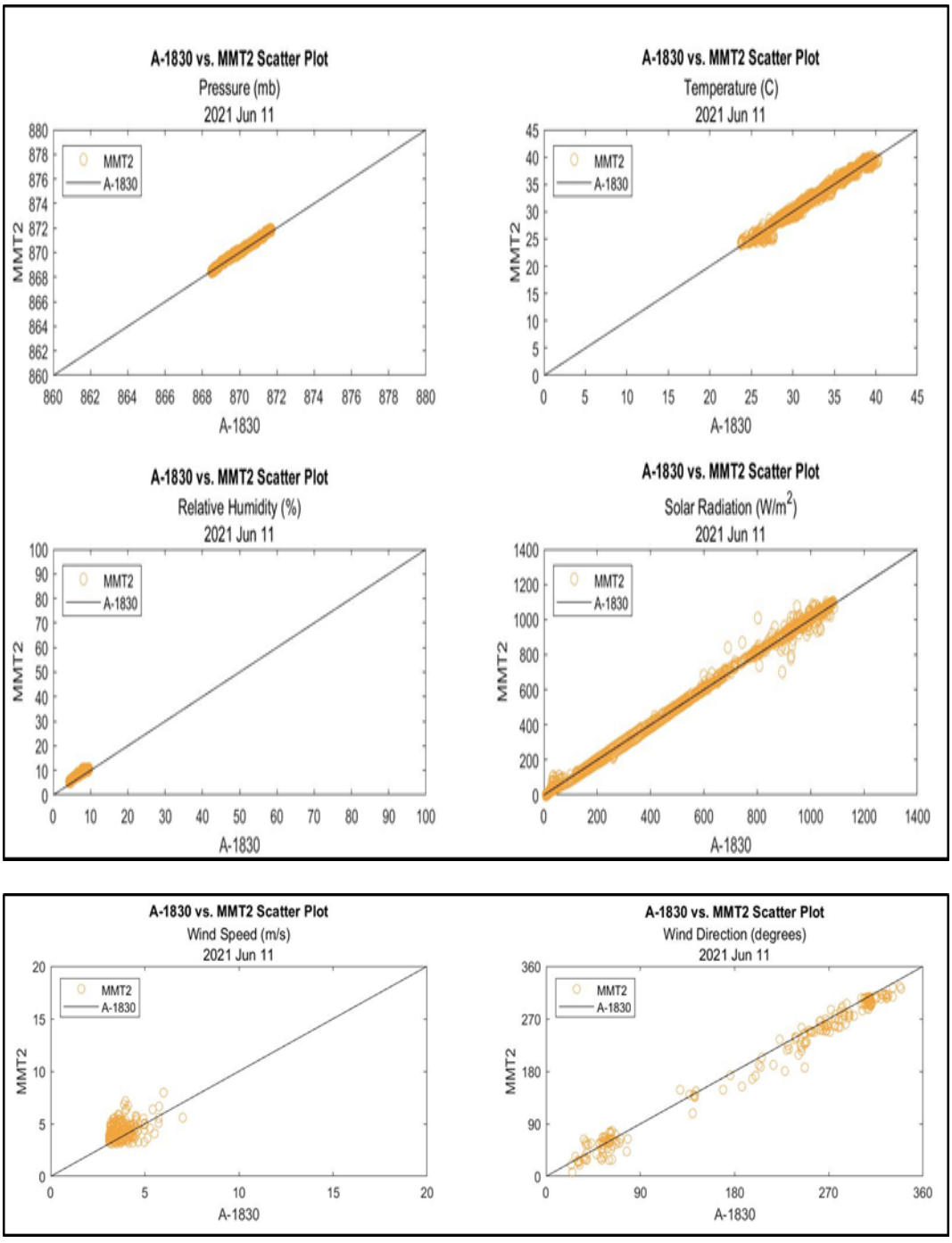


**Fig. B-7 2021 Jun 11, MMT2 vs. A-1830 data comparison**

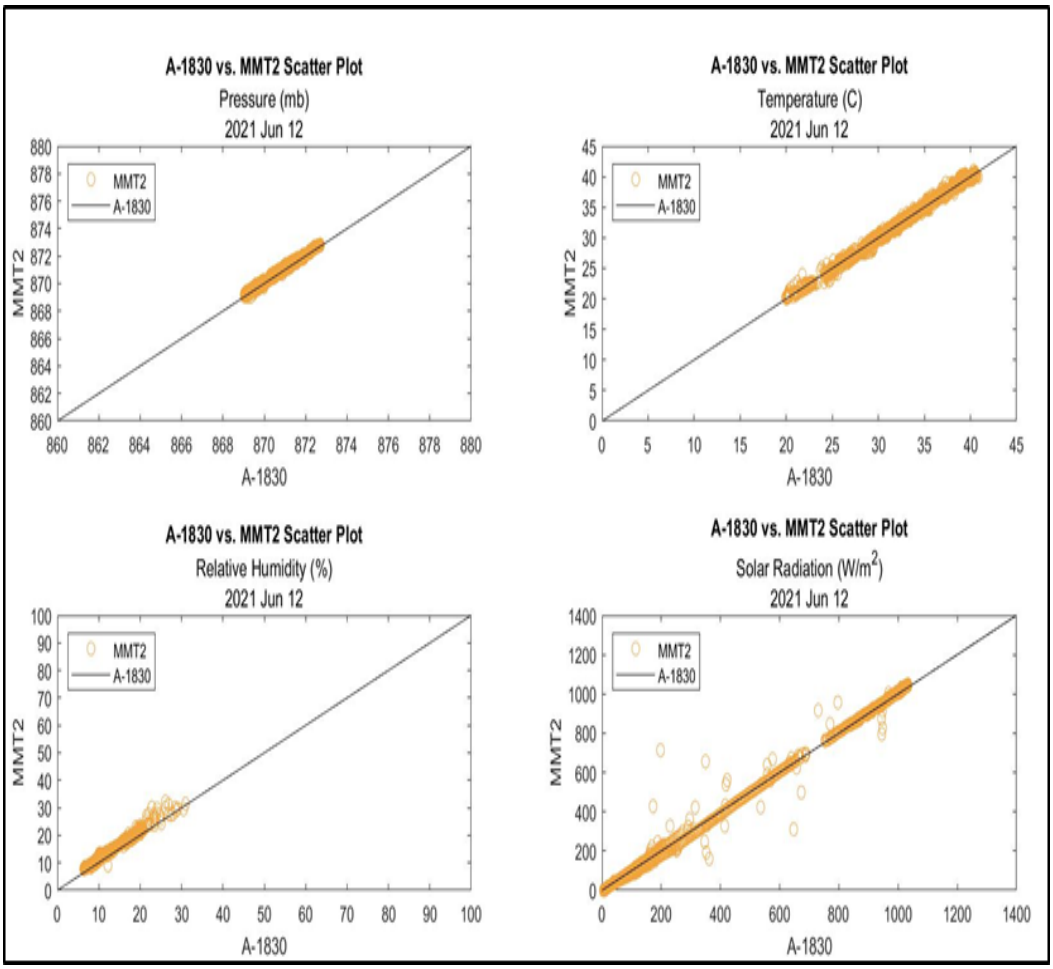


**Fig. B-8 2021 Jun 12, MMT2 vs. A-1830 data comparison**

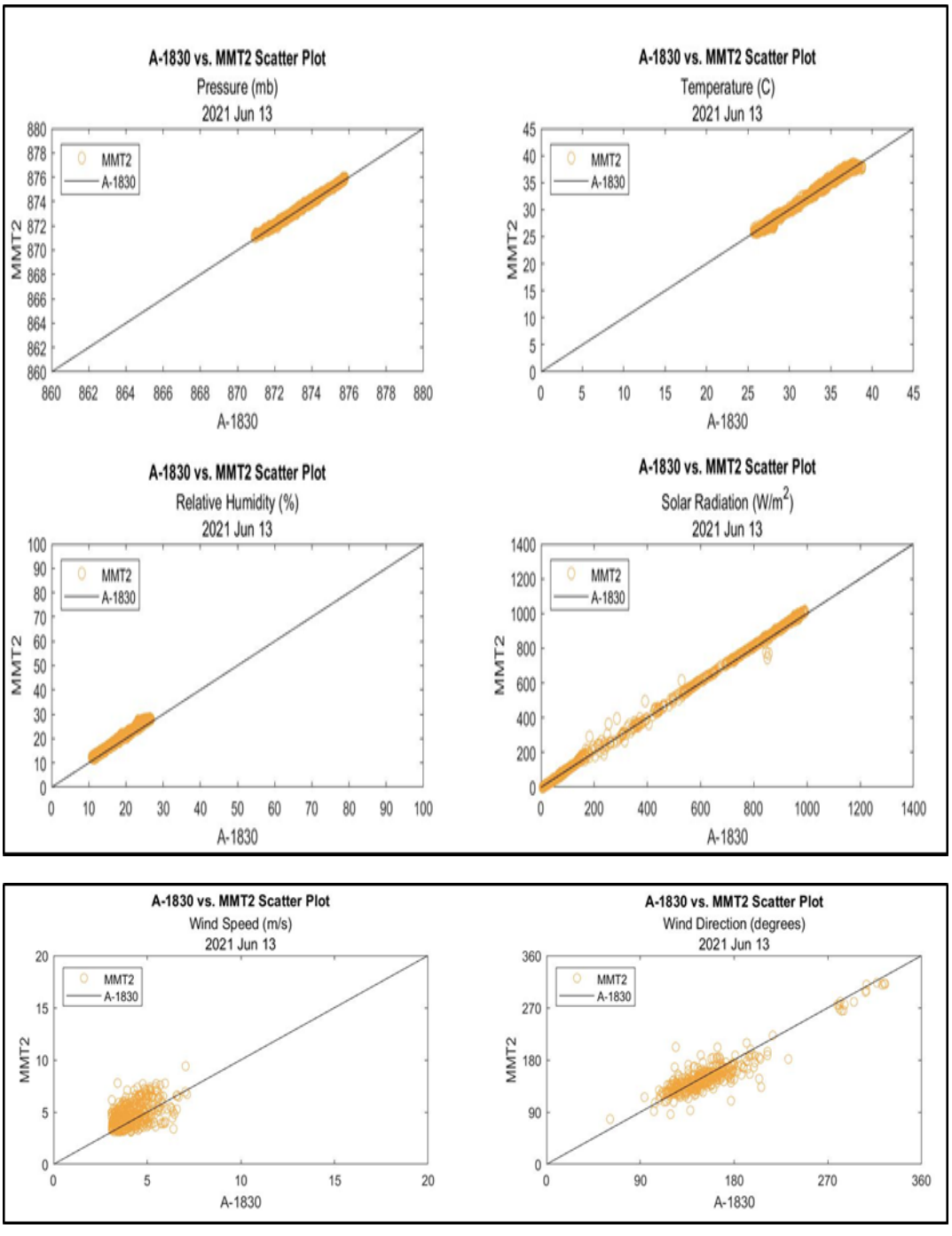


**Fig. B-9 2021 Jun 13, MMT2 vs. A-1830 data comparison**

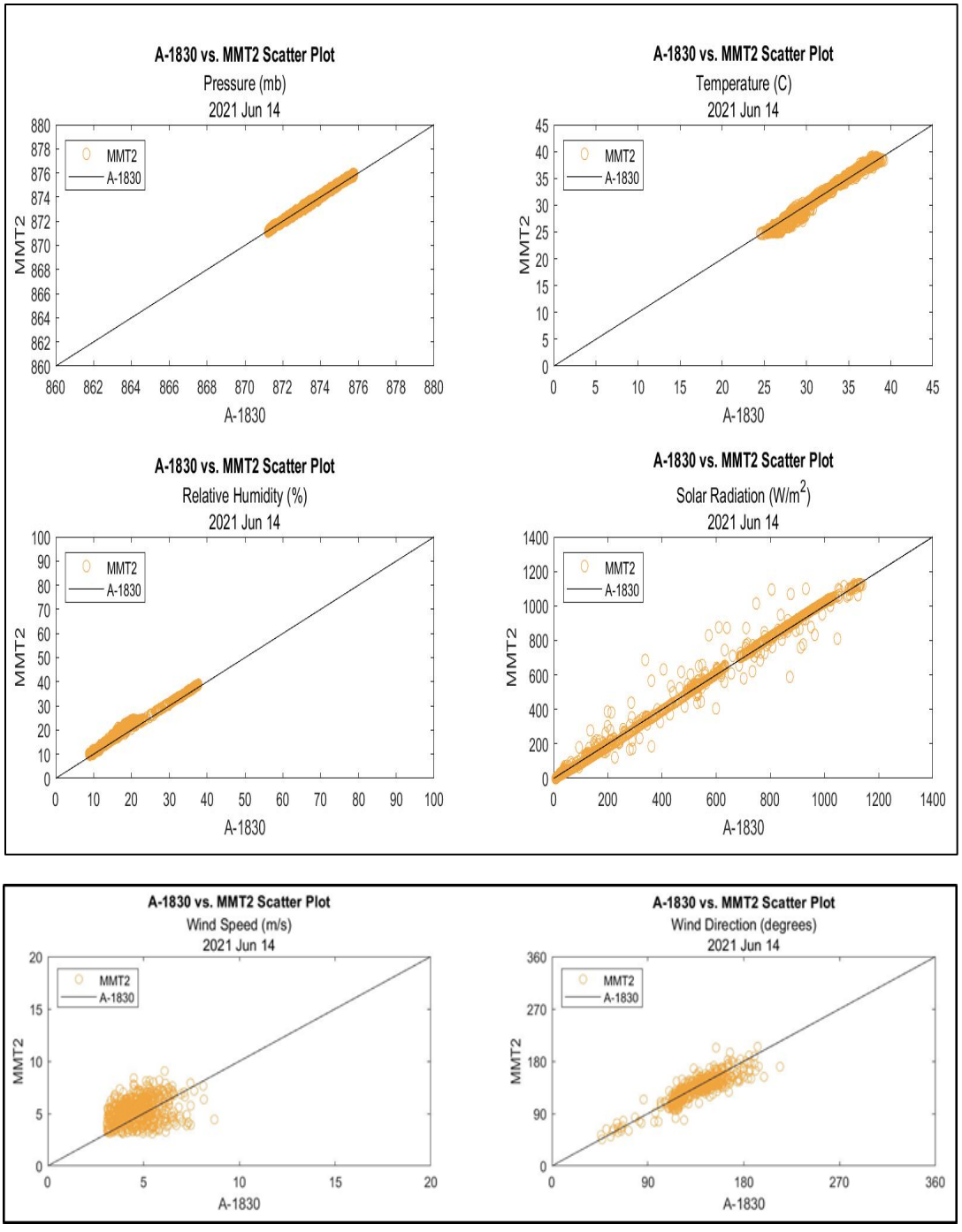


**Fig. B-10 2021 Jun 14, MMT2 vs. A-1830 data comparison**

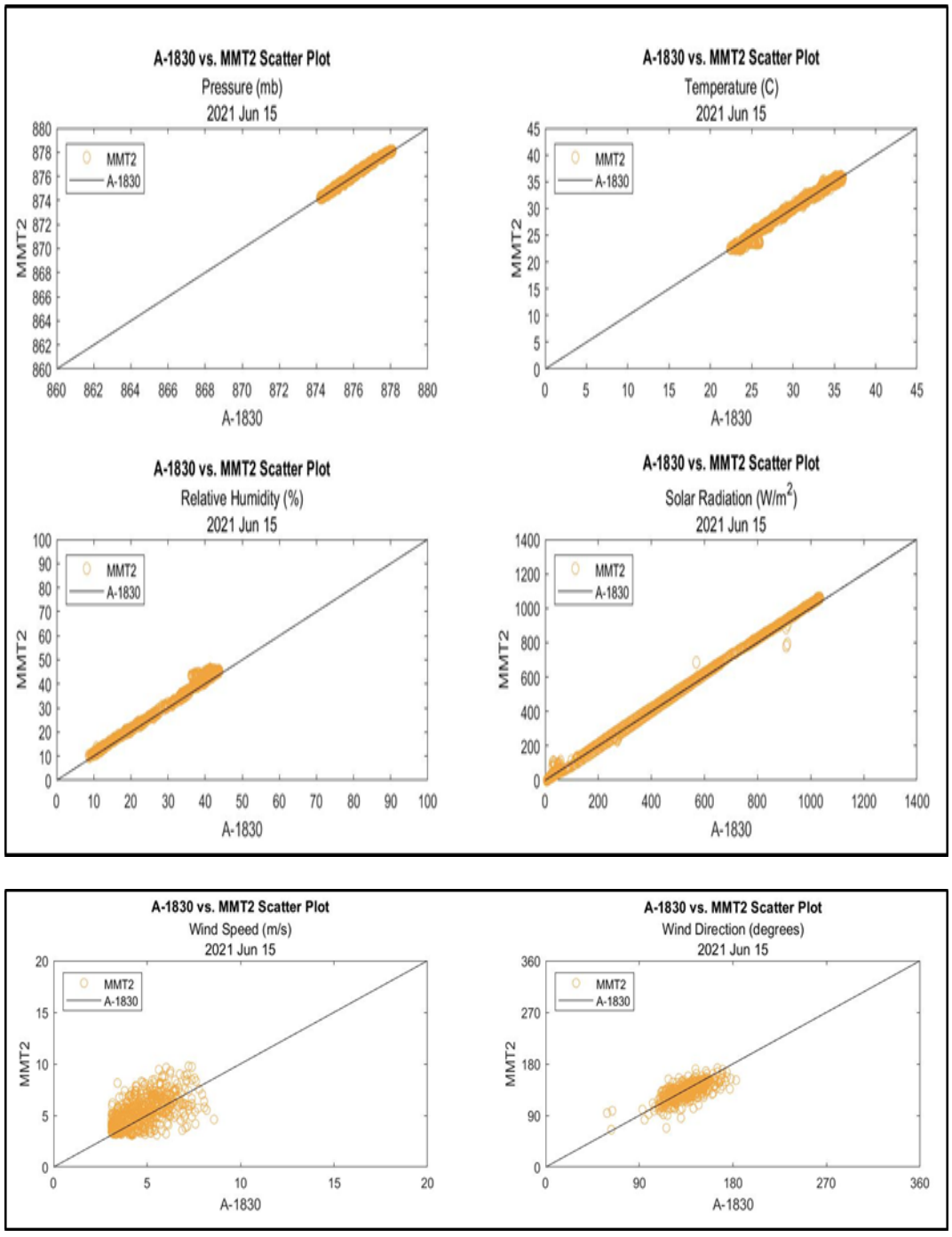


**Fig. B-11 2021 Jun 15, MMT2 vs. A-1830 data comparison**

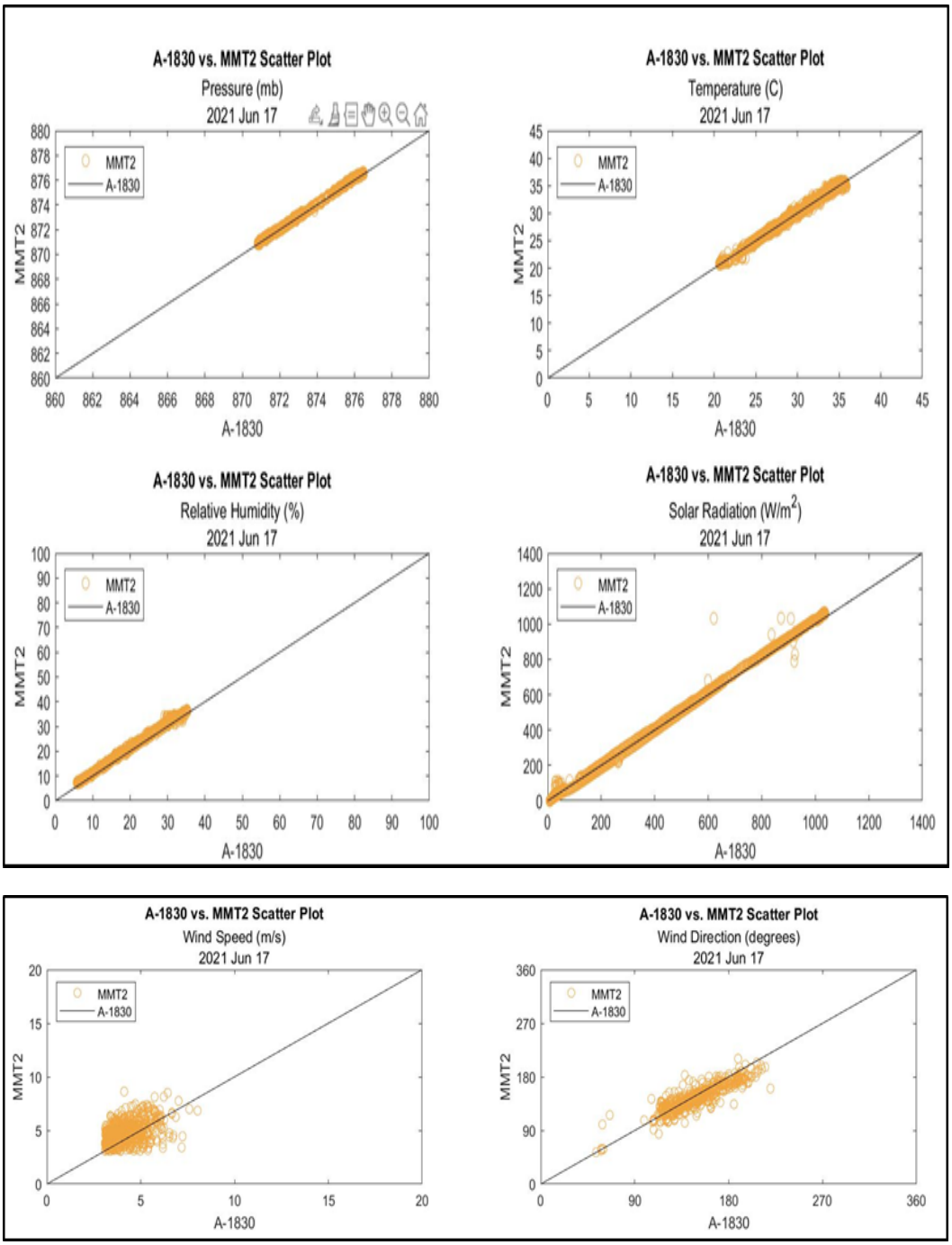


**Fig. B-12 2021 Jun 17, MMT2 vs. A-1830 data comparison**

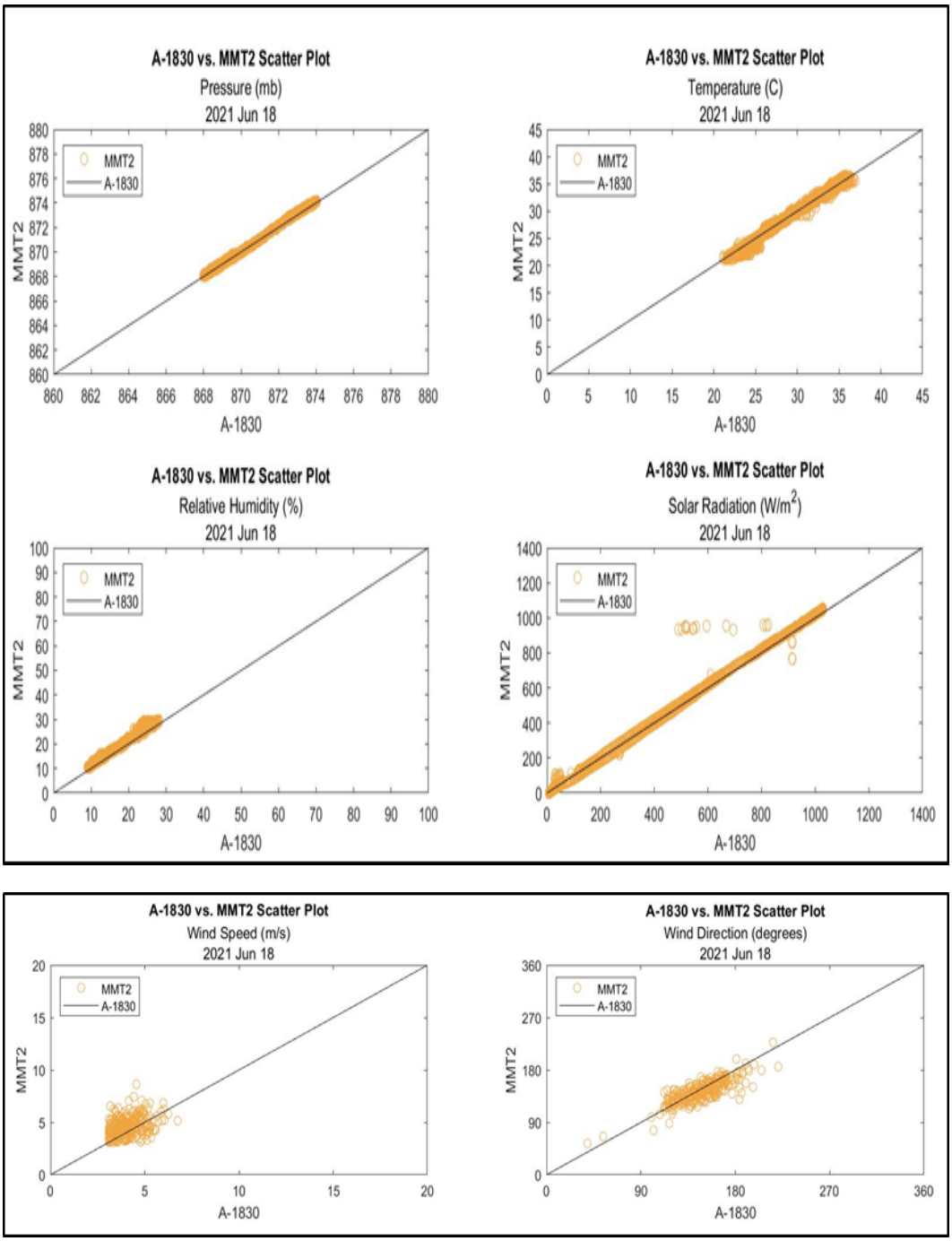


**Fig. B-13 2021 Jun 18, MMT2 vs. A-1830 data comparison**

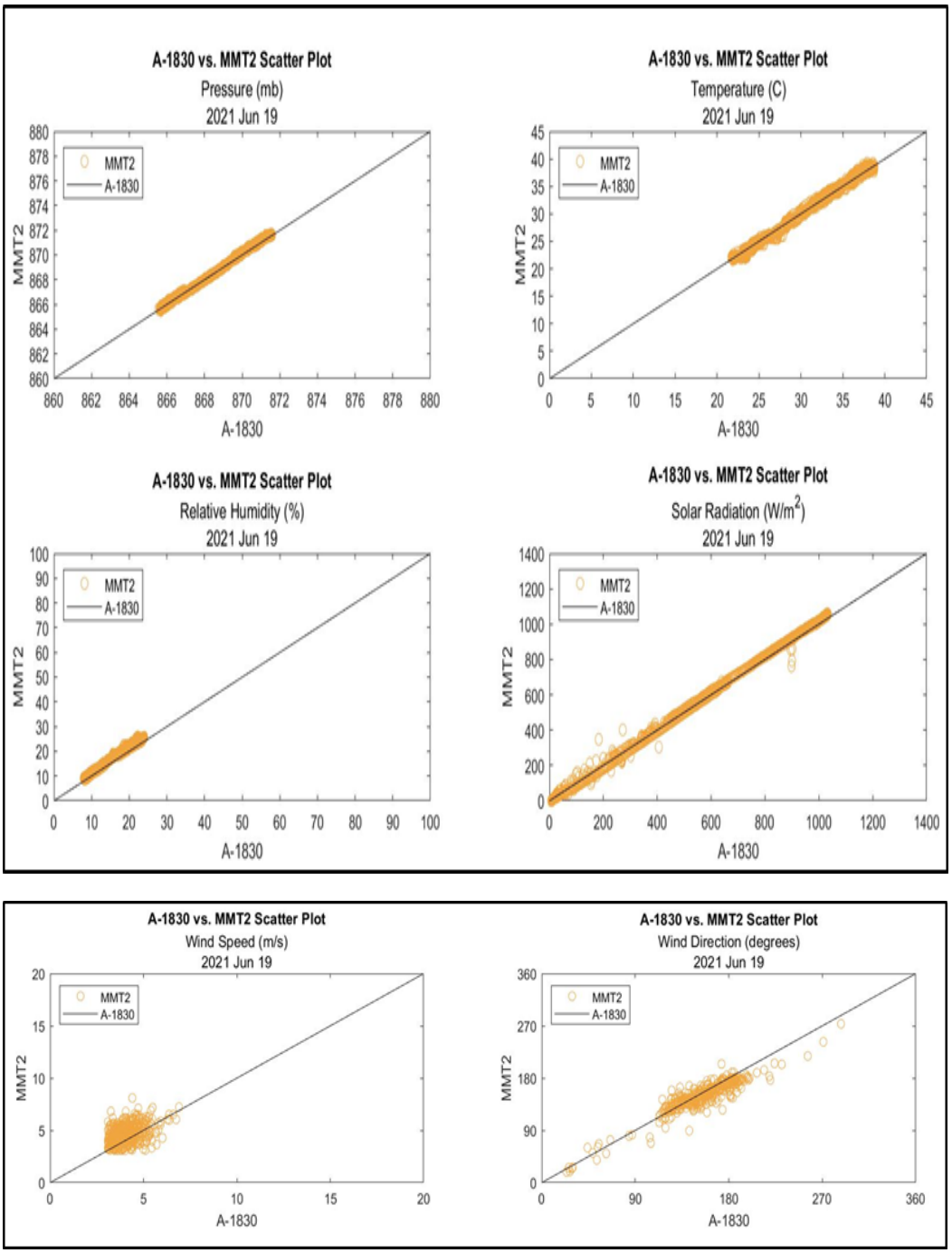


**Fig. B-14 2021 Jun 19, MMT2 vs. A-1830 data comparison**

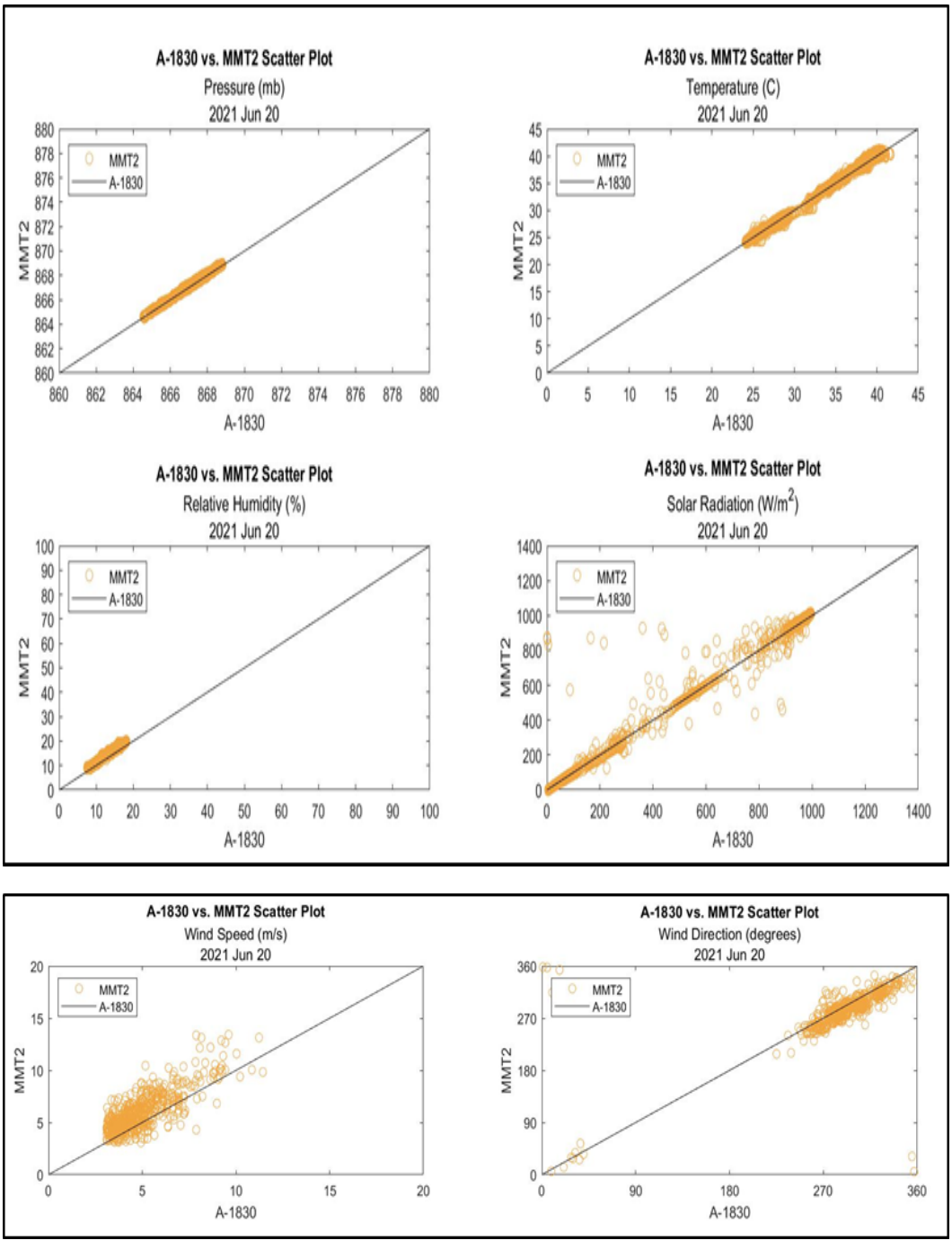


**Fig. B-15 2021 Jun 20, MMT2 vs. A-1830 data comparison**

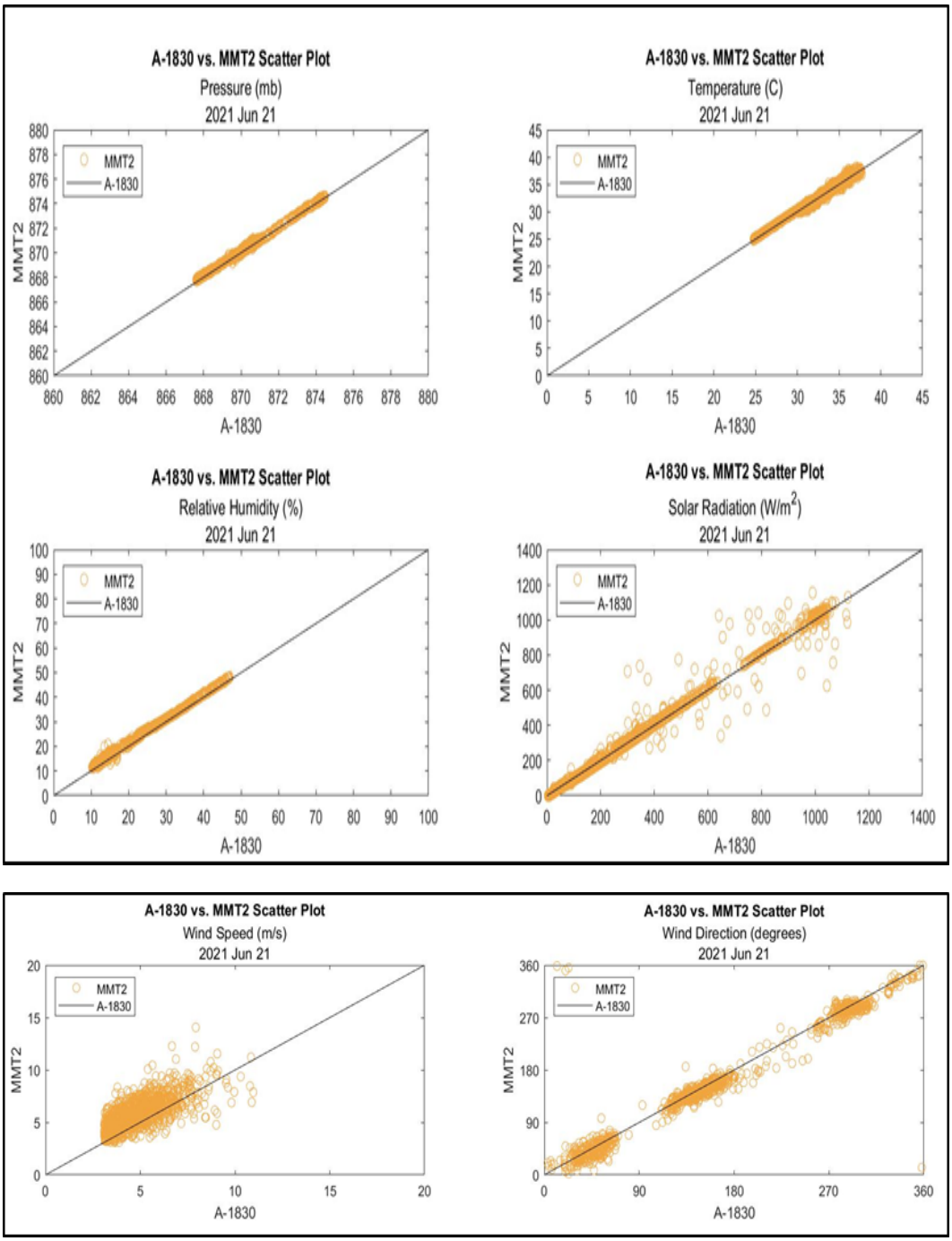


**Fig. B-16 2021 Jun 21, MMT2 vs. A-1830 data comparison**

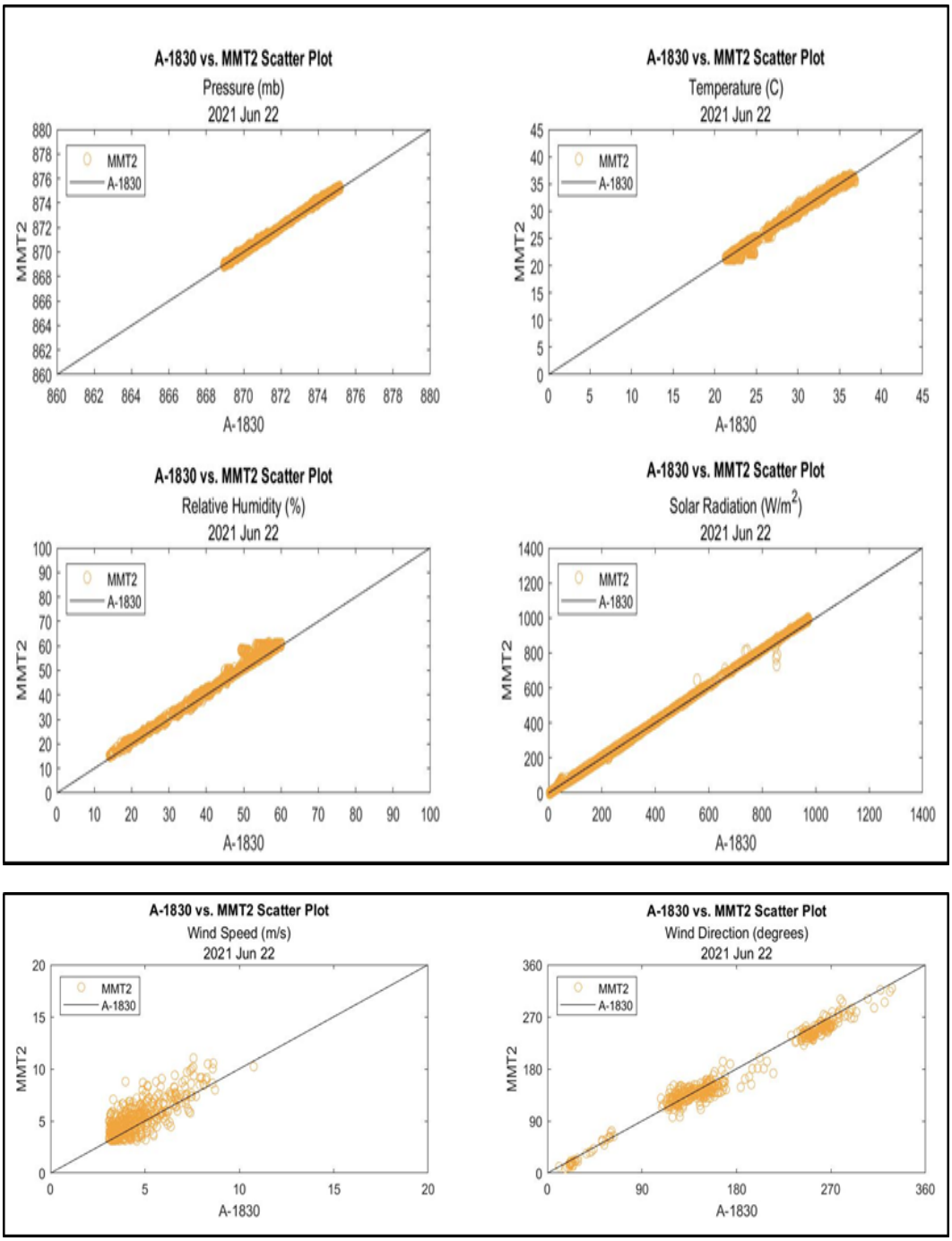


**Fig. B-17 2021 Jun 22, MMT2 vs. A-1830 data comparison**

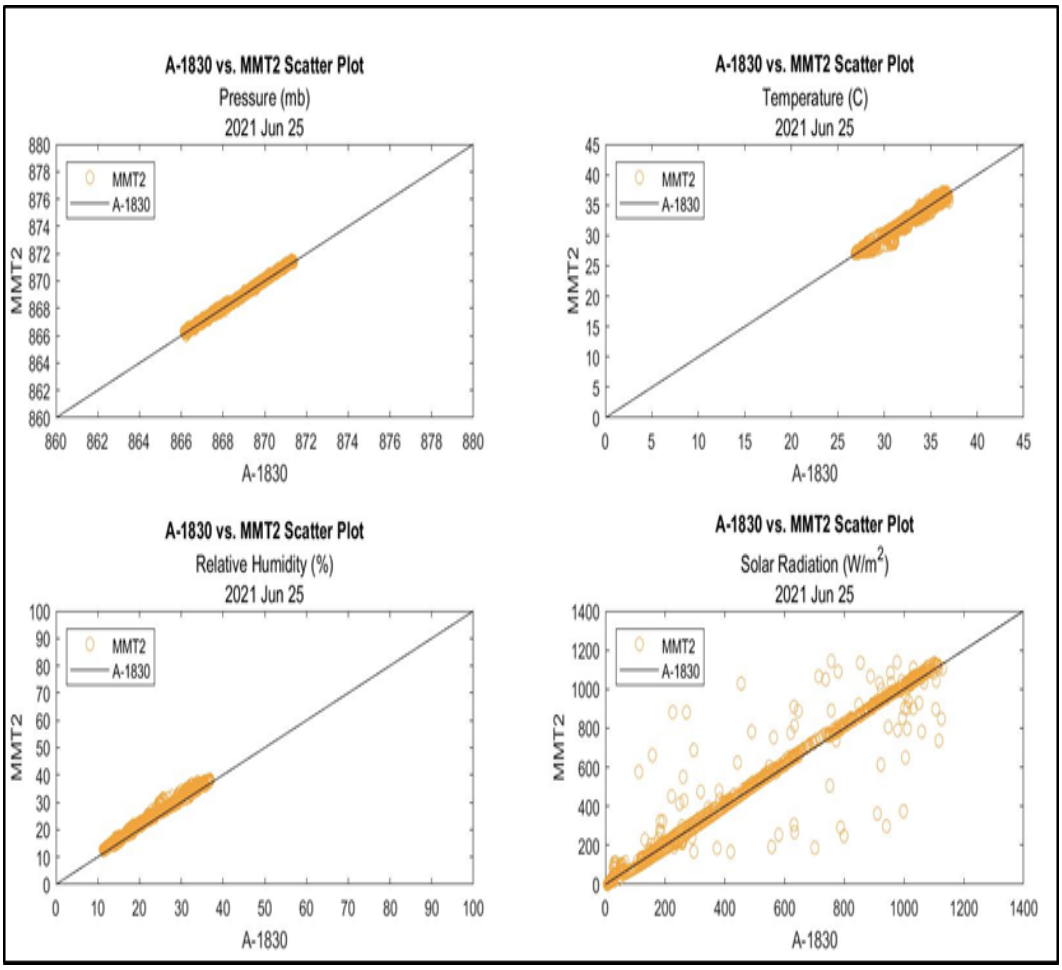


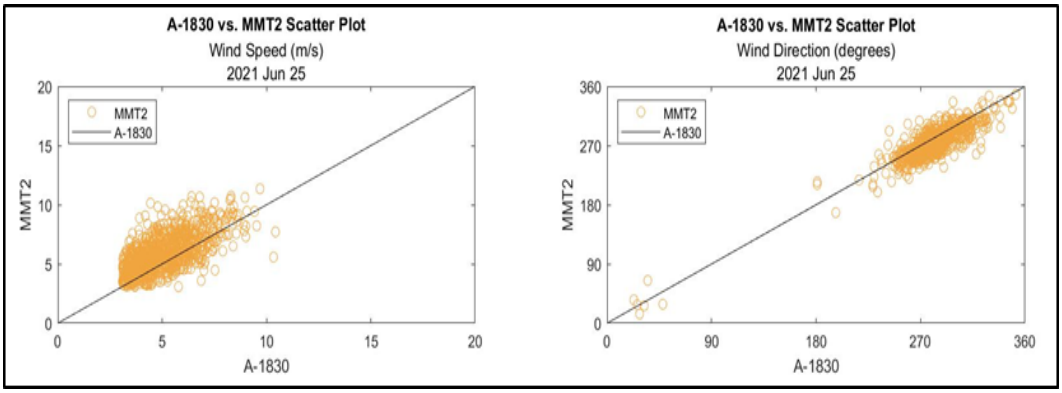


**Fig. B-18 2021 Jun 25, MMT2 vs. A-1830 data comparison**

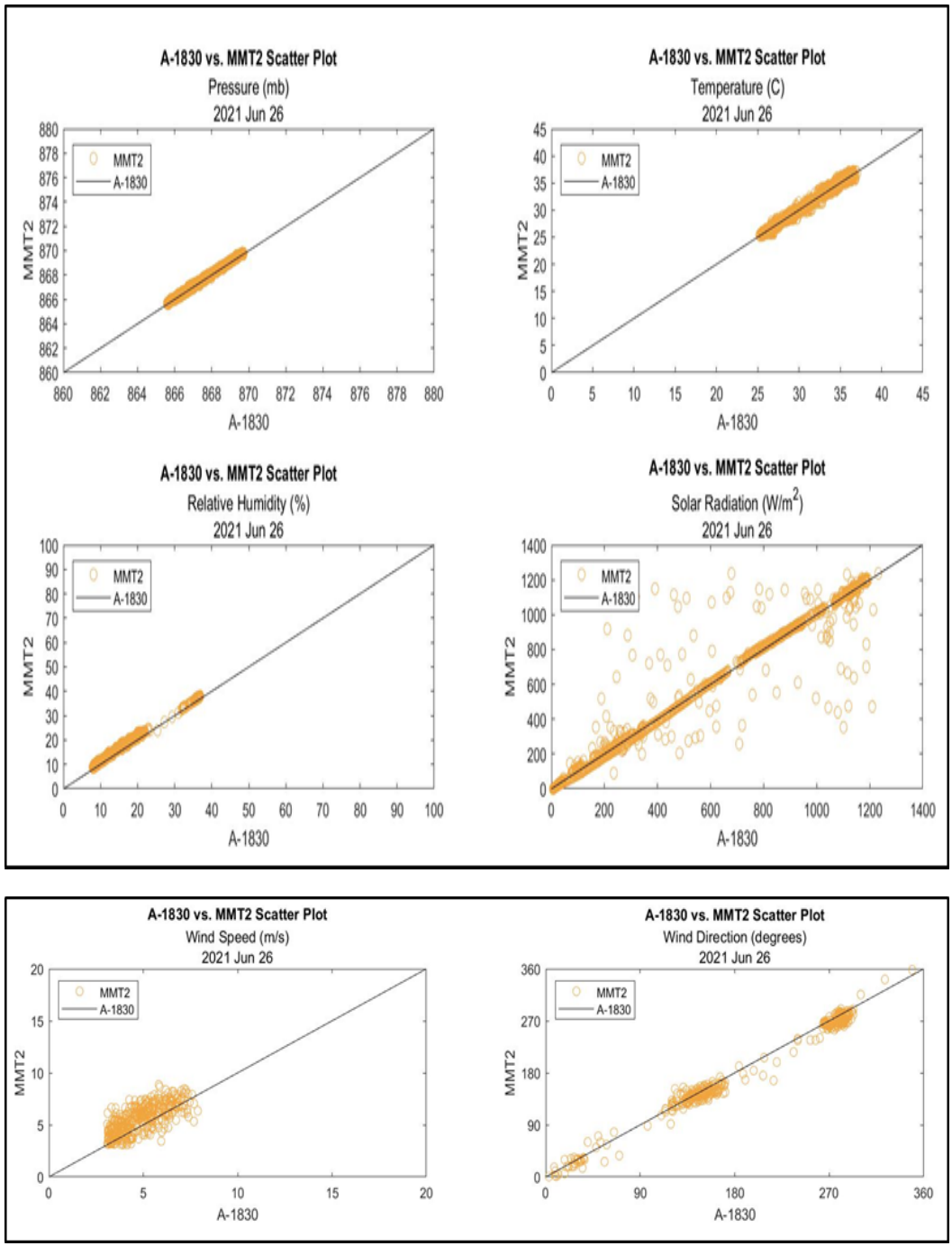


**Fig. B-19 2021 Jun 26, MMT2 vs. A-1830 data comparison**

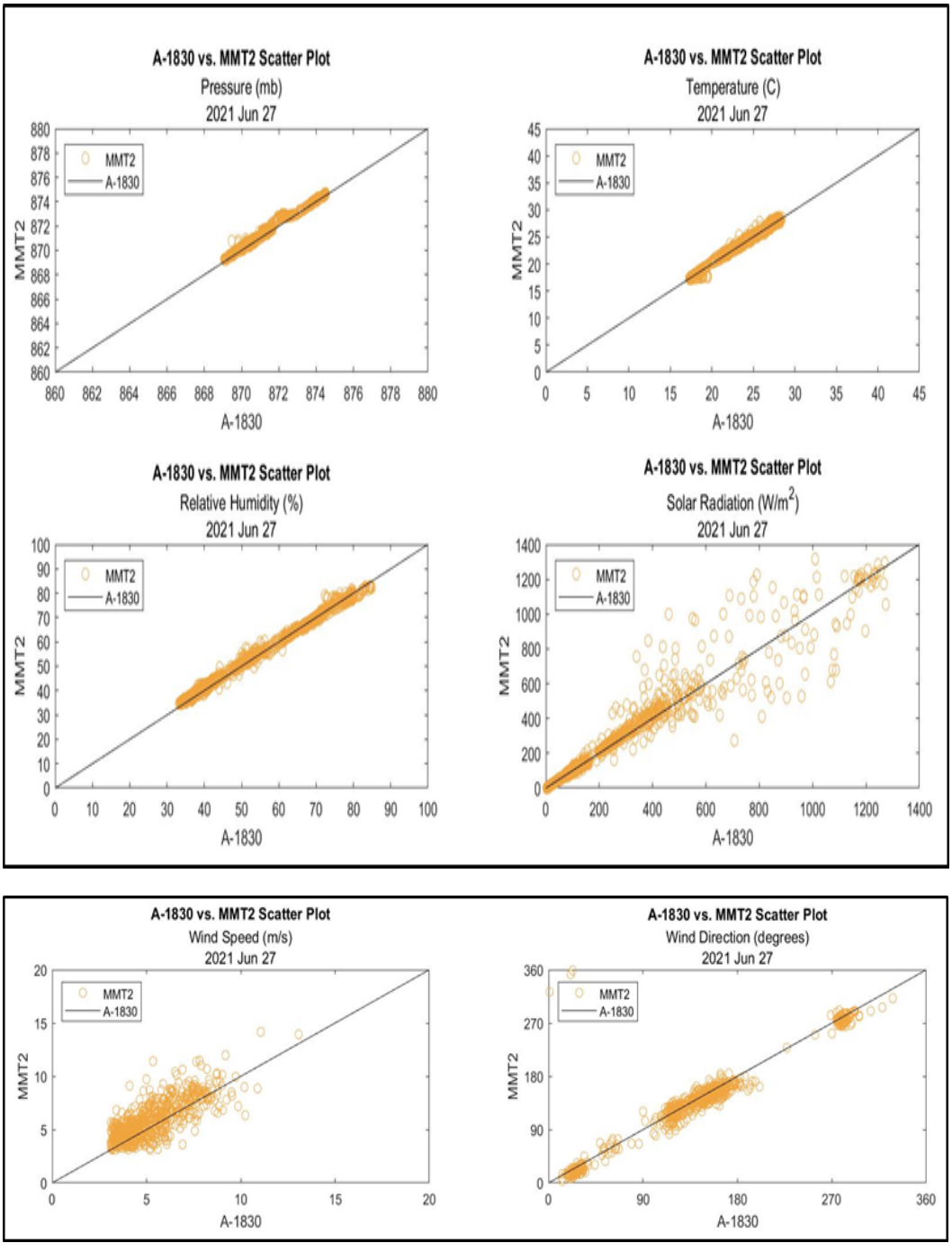


**Fig. B-20 2021 Jun 27, MMT2 vs. A-1830 data comparison**

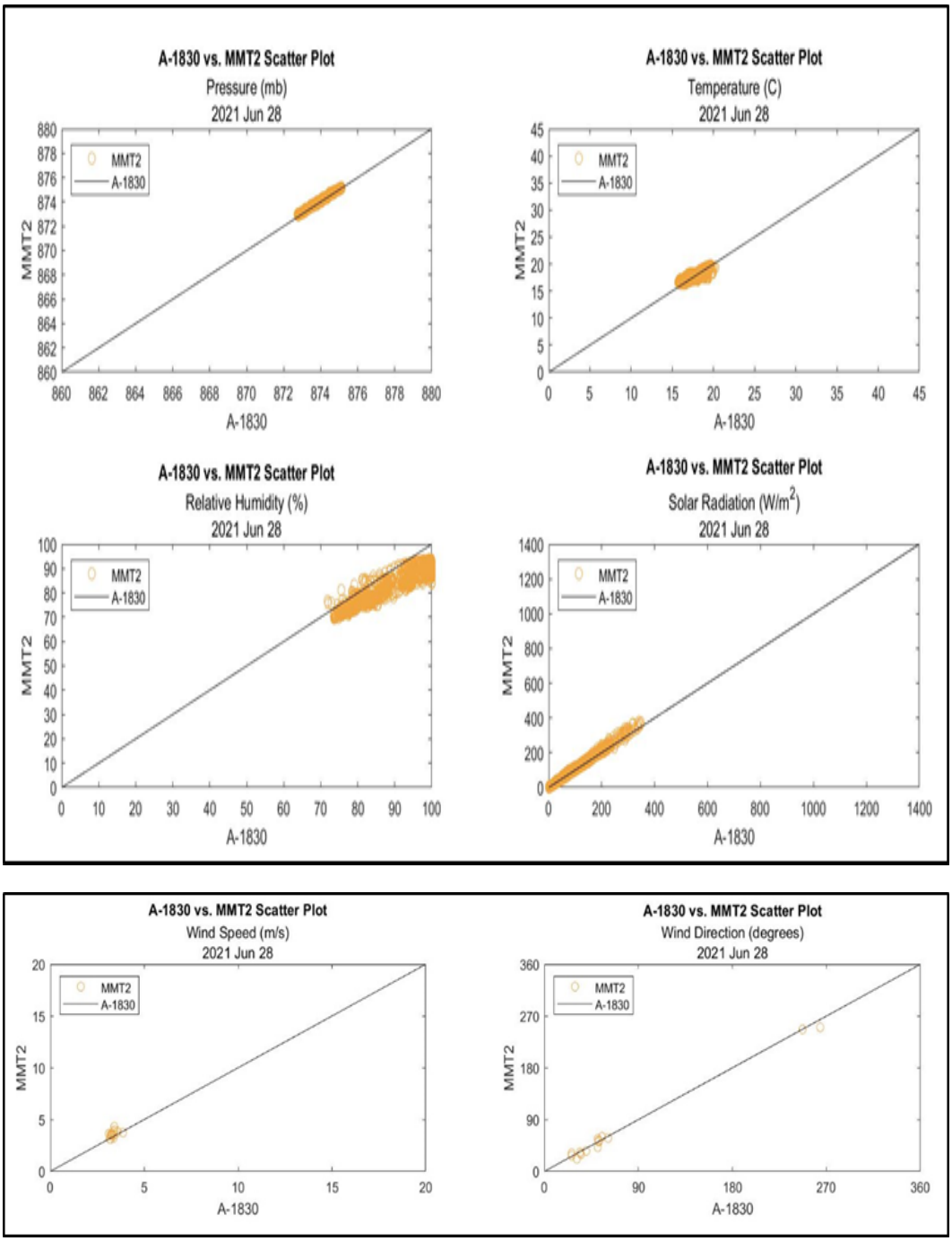


**Fig. B-21 2021 Jun 28, MMT2 vs. A-1830 data comparison**

## Appendix C. Daily Comparison-Error Analysis Tables

Appendix C displays 21 individual days of the daily error analysis tables, based on processed 2021 June (Meteorological Measurement Tripod #2 [MMT2] vs. A-1830) meteorological comparison data. The "truth" for the error analysis was defined as the A-1830 data. Each table includes the thermodynamic data—pressure (in mb), temperature (in °C), relative humidity (in %), solar radiation (in $W/m^2$) — and the dynamic variable wind speed, for a single 24-h period. Note: The wind speed (in m/s) is represented by its 2-D "u" and "v" components.

The statistical error analysis includes standard deviation (STD), mean absolute error (MAE), mean bias error (MBE), and root mean square error (RMSE). The percent of data points used in the statistical calculation is the final column. For more information on these terms, see Section 2.5.2.

**Table C-1 2021 Jun 05, MMT2 vs. A-1830 statistical comparison**

| 2021 Jun 05 | STD | MAE | MBE | RMSE | Percent included |
|---|---|---|---|---|---|
| **Pressure (mb)** | 0.16 | 0.14 | 0.09 | 0.14 | 100 |
| **Temperature (C)** | 0.40 | 0.31 | 0.40 | 0.02 | 100 |
| **Relative Humidity (%)** | 1.66 | 1.55 | 0.60 | 1.55 | 100 |
| **Solar Radiation ($\frac{W}{m^2}$)** | 47.74 | 22.12 | 47.07 | 8.11 | 56 |
| **Wind Speed u (m/s)** | 5.90 | 4.75 | –0.19 | 5.90 | 29 |
| **Wind Speed v (m/s)** | 5.85 | 4.82 | –0.05 | 5.84 | 29 |

**Table C-2 2021 Jun 06, MMT2 vs. A-1830 statistical comparison**

| 2021 Jun 06 | STD | MAE | MBE | RMSE | Percent included |
|---|---|---|---|---|---|
| **Pressure (mb)** | 0.14 | 0.13 | 0.08 | 0.12 | 100 |
| **Temperature (C)** | 0.28 | 0.23 | 0.25 | 0.12 | 100 |
| **Relative Humidity (%)** | 1.40 | 1.38 | 0.22 | 1.38 | 100 |
| **Solar Radiation ($\frac{W}{m^2}$)** | 56.23 | 25.08 | 55.33 | 10.17 | 57 |
| **Wind Speed u (m/s)** | 7.04 | 5.70 | –0.26 | 7.04 | 90 |
| **Wind Speed v (m/s)** | 6.86 | 5.51 | 0.08 | 6.86 | 90 |

**Table C-3 2021 Jun 07, MMT2 vs. A-1830 statistical comparison**

| 2021 Jun 07 | STD | MAE | MBE | RMSE | Percent included |
|---|---|---|---|---|---|
| **Pressure (mb)** | 0.15 | 0.14 | 0.06 | 0.14 | 100 |
| **Temperature (C)** | 0.30 | 0.24 | 0.26 | 0.16 | 100 |
| **Relative Humidity (%)** | 1.40 | 1.39 | 0.17 | 1.39 | 100 |
| **Solar Radiation ($\frac{W}{m^2}$)** | 25.55 | 19.90 | 22.36 | 12.38 | 56 |
| **Wind Speed u (m/s)** | 6.49 | 5.19 | 0.22 | 6.49 | 85 |
| **Wind Speed v (m/s)** | 6.58 | 5.28 | –0.17 | 6.58 | 85 |

**Table C-4 2021 Jun 08, MMT2 vs. A-1830 statistical comparison**

| 2021 Jun 08 | STD | MAE | MBE | RMSE | Percent included |
|---|---|---|---|---|---|
| **Pressure (mb)** | 0.15 | 0.15 | 0.06 | 0.14 | 100 |
| **Temperature (C)** | 0.34 | 0.26 | 0.32 | 0.10 | 100 |
| **Relative Humidity (%)** | 1.51 | 1.48 | 0.30 | 1.48 | 100 |
| **Solar Radiation ($\frac{W}{m^2}$)** | 47.75 | 29.55 | 46.73 | 9.94 | 57 |
| **Wind Speed u (m/s)** | 5.78 | 4.69 | –0.10 | 5.78 | 66 |
| **Wind Speed v (m/s)** | 5.67 | 4.55 | –0.19 | 5.67 | 66 |

**Table C-5 2021 Jun 09, MMT2 vs. A-1830 statistical comparison**

| 2021 Jun 09 | STD | MAE | MBE | RMSE | Percent included |
|---|---|---|---|---|---|
| **Pressure (mb)** | 0.16 | 0.14 | 0.09 | 0.13 | 100 |
| **Temperature (C)** | 0.48 | 0.38 | 0.48 | –0.03 | 100 |
| **Relative Humidity (%)** | 1.46 | 1.43 | 0.26 | 1.43 | 100 |
| **Solar Radiation ($\frac{W}{m^2}$)** | 26.62 | 18.66 | 25.61 | 7.32 | 56 |
| **Wind Speed u (m/s)** | 4.25 | 3.40 | –0.02 | 4.24 | 19 |
| **Wind Speed v (m/s)** | 4.52 | 3.65 | –0.03 | 4.51 | 19 |

**Table C-6 2021 Jun 10, MMT2 vs. A-1830 statistical comparison**

| 2021 Jun 10 | STD | MAE | MBE | RMSE | Percent included |
|---|---|---|---|---|---|
| **Pressure (mb)** | 0.16 | 0.14 | 0.10 | 0.12 | 100 |
| **Temperature (C)** | 0.51 | 0.37 | 0.51 | 0.01 | 100 |
| **Relative Humidity (%)** | 1.49 | 1.42 | 0.43 | 1.42 | 100 |
| **Solar Radiation ($\frac{W}{m^2}$)** | 19.45 | 14.14 | 17.74 | 7.99 | 56 |
| **Wind Speed u (m/s)** | 5.40 | 4.30 | –0.11 | 5.39 | 26 |
| **Wind Speed v (m/s)** | 5.08 | 4.10 | 0.53 | 5.10 | 26 |

**Table C-7 2021 Jun 11, MMT2 vs. A-1830 statistical comparison**

| 2021 Jun 11 | STD | MAE | MBE | RMSE | Percent included |
|---|---|---|---|---|---|
| **Pressure (mb)** | 0.15 | 0.13 | 0.09 | 0.12 | 100 |
| **Temperature (C)** | 0.50 | 0.38 | 0.50 | 0.05 | 100 |
| **Relative Humidity (%)** | 1.33 | 1.31 | 0.27 | 1.31 | 100 |
| **Solar Radiation ($\frac{W}{m^2}$)** | 24.70 | 15.58 | 24.31 | 4.44 | 57 |
| **Wind Speed u (m/s)** | 4.21 | 3.35 | 0.20 | 4.20 | 13 |
| **Wind Speed v (m/s)** | 4.31 | 3.45 | –0.07 | 4.30 | 13 |

**Table C-8 2021 Jun 12, MMT2 vs. A-1830 statistical comparison**

| 2021 Jun 12 | STD | MAE | MBE | RMSE | Percent included |
|---|---|---|---|---|---|
| **Pressure (mb)** | 0.18 | 0.16 | 0.10 | 0.15 | 100 |
| **Temperature (C)** | 0.39 | 0.29 | 0.39 | 0.06 | 100 |
| **Relative Humidity (%)** | 1.58 | 1.50 | 0.52 | 1.49 | 100 |
| **Solar Radiation ($\frac{W}{m^2}$)** | 34.06 | 13.66 | 34.00 | 2.26 | 58 |
| **Wind Speed u (m/s)** | 6.39 | 5.18 | –0.34 | 6.39 | 37 |
| **Wind Speed v (m/s)** | 5.81 | 4.61 | –0.03 | 5.81 | 37 |

**Table C-9 2021 Jun 13, MMT2 vs. A-1830 statistical comparison**

| 2021 Jun 13 | STD | MAE | MBE | RMSE | Percent included |
|---|---|---|---|---|---|
| **Pressure (mb)** | 0.13 | 0.11 | 0.08 | 0.10 | 100 |
| **Temperature (C)** | 0.37 | 0.29 | 0.34 | 0.14 | 100 |
| **Relative Humidity (%)** | 1.52 | 1.4 | 0.48 | 1.44 | 100 |
| **Solar Radiation ($\frac{W}{m^2}$)** | 16.87 | 12.63 | 14.23 | 9.09 | 56 |
| **Wind Speed u (m/s)** | 4.62 | 3.72 | 0.15 | 4.61 | 25 |
| **Wind Speed v (m/s)** | 4.59 | 3.61 | 0.10 | 4.58 | 25 |

**Table C-10 2021 Jun 14, MMT2 vs. A-1830 statistical comparison**

| 2021 Jun 14 | STD | MAE | MBE | RMSE | Percent included |
|---|---|---|---|---|---|
| **Pressure (mb)** | 0.11 | 0.10 | 0.09 | 0.08 | 100 |
| **Temperature (C)** | 0.60 | 0.45 | 0.60 | –0.00 | 100 |
| **Relative Humidity (%)** | 1.69 | 1.50 | 0.78 | 1.50 | 100 |
| **Solar Radiation ($\frac{W}{m^2}$)** | 43.38 | 22.98 | 42.39 | 9.30 | 57 |
| **Wind Speed u (m/s)** | 5.06 | 4.07 | –0.01 | 5.06 | 38 |
| **Wind Speed v (m/s)** | 5.20 | 4.23 | –0.19 | 5.20 | 38 |

**Table C-11 2021 Jun 15, MMT2 vs. A-1830 statistical comparison**

| 2021 Jun 15 | STD | MAE | MBE | RMSE | Percent included |
|---|---|---|---|---|---|
| **Pressure (mb)** | 0.14 | 0.12 | 0.09 | 0.11 | 100 |
| **Temperature (C)** | 0.49 | 0.36 | 0.48 | 0.07 | 100 |
| **Relative Humidity (%)** | 1.81 | 1.53 | 0.96 | 1.53 | 100 |
| **Solar Radiation ($\frac{W}{m^2}$)** | 22.47 | 19.67 | 16.35 | 15.43 | 57 |
| **Wind Speed u (m/s)** | 5.22 | 4.13 | –0.11 | 5.22 | 42 |
| **Wind Speed v (m/s)** | 5.20 | 4.15 | 0.11 | 5.19 | 42 |

**Table C-12 2021 Jun 17, MMT2 vs. A-1830 statistical comparison**

| 2021 Jun 17 | STD | MAE | MBE | RMSE | Percent included |
|---|---|---|---|---|---|
| **Pressure (mb)** | 0.14 | 0.12 | 0.08 | 0.11 | 100 |
| **Temperature (C)** | 0.36 | 0.28 | 0.34 | 0.11 | 100 |
| **Relative Humidity (%)** | 1.43 | 1.37 | 0.43 | 1.36 | 100 |
| **Solar Radiation ($\frac{W}{m^2}$)** | 30.48 | 19.86 | 26.59 | 14.92 | 57 |
| **Wind Speed u (m/s)** | 4.85 | 4.01 | 0.14 | 4.85 | 39 |
| **Wind Speed v (m/s)** | 4.69 | 3.79 | 0.11 | 4.69 | 39 |

**Table C-13 2021 Jun 18, MMT2 vs. A-1830 statistical comparison**

| 2021 Jun 18 | STD | MAE | MBE | RMSE | Percent included |
|---|---|---|---|---|---|
| **Pressure (mb)** | 0.16 | 0.14 | 0.10 | 0.13 | 100 |
| **Temperature (C)** | 0.53 | 0.38 | 0.53 | –0.06 | 100 |
| **Relative Humidity (%)** | 1.81 | 1.67 | 0.69 | 1.67 | 100 |
| **Solar Radiation ($\frac{W}{m^2}$)** | 50.47 | 23.24 | 47.38 | 17.46 | 57 |
| **Wind Speed u (m/s)** | 4.46 | 3.68 | 0.08 | 4.45 | 19 |
| **Wind Speed v (m/s)** | 4.48 | 3.68 | –0.43 | 4.49 | 19 |

**Table C-14 2021 Jun 19, MMT2 vs. A-1830 statistical comparison**

| 2021 Jun 19 | STD | MAE | MBE | RMSE | Percent included |
|---|---|---|---|---|---|
| **Pressure (mb)** | 0.16 | 0.13 | 0.11 | 0.12 | 100 |
| **Temperature (C)** | 0.42 | 0.32 | 0.41 | 0.08 | 100 |
| **Relative Humidity (%)** | 1.45 | 1.35 | 0.51 | 1.35 | 100 |
| **Solar Radiation ($\frac{W}{m^2}$)** | 21.41 | 17.52 | 18.72 | 10.41 | 56 |
| **Wind Speed u (m/s)** | 4.57 | 3.74 | –0.16 | 4.56 | 26 |
| **Wind Speed v (m/s)** | 4.45 | 3.53 | –0.36 | 4.46 | 26 |

**Table C-15 2021 Jun 20, MMT2 vs. A-1830 statistical comparison**

| 2021 Jun 20 | STD | MAE | MBE | RMSE | Percent included |
|---|---|---|---|---|---|
| **Pressure (mb)** | 0.14 | 0.12 | 0.08 | 0.12 | 100 |
| **Temperature (C)** | 0.40 | 0.31 | 0.39 | 0.08 | 100 |
| **Relative Humidity (%)** | 1.46 | 1.41 | 0.37 | 1.41 | 100 |
| **Solar Radiation ($\frac{W}{m^2}$)** | 82.82 | 26.80 | 82.10 | 11.28 | 57 |
| **Wind Speed u (m/s)** | 5.66 | 4.42 | –0.00 | 5.65 | 39 |
| **Wind Speed v (m/s)** | 5.62 | 4.40 | 0.12 | 5.61 | 39 |

**Table C-16 2021 Jun 21, MMT2 vs. A-1830 statistical comparison**

| 2021 Jun 21 | STD | MAE | MBE | RMSE | Percent included |
|---|---|---|---|---|---|
| **Pressure (mb)** | 0.15 | 0.13 | 0.08 | 0.13 | 100 |
| **Temperature (C)** | 0.36 | 0.29 | 0.33 | 0.15 | 100 |
| **Relative Humidity (%)** | 1.56 | 1.49 | 0.47 | 1.48 | 100 |
| **Solar Radiation ($\frac{W}{m^2}$)** | 54.70 | 24.08 | 54.16 | 7.86 | 57 |
| **Wind Speed u (m/s)** | 5.60 | 4.47 | 0.28 | 5.60 | 74 |
| **Wind Speed v (m/s)** | 5.84 | 4.71 | 0.729 | 5.89 | 74 |

**Table C-17 2021 Jun 22, MMT2 vs. A-1830 statistical comparison**

| 2021 Jun 22 | STD | MAE | MBE | RMSE | Percent included |
|---|---|---|---|---|---|
| **Pressure (mb)** | 1.64 | 0.16 | 1.64 | 0.06 | 100 |
| **Temperature (C)** | 0.49 | 0.34 | 0.49 | 0.01 | 100 |
| **Relative Humidity (%)** | 1.98 | 1.52 | 1.30 | 1.50 | 100 |
| **Solar Radiation ($\frac{W}{m^2}$)** | 16.47 | 13.76 | 12.40 | 10.84 | 57 |
| **Wind Speed u (m/s)** | 5.18 | 4.19 | –0.11 | 5.17 | 31 |
| **Wind Speed v (m/s)** | 5.11 | 4.03 | 0.42 | 5.12 | 31 |

**Table C-18 2021 Jun 25, MMT2 vs. A-1830 statistical comparison**

| 2021 Jun 25 | STD | MAE | MBE | RMSE | Percent included |
|---|---|---|---|---|---|
| **Pressure (mb)** | 0.12 | 0.10 | 0.07 | 0.09 | 100 |
| **Temperature (C)** | 0.44 | 0.32 | 0.44 | 0.02 | 100 |
| **Relative Humidity (%)** | 1.72 | 1.60 | 0.64 | 1.60 | 100 |
| **Solar Radiation ($\frac{W}{m^2}$)** | 95.30 | 38.62 | 94.48 | 12.89 | 57 |
| **Wind Speed u (m/s)** | 5.85 | 4.76 | –0.09 | 5.85 | 65 |
| **Wind Speed v (m/s)** | 5.80 | 4.70 | –0.14 | 5.80 | 65 |

**Table C-19 2021 Jun 26, MMT2 vs. A-1830 statistical comparison**

| 2021 Jun 26 | STD | MAE | MBE | RMSE | Percent included |
|---|---|---|---|---|---|
| **Pressure (mb)** | 0.13 | 0.11 | 0.08 | 0.10 | 100 |
| **Temperature (C)** | 0.40 | 0.32 | 0.38 | 0.13 | 100 |
| **Relative Humidity (%)** | 1.45 | 1.40 | 0.40 | 1.39 | 100 |
| **Solar Radiation ($\frac{W}{m^2}$)** | 118.63 | 43.30 | 118.54 | 6.28 | 56 |
| **Wind Speed u (m/s)** | 5.54 | 4.44 | 0.03 | 5.53 | 25 |
| **Wind Speed v (m/s)** | 5.36 | 4.38 | 0.18 | 5.36 | 25 |

**Table C-20 2021 Jun 27, MMT2 vs. A-1830 statistical comparison**

| 2021 Jun 27 | STD | MAE | MBE | RMSE | Percent included |
|---|---|---|---|---|---|
| **Pressure (mb)** | 1.64 | 0.23 | 1.64 | 0.14 | 100 |
| **Temperature (C)** | 0.29 | 0.20 | 0.27 | 0.11 | 100 |
| **Relative Humidity (%)** | 1.32 | 1.09 | 1.06 | 0.79 | 100 |
| **Solar Radiation ($\frac{W}{m^2}$)** | 87.61 | 39.17 | 87.11 | 9.79 | 57 |
| **Wind Speed u (m/s)** | 5.70 | 4.46 | 0.10 | 5.70 | 46 |
| **Wind Speed v (m/s)** | 5.93 | 4.67 | 0.30 | 5.94 | 46 |

**Table C-21 2021 Jun 28, MMT2 vs. A-1830 statistical comparison**

| 2021 Jun 28 | STD | MAE | MBE | RMSE | Percent included |
|---|---|---|---|---|---|
| **Pressure (mb)** | 0.12 | 0.11 | 0.05 | 0.11 | 100 |
| **Temperature (C)** | 0.40 | 0.27 | 0.37 | 0.15 | 100 |
| **Relative Humidity (%)** | 7.86 | 7.08 | 3.60 | -6.99 | 100 |
| **Solar Radiation** $(\frac{W}{m^2})$ | 10.82 | 7.35 | 8.19 | 7.08 | 57 |
| **Wind Speed u (m/s)** | 3.63 | 3.56 | 1.99 | 4.03 | 1 |
| **Wind Speed v (m/s)** | 3.24 | 3.12 | 1.43 | 3.44 | 1 |

# Appendix D. Verification of Error Calculations

**Checking Error Calculations**

Hand-calculations were performed on a small sample of data to verify the validity of the equations used. The "T" were equivalent to the Meteorological Measurement Tripod #2 (MMT2) sensor data. "O" data were equivalent to the defined "Standard", or A-1830 data. The results of these calculations are shown.

**Mean Absolute Error**

T = [20 22 21 25 22 24]

O = [20 21 21 24 23 24]

Mean Absolute Error (MAE): $\frac{1}{n}\sum_{i=1}^{n}|O_i - T_i|$

$$MAE = \frac{1}{6} \times ((|20-20|) + (|21-22|) + (|21-21|) + (|24-25|) + (|23-22|) + (|24-24|))$$

$$MAE = \frac{1}{6} \times (0+1+0+1+1+0)$$

$$MAE = \frac{1}{6} \times (3)$$

$$MAE = 0.5$$

**Mean Bias Error**

Mean Bias Error (MBE): $\frac{1}{n}\sum_{i=1}^{n}(O_i - T_i)$

$$MBE = \frac{1}{6} \times ((20-20) + (21-22) + (21-21) + (24-25) + (23-22) + (24-24))$$

$$MBE = \frac{1}{6} \times (0-1+0-1+1+0)$$

$$MBE = \frac{1}{6} \times (-1)$$

$$MBE = -\frac{1}{3} \approx -0.1667$$

**Root Mean Square Error**

$$RMSE = \sqrt{\frac{\sum_{i=1}^{n}(O_i - T_i)^2}{n}}$$

$$RMSE = \sqrt{\frac{((20-20)^2 + (21-22)^2 + (21-21)^2 + (24-25)^2 + (23-22)^2 + (24-24)^2}{6}}$$

$$RMSE = \sqrt{\frac{((0)^2 + (-1)^2 + (0)^2 + (-1)^2 + (1)^2 + (0)^2}{6}}$$

$$RMSE = \sqrt{\frac{(0) + (1) + (0) + (1) + (1) + (0)}{6}}$$

$$RMSE = \sqrt{\frac{3}{6}}$$

$$RMSE = \sqrt{\frac{1}{2}} \approx 0.7071$$

**MATAB Error Calculation**

Figure D-1 shows the MATLAB command window when the sample data were used as an input. The results agree with the previous hand-calculations.

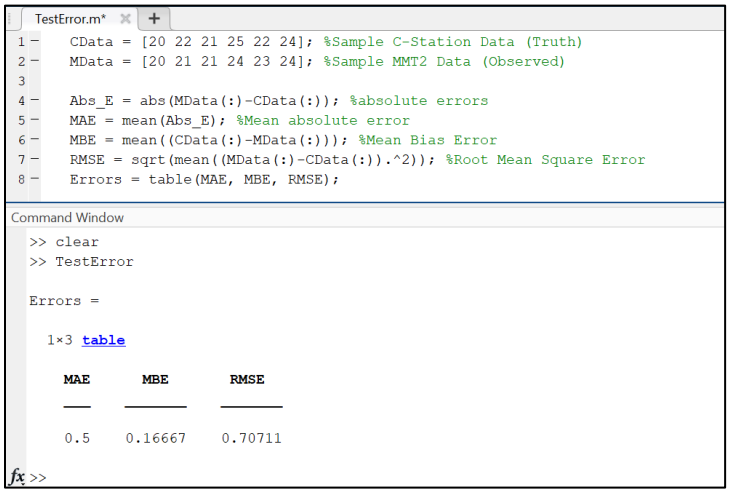


**Fig. D-1 MATLAB validation of error equations**

## List of Symbols, Abbreviations, and Acronyms

| | |
|---|---|
| 2-D | two-dimensional |
| 3-D | three-dimensional |
| AC | alternating current |
| ACORE | American Council on Renewable Energy |
| ARL | Army Research Laboratory |
| ATEC | Army Test and Evaluation Command |
| DEVCOM | US Army Combat Capabilities Development Command |
| DOD | Department of Defense |
| L-REAC | Local-Rapid Evaluation of Atmospheric Conditions |
| MAE | mean absolute error |
| MBE | mean bias error |
| MMT | Meteorological Measurement Tripod |
| MMT2 | Meteorological Measurement Tripod #2 |
| MST | Mountain Standard Time |
| NOAA | National Oceanic and Atmospheric Administration |
| P | pressure |
| PV | photovoltaic |
| RH | relative humidity |
| RSME | root mean square error |
| SR | solar radiation |
| STD | standard deviation |
| T | temperature |
| WD | wind direction |
| WS | wind speed |

1 (PDF) DEFENSE TECHNICAL INFORMATION CTR
DTIC OCA

1 (PDF) DEVCOM ARL
FCDD RLD DCI
TECH LIB

3 (PDF) ATEC
B THOMAS
S STARTZ
S HALVORSON

1 (PDF) MTU
G PARKER

1 (PDF) WEST POINT
C JAMES

1 (PDF) C5ISR
M BAILEY

1 (PDF) GVSC
D RIZZO

2 (PDF) ROTC INTERN
S BERGEN
H GOODMAN

12 (PDF) DEVCOM ARL
FCDD RLC E
5 (HC) B MCCALL
T JAMESON
FCDD RLC ED
G VAUCHER (5 HC)
C HOCUT
R BRICE
R RANDALL
M LEE
M S DARCY
J RABY
FCDD RLS RP
M BERMAN
B GEIL
R JANE